The use of spectral reflectance data to assess plant stress and improve irrigation water management

Samuel Onyekachi Ihuoma

Department of Bioresource Engineering

McGill University, Montreal.

Submitted April 2020

A Thesis Submitted to McGill University in partial fulfillment of the requirements for the degree of Doctor of Philosophy

Abstract

Early identification and prediction of plant abiotic stress are required to ensure sustainable agricultural management. Traditional plant and soil-based methods of estimating plant stress are destructive, labour intensive, and time-consuming. These methods often do not represent the heterogeneity of soil and crop parameters at large spatial scales. Spectral reflectance data provide near real-time and non-destructive estimates of plant stress, and account for spatial and temporal variability of crops and soil. This research focused on the use of spectral reflectance data to estimate plant water and nitrogen requirements to improve field management of high-value vegetable crops.

The first study in this thesis investigated the potential of crop reflectance indices for detecting water stress, in order to improve the irrigation of greenhouse-grown vegetable crops. Two widely grown vegetable crops (tomato plants: *Solanum Lycopersicum L.* and bell pepper: *Capsicum annuum L.*) were chosen due to their canopy architecture and sensitivity to water stress. Spectral data and plant stress parameters (stomatal conductance, leaf temperature, relative water content, and crop yield) were concurrently acquired from plants subjected to different irrigation treatments (100, 80, 60, 40, and 20% of plant available water). Various reflectance indices were obtained from the spectral data. The relationships between crop reflectance indices and water stress indicators were statistically examined to evaluate the most useful indices for detecting water stress. The results indicate that the photochemical reflectance indices (PRI) centered at 553 nm (PRI_{553}) was the most useful index for detecting water stress in bell pepper plants, while the PRI centered at 550 nm (PRI_{550}) was suitable for tomato crops. These results contrast the findings of previous studies, which recommended the use of PRI_{570} for monitoring water stress in most field crops.

Given that the spectral vegetation indices for monitoring plant water status are affected by microclimatic conditions, it was hypothesized that the findings of the greenhouse studies will not be applicable to open field conditions. The second study in this thesis assessed the use of reflectance indices for monitoring water and nitrogen stresses in field-grown tomato crops. Spectral reflectance data and plant stress indicators (leaf temperature, relative water content, crop yield, and leaf chlorophyll content) were measured from tomato plants subjected to three irrigation water treatments (100, 70, and 30% of field capacity) and three nitrogen treatments (100, 70, and 30% of crop nutrient requirement). The results showed that the PRI_{550} and water index (R_{900}/R_{970}) were the most sensitive indices for distinguishing crop water stress, while renormalized difference vegetation index and Transformed Chlorophyll Absorption in Reflectance Index had the best correlation with nitrogen stress indicators. Normalized PRI was the most sensitive index for detecting the combined effect of water and nitrogen stress.

The last study in this thesis compared the suitability of multispectral images acquired from unmanned aerial vehicles, PlanetScope, and Sentinel-2 satellite platforms for estimating crop coefficient and evapotranspiration. Sentinel-2 data were used to predict crop evapotranspiration (ETc) and the results were compared with ETc estimated from the FAO 56 Penman-Monteith module of the AquaCrop model. ETc data were coupled with time domain reflectometry soil moisture measurements to estimate irrigation water requirements (IWR). The estimated seasonal IWR was less than the actual amount of water applied by the grower, indicating that the field was over irrigated by 17% and 20% in the 2017 and 2018 growing seasons, respectively. This thesis concludes that leaf spectral data are advantageous over conventional methods of crop stress assessment for improving irrigation water management.

Résumé

L'identification précoce et la prévision du stress abiotique des cultures s'avèrent nécessaires à une gestion agricole durable. Fondées sur l'état des plantes et du sol, les méthodes d'antan pour estimer le stress subi par une culture s'avérèrent destructrices et intenses en temps et travail, en plus de ne pas tenir compte de l'hétérogénéité des cultures et du sol. Les données de réflectance spectrale fournissent des estimations non destructives et en temps quasi-réel du stress subi par les plantes, tout en tenant compte de la variabilité spatiotemporelle des cultures et du sol. Visant à améliorer la gestion des besoins en eau et en azote des cultures maraîchères à l'échelle du champ, par l'emploi des données de réflectance spectrale, une première étude, axée sur l'amélioration de l'irrigation des cultures maraîchères en serre, s'attarda à l'étude du potentiel des indices de réflectance des cultures à détecter le stress hydrique. Deux cultures maraîchères (tomate - *Solanum lycopersicum* L. et poivron — *Capsicum annuum* L.) furent choisies pour l'architecture de leur canopée et leur sensibilité au stress hydrique. Le recueil simultané auprès de plantes soumises à différents régimes d'irrigation (100, 80, 60, 40 et 20% de l'eau disponible aux plantes), des données spectrales et paramètres de stress (conductance stomatique, température des feuilles, teneur en eau relative, rendement des cultures), permit de calculer divers indices de réflectance et d'évaluer statistiquement leurs relations aux indicateurs de stress hydrique, afin d'identifier les indices les plus utiles à la détection du stress hydrique. En contraste aux résultats d'études précédentes recommandant l'utilisation du PRI_{570} pour surveiller le stress hydrique, dna sla présente étude les indices de réflectance photochimique (PRI) centrés à 553 nm (PRI_{553}) se révélèrent les plus utiles à la détection du stress hydrique des poivrons, tandis qu'un PRI centré à 550 nm (PRI_{550}) fut le plus utile pour les tomates.

Les indices de végétation spectrale utilisés pour surveiller the stress hydrique des plantes étant affectés par les conditions microclimatiques, nous émîmes l'hypothèse que les résultats d'une culture en serre n'aurait pas leur application en plein champ. La deuxième partie de l'étude évalua donc l'utilisation d'indices de réflectance pour surveiller les stress hydriques et azotés des tomates cultivées en plein champ. La réflectance spectrale et les indicateurs de stress des plantes (température des feuilles, teneur en eau relative, rendement et teneur en chlorophylle des feuilles) furent mesurés pour des plants de tomates soumis à trois traitements d'irrigation (100, 70 et 30% de la capacité au champ) combinés de manière factorielle à trois niveaux de fertilisation azotée (100, 70 et 30% des besoins). L'indice PRI_{550} et l'indice d'eau (R_{900}/R_{970}) permirent la meilleure discrimination entre niveaux de stress hydrique, tandis que l'indice de végétation par différence renormalisée et l'indice d'absorption de chlorophylle transformée en réflectance furent le plus fortement corrélés aux indicateurs de stress azoté. Le PRI normalisé s'avéra l'indice le plus sensible à l'effet combiné du stress hydrique et azoté.

La dernière étude présentée dans cette thèse compara l'aptitude des images multispectrales acquises à partir de véhicules aériens sans pilote, de PlanetScope et de plateformes satellites Sentinel-2 pour estimer le facteur culture et l'évapotranspiration. Ces dernières données ont permi à prédire l'évapotranspiration des cultures (ET_c) et de comparer ces résultats à l'ET_c estimé par la méthode Penman-Monteith. Les données ET_c furent couplées à des mesures d'humidité du sol acquises par réflectométrie temporelle afin d'estimer les besoins en eau d'irrigation (IWR). L'IWR saisonnier s'avéra inférieur à la quantité d'eau appliquée par le producteur, indiquant une surirrigation du champ de 17% et de 20% lors des saisons 2017 et 2018, respectivement. Pour améliorer la gestion de l''irrigation, les données spectrales foliaires offrent une meilleure évaluation du stress des cultures que les méthodes conventionnelles.

Dedication

This piece of work is dedicated to the Holy Trinity*, God the Father, God the Son, and God the Holy Spirit*, for His infinite mercies during my academic pursuits.

Acknowledgements

Kindness elicits gratitude; it is on this strength that my unalloyed gratitude goes to my supervisor, Prof. Chandra A. Madramootoo, for accepting to supervise and fully fund my Ph.D. program. His diligent supervision, mentoring, and encouragement helped me to successfully navigate this journey. As my academic role model, I have immensely benefitted from your intellectual prowess, wealth of experience, and strive for excellence. Thank you so very much, Dr. Chandra.

I am grateful to all the members of Water Innovation Lab, McGill University, for their support and motivation throughout my study. I say a very big thank you to Wendy Ouellette, Yari Aghil, Divya Gupta, Naresh Gaj, Genevieve Grenon, Naeem Abbasi, Bhesram Singh, Mfon Essien, Kosoluchukwu Ekwunife, Aidan De Sena, Naresh Arumugagounder Thangaraju, Harsimar Sidana, Anshika Jain, and Rebecca Seltzer.

I also appreciate Kenton Ollivierre for his help and support during my field and greenhouse experiments. Many thanks to Michael Bleho and Guy Rimmer Plant Science Department, Macdonald Campus of McGill University, for providing technical assistance during my greenhouse and field experiments. A very big thank you to Wayne Palichuk, for allowing us to use his field for my drone experiment. Thank you to Dr. Michael Ngadi, Dr. Christopher Nzediegwu, Ms. Nathalie Beaudry, and my numerous friends on campus for their support during this program.

Special thanks to my parents and siblings for their love, support, prayers, and encouragement during the pursuit of my doctoral degree. A million thanks to my lovely wife, Ifeoma Juliet Ihuoma, for her understanding, prayers, inspiration, and support during my studies. Ekene diri Chukwu maka nwa m nwoke, Chinaraekene Jeffrey Ihuoma, onye amuru otu izu mmechara Ph.D. m.

Above all, I remain highly indebted to God Almighty for making my Ph.D. dream a reality.

Contributions of the Authors

Samuel Onyekachi Ihuoma is the principal author of this work which was supervised by Dr. Chandra A. Madramootoo, James McGill Professor, Department of Bioresource Engineering, McGill University, Sainte-Anne-de-Bellevue, Quebec, Canada. All the research protocols were jointly designed by Samuel and Dr. Chandra. Samuel executed all the greenhouse and field experiments and drafted the manuscripts while Dr. Chandra reviewed and edited the manuscripts. The authors of all the scientific papers in this thesis are Samuel O. Ihuoma and Chandra A. Madramootoo. Dr. Margaret Kalacska, Applied Remote Sensing Laboratory, Department of Geography, McGill University, contributed to the last paper. Details of the papers from this thesis are provided below.

A. Manuscripts

1. **Ihuoma, S. O.,** Madramootoo, C. A., 2017. Recent advances in crop water stress detection. *Computers and Electronics in Agriculture,* 141, 267–275.
2. **Ihuoma, S. O.,** Madramootoo, C. A., 2019. Crop reflectance indices for mapping water stress in greenhouse-grown bell pepper. *Agricultural Water Management,* 219, 49–58.
3. **Ihuoma, S. O.,** Madramootoo, C. A., 2019. Sensitivity of spectral vegetation indices for monitoring water stress in tomato plants. *Computers and Electronics in Agriculture*, 163, 104860.
4. **Ihuoma, S. O.,** Madramootoo, C. A., 2019. Narrow-band reflectance indices for mapping the combined effects of water and nitrogen stress in tomato crops. *Biosystems Engineering, 192, 133 - 143*.

5. **Ihuoma, S. O.,** Madramootoo, C. A., Kalacska, M., 2019. Integration of satellite imagery and spatially-variable soil moisture data for estimating irrigation water requirements in high value processing crops (To be submitted).

B. Papers presented at conferences

1. **Ihuoma, S. O.,** Madramootoo, C. A., Sensitivity of Spectral Vegetation Indices for Monitoring Water Stress in Greenhouse Grown Tomato Plants. Annual International Meeting of American Society of Agricultural and Biological Engineers. July 2017.
2. **Ihuoma, S. O.,** Madramootoo, C. A., Integration of multispectral and thermal data for mapping crop water stress. The 14th International Conference on Precision Agriculture. June 2018.
3. **Ihuoma, S. O.,** Madramootoo, C. A., Spectral vegetation indices for mapping the combined effects of water and nitrogen stress. Annual International Meeting of American Society of Agricultural and Biological Engineers. July 2018.
4. **Ihuoma, S. O.,** Madramootoo, C. A., A comparison of UAVs and remote sensing to schedule irrigation for high-value processing crops. Annual International Meeting of American Society of Agricultural and Biological Engineers. July 2019.

Table of Contents

List of Figures

List of Tables

List of Abbreviations

A	Area
ANOVA	One-way Analysis of variance
CO_2	Carbon (IV) oxide
CWSI	Crop Water Stress Index
DACT	Degrees Above Canopy Threshold
DANS	Degrees Above Non-Stressed
DW	Dry weights
ET	Evapotranspiration
ETa	Actual evapotranspiration
ETc	Crop evapotranspiration
ETo	Reference evapotranspiration
EWT	Equivalent Water Thickness
EWT_{canopy}	Equivalent Water Thickness, at the canopy level
FAO	Food and Agricultural Organisation
FC	Field capacity
FW	Fresh Weights
GLM	General Linear Model
GNDVI	Normalized difference vegetation index on greenness
Gs	stomatal conductance
GVI	Green vegetation index
IWUE	Irrigation Water Use Efficiency
Kc	crop coefficient

Kcb	Basal crop coefficient
Ke	Soil evaporation
Ks	Stress coefficient
LAI	Leaf Area Index
LCC	Leaf chlorophyll content
LSD	Least Significant Difference
METRIC	Mapping EvapoTranspiration at High Resolution with Internalized Calibration
MODIS	Moderate-resolution Imaging Spectroradiometer
NDVI	Normalized Difference Vegetation Index
NDWI	Normalized Difference Water Index
NIR	Near Infrared
N-P-K	Nitrogen-Phosphorus-Potassium
OLS	Ordinary Least Square
OMAFRA	Ontario Ministry of Agriculture, Food and Rural Affairs
OSAVI	Optimized Soil Adjusted Vegetation Index
P	Precipitation
PM	Penman-Monteith
PRI	Photochemical Reflectance Index
PRI	Photochemical Reflectance Index
PRInorm	Normalised Photochemical Reflectance Index
P_{tot}	Gross monthly precipitation
RDVI	Renormalized Difference Vegetation Index
Re	Effective rainfall

RWC	Relative Water Content
SEB	Surface energy balance
SEBAL	Surface Energy Balance Algorithm for Land
SMC	Volumetric soil moisture content
SR	Surface runoff
SRWI	Simple Ratio Water Index
SWIR	Short Wave Infrared
Ta	Air Temperature
Tc	Canopy temperature
TCARI	Transformed Chlorophyll Absorption in Reflectance Index
TDR	Time Domain Reflectometers
Tdry	Water-stressed canopy Temperature
Tnws	Non-water stressed canopy Temperature
TTT	Time-Temperature Threshold
TW	Turgid Weight
UAS	Unmanned Aircraft Systems
UAVs	Unmanned Aerial Vehicles
USDA	United States Department of Agriculture
VIs	Vegetation indices
VIS	Visible light
GR	Groundwater recharge
W	Soil water content
WI	Water index

CHAPTER I

General Introduction

1.1. Background of the study

Vegetable crop production is an essential component of Canada's agricultural industry and is largely dependent on irrigation for its viability. The major vegetables grown in Canada include tomato, bell pepper, cucumber, and sweet corn, and they are highly sensitive to water stress (Ferrara et al., 2011, Yildirim et al., 2012). The crops require supplemental irrigation to offset the deficiencies in rainfall and high evaporative demand during the growing season, to sustain high production levels. However, irrigated agriculture faces tremendous uncertainty in water supply due to prolonged drought associated with climate change, as well as increased competition from environmental, municipal and industrial water needs (DeJonge *et al.,* 2015). Within the past few years, nearly a third of the Canadian communities have faced threats to the security of the quantity or quality of their water supply (Aladenola and Madramootoo, 2014). Some important agricultural regions in Canada are already water-stressed, and there are growing concerns about water quality in agricultural lands (Stewart et al., 2011). Previous studies have shown that water stress adversely affects physiological and nutritional development, and yield of vegetable crops (Kirnak et al., 2003). Therefore, regular assessment of plant water status is required to properly manage irrigation and optimize agricultural water use.

1.2. Problem statement

Conventional irrigation applications rely mostly on soil moisture measurements and estimates of meteorological variables to assess water loss from the plant-soil-continuum (Ihuoma and Madramootoo, 2017). These measurements are invasive, laborious, and time-consuming, and are affected by spatial heterogeneity of soil and crop parameters. Irrigation scheduling can be improved by monitoring the plant water status directly, rather than depending only on soil water content measurements (Jones, 2007). Water stress induces stomatal closure, which reduces the transpiration rate, thus decreasing evaporative cooling and increasing leaf temperature. The increase in leaf temperatures as a result of water deficit was measured using thermal infrared thermometers (Idso et al., 1981, Jackson and Center, 1981).

The Photochemical Reflectance Index (PRI), an index sensitive to the epoxidation state of the xanthophyll cycle pigments and to photosynthetic efficiency, has been identified as a pre-visual indicator of water stress and serves as a proxy for water stress detection (Gamon et al., 1992). The functional basis of the PRI is related to its sensitivity to rapid changes in carotenoids through the de-epoxidation of the xanthophyll pigments (Gamon et al., 1992, Magney et al., 2016) and to heat dissipation increasing under water stress conditions (Panigada et al., 2014). Several other reflectance indices, such as Normalized Difference Vegetation Index (NDVI), Normalised PRI (PRInorm), Water index (WI), etc., obtained from UAVs have been suggested for detecting water stress in various crops (Ihuoma and Madramootoo, 2017).

Presently, only a few studies have focused on the use of vegetation indices (VIs) from remote sensing imagery to detect early stages of water stress for improving irrigation scheduling (Suárez et al., 2010, Zarco-Tejada et al., 2012, Rossini et al., 2013, Panigada et al., 2014, Magney et al., 2016). Although the VIs threshold for water stress detection is crop-specific, most of the recent studies only focused on different species of tree and cereal crops. The use of narrow-band optical indices for detecting crop abiotic stress in greenhouse and field-grown vegetables has not been extensively investigated in water-stressed regions and environments. Monitoring plant stress from vegetation indices, acquired from proximal and remote sensing platforms, presents an opportunity to better assess crop health status on a near real-time basis to improve agricultural productivity.

1.3. Research Objectives

The overall objective of this research was to develop an approach to crop stress management based on spectral reflectance data for precision irrigation of vegetable crops**.** The study focused on the use of spectral vegetation indices to provide a better estimate of plant stress for improving agricultural water management.

The overall objective was achieved through the following **specific objectives**:

i. Evaluate various spectral reflectance indices for detecting crop water stress in high-value vegetable crops.
ii. Identify suitable vegetation indices for mapping the combined effects of water and nitrogen stress in vegetable crops at different growth stages.
iii. Assess the suitability of Unmanned Aerial Vehicles, PlanetScope and Sentinel-2A & 2B imagery for estimating crop coefficient, evapotranspiration, and irrigation water requirements of high-value vegetable crops.

Connecting text

Chapter II contains an extensive literature review, which reviewed the concept of spectral reflectance indices for assessing plant abiotic stress. The review outlined recent developments in monitoring crop stress and the constraints experienced. It concluded with the future research needs and perspectives that formed the core of this research.

A version of this literature review titled, *"Recent advances in crop water stress detection"*, has been published as a review paper in *Computers and Electronics in Agriculture*. The manuscript is co-authored by Dr. Chandra A. Madramootoo, my supervisor. In order to ensure consistency with the thesis format, the original draft has been modified, and the cited references are listed in the reference section.

Chapter II

Literature Review

Recent advances in crop water stress detection

2.1. Abstract

In order to meet the demand for increased global food production under limited water resources, the implementation of suitable irrigation scheduling technique is crucial, particularly in irrigated basins experiencing water stress. Optimizing water use in agriculture requires innovations in detection of plant water stress, at various stages of the growing season to minimize crop physiological damage, and yield loss. Remotely sensed plant stress indicators, based on the visible and near-infrared spectral regions, have the advantage of high spatial and spectral resolutions, low cost, and quick turnaround time. This paper outlines recent developments in monitoring crop water stress, for scheduling irrigation, some of the constraints experienced, and future research needs.

Keywords: Plant water stress, irrigation scheduling, remotely sensed, spatial resolution, spectral region.

2.2. Introduction

Irrigated agriculture is essential to global food production, utilizing only 20% of cultivated land to provide 40% of the world's food supply (Garces-Restrepo et al., 2007). However, climate change, increasing worldwide shortages of water, frequent droughts, and global warming (Hirich et al., 2016) are threatening the reliability of irrigation water supplies. While the human population and demands for freshwater resources are increasing, drought and regular water scarcity can put global food security at risk (Lei et al., 2016), by severely disrupting agricultural production. The challenge is to meet rising productivity demands by improving methods of crop management

(Behmann et al., 2014), and this requires a deeper understanding of plant response to abiotic stresses.

Conventional methods for monitoring crop water stress rely on in situ soil moisture measurements and meteorological variables to estimate the amount of water lost from the plant-soil system during a given period (González-Dugo et al., 2006). Regular sampling of soil to assess water depletion from the plant root zone assumes that the water holding capacity of the entire soil is uniform, so only a few point measurements are used to represent water retention characteristics (Clarke, 1997). The method is time consuming, assumes uniform plant density, and the same rate of transpiration, over an entire field, which is rarely the case. Similarly, evapotranspiration models assume a freely transpiring reference crop with uniform cover and soil type within a field. These methods are time consuming and produce point information that give poor indications of the overall status of the field. Other methods of detecting plant water status involve soil water balance calculations, direct and indirect measurement of plant water status, via stomatal conductance and leaf water potential. These approaches, though reliable, are labour intensive, destructive, and unsuitable for automation, due to heterogeneity of soil and crop canopy.

In order to increase water savings and enhance agricultural sustainability, implementation of suitable irrigation scheduling methods is essential (Osroosh et al., 2015), and requires early detection of water stress in crops, before it causes irreversible damage and yield loss. Recently, studies have focused on the use of remotely sensed data as an alternative to traditional field measurements of plant stress parameters, as this provides information about the spatial and temporal variability of crops (Dangwal et al., 2015; Leroux et al., 2016; Panigada et al., 2014; Rossini et al., 2013; Suárez et al., 2010; Zarco-Tejada et al., 2013; Zhao et al., 2015). Spectral reflectance indices obtained from high resolution hyperspectral sensors, onboard small Unmanned Aircraft Systems (sUAS), can be used in precision agriculture for monitoring crop water status and scheduling irrigation (Berni et al., 2009a, 2009b; Gago et al., 2015). However, due to several confounding factors affecting the vegetation indices (VIs) at the canopy and landscape scales, and that the threshold for water stress detection is crop specific, a general agreement for their use as a pre-visual indicator of water stress is yet to be achieved. This paper reviews the recent advances in crop water stress detection that can potentially be applicable to improve irrigation scheduling of vegetable crops and aims to identify the most promising approach for large-scale application.

2.3. Plant response to water stress

Crop water stress is a deficiency in water supply, detected as a reduction in soil water content or from the physiological responses of the plant to water deficit. Plants absorb root zone soil water to meet their evapotranspiration needs, and this depletes soil available water. Under limiting soil moisture conditions, chemical and hydraulic signals are transmitted to the plant leaf through xylem pathways (Limpus, 2009), which leads to physiological responses such as stomatal closure and reductions in photosynthesis rate. Wang et al. (2015) indicated that water stressed crops have reduced evapotranspiration, and manifest other symptoms such as leaf wilting, stunted growth, and leaf area reduction. Also, water stress adversely affects the physiological and nutritional development of crops, leading to reduced biomass, yield, and quality of crops (Aladenola and Madramootoo, 2014; Rossini et al., 2013; Zhang et al., 2017a, 2017b). Plant water status measures the response of a plant to the combined effects of soil moisture availability, evaporative demand, internal hydraulic resistance, and uptake capacity of the plant-root interface. It is a more sensitive indicator of stress than soil moisture (Jones, 2010). Plant response to water stress depends on environmental conditions and crop evapotranspiration needs, as irrigation must replenish soil moisture deficit from evapotranspiration losses. FAO-56 defines the irrigation water requirement for a well-watered crop as water loss through evapotranspiration of a disease-free crop under nonlimiting soil conditions (Allen et al., 1998). Measures of plant water status are required to better understand the mechanisms of plant response and adaptation to water stress, and for the optimisation of crop production (Osakabe et al., 2014), through precision irrigation.

Similarly, evapotranspiration (ET) models are used to predict how changes in weather parameters can affect plant water status (Osroosh et al., 2016). The frequently used ET models are the Penman-Monteith (PM) (Allen et al., 1998) and Hargreaves (Hargreaves and Samani, 1985) equations. The Hargreaves model needs fewer data than the PM model and can estimate ET using air temperature as only input. Other researchers have used the CROPWAT-8, which is based on the Penman-Monteith method, to assess reference evapotranspiration (ETo), crop evapotranspiration (ETc), and irrigation water requirements (Bouraima et al., 2015; Patel et al., 2017; Surendran et al., 2017). The most common and practical approach widely used for estimating crop water requirement, and the operational monitoring of soil-plant water balance is the FAO-56 method. In the FAO-56 approach, crop evapotranspiration is estimated by the combination of ETo and crop coefficients.

There are two different FAO-56 approaches: single and dual crop coefficients. The single crop coefficient approach is used to express both plant transpiration and soil evaporation combined into a single crop coefficient (Kc). The dual crop coefficient approach uses two coefficients to separate the respective contribution of plant transpiration (Kcb) and soil evaporation (Ke), each by individual values (Allen et al., 2005). Kcb is multiplied by water stress coefficient (K_s) (range 0 -

1) to account for the reduction of ET due to soil moisture depletion. It has been shown that K_s is related to crop water stress index (CWSI) according to Eq. (2.1).

$$K_s = 1 - CWSI \quad \text{...} \quad (2.1)$$

Several researchers have evaluated the accuracy of water stress coefficient methods for estimating crop ETc under different levels of deficit irrigation. For instance, Bausch et al. (2011) successfully used a ratio of canopy temperature (Tc) as a substitute for the soil moisture-based Ks. Kullberg et al. (2017) observed that using appropriate Ks method has the potential to improve irrigation scheduling to properly manage stress and ensure optimum crop yield under limited irrigation water supply. The main methods that are used for monitoring plant water stress have been summarized in Table 2.1 and are discussed below.

2.4. Plant-based approach

Stress quantification from plant-based approaches include the direct measurement of leaf water potential with a pressure chamber (Scholander et al., 1965). Leaf water potential is assumed to represent the mean soil water potential next to the plant roots (Ameglio et al., 1999), and provides good indication of leaf water status. It is widely adopted for scheduling irrigation in various crops (Alchanatis et al., 2010; Ameglio et al., 1999; Bellvert et al., 2016; Zarco-Tejada et al., 2012). However, the approach is slow and destructive, with limited temporal and spatial resolution, and is not suitable for strongly isohydric crops, which maintain a stable leaf water status over a wide range of evaporative demand or soil water supplies (Limpus, 2009). The amount of water in plant leaves can be measured by laboratory analysis, using Relative Water Content (RWC) and Equivalent Water Thickness (EWT) (Colombo et al., 2011). The EWT is the hypothetical thickness of a single layer of water averaged over the whole leaf area and can be computed in laboratory by measuring Fresh Weights (FW) and Dry weights (DW) and the one-sided leaf Area (A), as shown in Eq. (2.2).

$$ETW = \frac{FW - DW}{A} \text{ .... (2.2)}$$

At the canopy level, Equivalent Water Thickness (EWT_{canopy}) (shown in Eq. (2.3)) can be obtained by scaling the EWC with Leaf Area Index (LAI), defined as the one-sided green leaf area per unit ground surface area (LAI = leaf area/ground area, cm^2/cm^2).

$$EWT_{canopy} = LAI * EWT \text{ .... (2.3)}$$

The RWC compares the water content of a leaf with the maximum water content at full turgor and can be considered as an indicator of vegetation status. It can be obtained from laboratory measurements of leaf weight and leaf Turgid Weight (TW) according to the following expression:

$$RWC = \frac{FW - DW}{TW - DW} * 100(\%) \text{.................................. (2.4)}$$

The RWC reflects the balance between water supplied to the leaf tissue and transpiration ratio, and indicates the amount of water present at the time of sampling relative to the amount of water in a saturated leaf. Both RWC and EWC are good indicators of plant water status and have been successfully used for scheduling irrigation in various crops (Danson et al., 1992; Jones, 2004; Panigada et al., 2014; Wang et al., 2015). The approaches require less sophisticated equipment but are also destructive and time consuming.

Table 2. 1**.** A summary of the methods for monitoring plant water stress, indicating their main advantages and disadvantages.

Methods	Description	Advantages	Disadvantages
1. Soil water measurement			
(a) Gravimetric method	Sampling of soil, which is weighed, oven-dried and reweighed to estimate the amount of water lost from the plant-soil system.	It is reliable and serves as a guide on the amount of water to apply during irrigation.	The method is labour intensive, destructive, and time consuming.
(b) Soil moisture sensors			
(I) Neutron probe	Based on the emission of high energy neutrons by a radioactive source into the soil.	Fast, non-destructive, and repetitive.	Requires adequate operator training, storage, licencing, and inspection, due to its radioactive source.
(II) TDR and FDR	Based on the difference between the dielectric constant of water and soil.	Precise and easy to apply in practice. Estimates soil water levels at different depths along the soil profile. Readings can be logged automatically.	Several sensors are required for an entire field. High cost of installation of sensors.
(III) Tensiometers	Measures soil water potential	Easy to use for irrigation scheduling.	Useful in coarse textured soils or in high frequency irrigation only. Used for a narrow range of available soil water.
2. Soil water balance approach	Indirect estimate of soil moisture status based on soil water balance calculations.	Good indicator of the amount of irrigation water and easy to apply.	Not very accurate and requires calibration with actual soil measurements. Requires estimate of evaporation, rainfall, and irrigation events.

3. Plant-based approaches			
(a) Stomatal conductance	Indirect indicator of plant water stress by measuring the stomata opening.	Good measure of plant water status. Used as benchmark for most research studies.	Labour intensive and unsuitable for automation and commercial application. Not very accurate for anisohydric crops.
(b) Leaf water potential	Direct measurement of leaf water content.	Widely accepted reference technique.	Slow, destructive, and unsuitable for isohydric crops.
(c) Relative water content	Direct measurement of leaf water status.	Good indicator plant water status, requiring less sophisticated equipment.	Destructive and time consuming.
(d) Sap flow measurement	Measures the rate of transpiration through heat pulse.	Sensitive to stomatal closure and water deficits. Adapted for automated recording and control of irrigation systems.	Needs calibration for each tree and is difficult to replicate. Requires complex instrumentation and expertise.
(e) Stem and fruit diameter	Measures fluctuation in stem and fruit diameters in response to changes in water content.	Sensitive measure of plant water stress.	Not useful for the control of high-frequency irrigation systems.
4. Remote sensing methods			
(a) Infrared thermometry	Measures canopy temperature, which increases as a result of water stress.	Reliable and non-destructive.	Based on only a few point measurements. Does not account for soil and crop heterogeneity.
(I) CWSI	Uses the difference between canopy and air temperatures to quantify crop water stress.	Sensitive to stomatal closure and crop water deficit.	Influenced by cloud cover, requires different baselines for different crops.

(II) DANS, DACT, and Tc ratio	Measure single canopy temperature for quantifying water stress.	Require less data than CWSI for detecting water stress. Tc ratio gives quantitative water stress coefficient (Ks) for calculating crop ET.	Difficult to scale up to large cropped fields.
(b) Spectral vegetation indices			
(i) Structural indices	Measures reflectance indices within the VIS and NIR spectral range (NDVI, RDVI, OSAVI, TCARI) to indicate canopy changes due to water stress.	Non-destructive with high temporal and spectral resolution.	Requisite image analysis is still a challenging task. Precision reduces from leaf scale to canopy scale.
(ii) Xanthophyll indices	Measures PRI and PRI_{norm}, which are sensitive to the epoxidation state of the xanthophyll cycle pigments.	Account for physiological changes in photosynthetic pigment changes due to water stress.	More work is needed to convert raw imagery to user-friendly irrigation application.
(iii) Water indices	Measures the reflectance trough in the near-infrared region (WI, SRWI, and NDWI) used to represent canopy moisture content.	Rapid and non-destructive measure of leaf water content.	Problem of scaling up to canopy level.

Several other approaches are available that give indirect indications of stress such as measurement of stomatal conductance (Agam et al., 2013; Ballester et al., 2013; Lorenzo-Minguez et al., 1985; Maes et al., 2011), measurement of fruit and stem diameter (Gallardo et al., 2006; Huguet et al., 1992), and sap-flow measurement (Giorio and Giorio, 2003; Granier, 1987; Singh et al., 2010). Most plants exercise some measure of control over their leaf water status, by minimizing changes in leaf water status as the soil dries, through stomatal closure. Therefore, stomatal conductance is a very sensitive plant response to soil water deficit (Jones, 2004), except for some anisohydric species, which have less effective control of leaf water status under declining soil moisture conditions. The recognition that water stressed plants tend to close their stomata, which leads to increase in leaf temperature, has been used to develop thermal sensing methods, for the detection of plant stress (Idso et al., 1981). The approach provides a good indication of irrigation needs in many crops. However, measurements of stomatal conductance are tedious, and large leaf-to-leaf variation of the plant canopy requires much replication to obtain reliable data for irrigation scheduling.

The sap flow technique is used to assess transpiration rates of plants, by measuring the rate at which sap ascends stems using heat pulse. In this approach, short pulses of heat are applied in the stem, and the mass flow of sap is determined from the velocity of the heat pulses moving along the stem. The changes in transpiration rate indicated by sap flow are mainly determined by changes in stomatal opening. Singh et al. (2010) used sap flow sensors to schedule irrigation in corn field, but noted that the approach only gives indirect estimates of changes in conductance, as flow is also dependent on atmospheric conditions such as humidity. Therefore, changes in sap flow can occur without changes in stomatal aperture. Several other studies used sap-flow measurement for irrigation scheduling and control in a diverse range of crops, including grapevine (Eastham and

Gray, 1998), fruit and olive trees (Ameglio et al., 1999; Giorio and Giorio, 2003) and even greenhouse crops (Ehre et al., 2001), with varying degrees of success. However, Jones (2004) stated that sap flow method requires a heat source, complex instrumentation, technical expertise, and needs calibration for each crop and for definition of irrigation control thresholds.

The use of plant-based indicators for irrigation scheduling requires the definition of threshold values, beyond which irrigation is essential. Therefore, it is important to regularly check the plant water status to avoid exceeding the reference values (Ballester et al., 2013). The threshold values, which are determined for plants growing under a well-watered condition, are difficult to obtain in a changing environment (Fereres and Goldhamer, 2003). Another limitation of plant-based approaches is that they do not usually provide information on the quantity of irrigation water to apply at any time, but only indicates that irrigation is required. This implies that soil moisture measurements or other estimation procedures are needed to determine the quantity of water to apply to optimize crop water use (Stockle and Dugas, 1992). A general drawback of both direct measurements of soil water status and plant-based approaches is the costs of installation of sensors or the difficulty with obtaining representative measurements, with single point sampling that would adequately account for soil and crop heterogeneity (Ballester et al., 2013; Jones, 2012).

2.4.1. Environmental canopy sensing

Infrared thermometry and thermal imagery, along with additional environmental measurements, have been acknowledged as an alternative approach to soil moisture-based methods of plant water stress detection (Berni et al., 2009a; Cohen et al., 2005; Jones, 2010; Osroosh et al., 2015). Water stress detection based on canopy temperature measurements is probably the most widely used plant-based approach for remote sensing that is applicable to irrigation scheduling of several crops.

As plants absorb solar radiation, canopy temperature increases, but is cooled when that energy is used for evapotranspiration.

Water stressed plants have reduced transpiration and higher leaf temperature compared to non-stressed crops. González-Dugo et al. (2006) used variability of canopy temperature to indicate water stress, and emphasised the need to quantify the complex relationship between canopy temperature, water stress, and spatial water availability. Collaizzi et al. (2012) revealed that canopy temperature-based algorithms are strongly correlated to crop outputs such as yield, water use efficiency, irrigation rates, seasonal evapotranspiration, and midday leaf water potential. Many indices have been established for evaluating water stress using infrared canopy temperature (Idso et al., 1981; Jones, 2004; Nielsen and Gardner, 1988; Osroosh et al., 2015; O'Shaughnessy et al., 2012; Payero and Irmak, 2006). Most of the indices use crop canopy temperature as a main driver for evaluation, typically as a single daily measurement at an assumed peak stress time, or by evaluating time above a temperature threshold. The approach is sensitive to small stresses, and relies on stomatal closure as an early indicator of water deficits.

2.4.2. Canopy temperature-based crop water stress index (CWSI)

The CWSI derived from canopy temperature has been largely adopted as a tool to indicate plant water status and schedule irrigation in many crops (Aladenola and Madramootoo, 2014; Alchanatis et al., 2010; Bellvert et al., 2016; Yildirim et al., 2012). CWSI theory is based on the principle that transpiration cools the leaf surface and as root zone soil moisture is depleted, stomatal conductance and transpiration decrease and leaf temperature increases. The concept of using CWSI for improving irrigation scheduling gained popularity when Idso et al. (1981) observed a linear relationship between canopy temperatures measured using infrared thermometry and air temperature and vapour pressure deficit, and developed an empirical method of quantifying crop water stress. The empirical CWSI (Eq. (2.5)) uses two baselines. The lower baseline represents canopy Temperature (Tc) minus air Temperature (Ta) of a well-watered crop transpiring at maximum potential rate and the upper baselines represents (Tc–Ta) of a non-transpiring crop.

$$CWSI = \frac{[(T_c - T_a) - (T_{nws} - T_a)]}{[(T_{dry} - T_a) - (T_{nws} - T_a)]} \quad \text{.................................} \quad (2.5)$$

where, Tc: canopy Temperature (°C), Ta: air Temperature (°C), Tnws: non-water stressed canopy Temperature (°C), and Tdry: water-stressed canopy Temperature (°C).

Within the past few years, there have been improvements in the use of CWSI for monitoring water stress and scheduling irrigation in different crops (Berni et al., 2009a, 2009b; Gonzalez-Dugo et al., 2014; O'shaughnessy et al., 2011; Paltineanu et al., 2013). O'Shaughnessy et al. (2012) incorporated a Time-Temperature Threshold (TTT) into a theoretical index (CWSI-TTT), and used it to successfully automate irrigations of grain sorghum. The study however, reported an under-irrigation problem during the growing season, caused by cloud cover and the influence of changing crop aspect on infrared thermometer measurements. Osroosh et al. (2015) developed an adaptive irrigation scheduling algorithm relying on a theoretical CWSI. This, unlike the traditional CWSI algorithm where the threshold is a constant value, uses a dynamic threshold determined by following the CWSI trend. However, large discrepancies in their thermal readings, attributed to infrared thermal and microclimatic measurements, resulted in dissimilar values of measured temperature and midday CWSI.

Recent studies have evaluated additional indices based on infrared thermometry that require less information than CWSI for detecting crop water stress. Bausch et al. (2011) investigated the use of a ratio of canopy temperature (Tc ratio) measured over fully irrigated and water-stressed corn as a substitute for the Ks presently used in the reference ET-crop coefficient. The result indicated that the Tc ratio is a reasonable quantitative estimate of Ks for calculating crop ET under water stress conditions and that the ratio allows application of the crop coefficient method for scheduling deficit irrigation. Taghvaeiana et al. (2014) indicated that the Degrees Above Non-Stressed (DANS), which is based solely on canopy temperature, was effective in monitoring water stress and scheduling irrigations in deficit-irrigated sunflower in arid/semi-arid regions. DeJonge et al. (2015) recommended the Degrees Above Canopy Threshold (DACT) as a suitable index that requires a single canopy temperature measurement for quantifying water stress in maize. Kullberg et al. (2017) compared four thermal remote sensing indices based methods for estimating crop evapotranspiration coefficients: CWSI, DANS, DACT, Tc ratio, and observed that thermal indices DANS and DACT are responsive to crop water stress, comparable to more data intensive methods such as CWSI.

While canopy temperature measurements by infrared thermometers are reliable and non-invasive (Cohen et al., 2005), they are usually based on only a few point measurements. Therefore, uniformity of soil water content and of plant canopy for large areas is assumed. Most researchers, however, assume that weather conditions are constant if the measurements required to locally calibrate the baselines are made close to solar noon and under clear sky conditions. This assumption is problematic because weather conditions change with location, time of day and day of the year, and the baselines for the same crop will consequently change with weather conditions (Payero and Irmak, 2006). Researchers from different places have, therefore, reported different baselines for the same crop (Idso et al., 1981; Irmak et al., 2000; Nielsen and Gardner, 1988;

Payero and Irmak, 2006; Steele et al., 1994; Yazar et al., 1999). The lack of transferability of the baselines, together with the restriction of having to make required measurements close to solar noon and under clear sky conditions, are major drawbacks of using the empirical CWSI method for irrigation scheduling (Alves and Pereira, 2000).

2.5. Remote sensing methods

Even though the usefulness of canopy temperature, measured from infrared thermometry, has been established in several studies for monitoring plant water stress, there are physiological and operational concerns that support the development of alternative narrow-band indices, based on the visible and red edge spectral region for detecting water stress in crops (Berni et al., 2009b; Dangwal et al., 2015; Panigada et al., 2014; Rossini et al., 2013; Wang et al., 2015; Zarco-Tejada et al., 2013; Zhao et al., 2015). In some plants, the diurnal fluctuations in stomatal conductance are such that the relationships between canopy temperature and stress levels are not clear-cut. An increase in evaporative demand due to high vapor pressure deficits induces a constant decline in leaf conductance, even when the crops are well watered (Zarco-Tejada et al., 2012). Again, monitoring of large cropped fields requires appropriate imagery at high spatial and spectral resolutions, as well as short revisit periods (Berni et al., 2009b). Although the use of remote sensing in agriculture was proposed few decades ago, it has not been widely adopted until recently, mainly because of the widespread adoption of emerging technologies that integrate high-resolution thermal cameras on board UAS (Berni et al., 2009a; Elston, 2016; Suárez et al., 2010; Zarco-Tejada et al., 2013). The potential applications of UAS in agriculture include; crop scouting, mapping canopy coverage, determining plant stresses, measuring soil moisture, managing variable-rate irrigation, and crop yield estimation (Ehsani et al., 2016).

Recent researchers have proposed the integration of remotely sensed data with soil water balance method to improve irrigation water management. For instance, Campos et al. (2016) estimated total available water in soil by integrating evapotranspiration data and multispectral imagery. Filion et al. (2016) used remotely sensed image to map soil moisture in the Mediterranean regions to support water management and agricultural practice. Zhang et al. (2017a, 2017b) integrated airborne imagery data into a soil water balance model to improve the estimation of soil water deficit for maize and sunflower grown under full and deficit irrigation treatments. Therefore, UAS will be a vital tool for growers soon, because they can cover large areas, and take advantage of new sensing, mapping and data analytic technologies. Image resolution is improving, and costs are also decreasing with time. Real time mapping and rapid image analysis also provide for early detection of plant water stress for timely irrigation scheduling, due to the potential to scale up information from the leaf to canopy/field levels (Gago et al., 2015).

2.5.1. Spectral reflectance indices

The focus on indicators other than thermal infrared indices for monitoring water stress is because leaf temperature, though a direct indicator of plant transpiration, does not directly account for other physiological changes such as photosynthetic pigment changes or non-stomatal reductions of photosynthesis under water stress conditions (Zarco-Tejada et al., 2013). The spectral vegetation indices that have been correlated to plant water stress are given in Table 2.2. These indices are classified into three; the xanthophyll, structural/greenness, and water indices.

2.5.1.1. Xanthophyll indices

The Photochemical Reflectance Index (PRI) (Gamon et al., 1992), and solar-induced chlorophyll fluorescence emission (Flexas et al., 2002; Moya et al., 2004), are pre-visual indicators of water stress which serve as an indirect means for water stress detection (Berni et al., 2009b; Suárez et al., 2010). The PRI is sensitive to the epoxidation state of the xanthophyll cycle pigments and to photosynthetic efficiency (Gamon et al., 1992; Suárez et al., 2010). The functional basis of the PRI is based on its sensitivity to rapid changes in carotenoids through the deepoxidation of the xanthophyll pigments (Magney et al., 2016), and to heat dissipation increasing under water stress conditions (Panigada et al., 2014). When the light absorbed by plants exceeds their photosynthetic demand, energy dissipation occurs to avoid damage to the tissues (Rossini et al., 2013). The plants dissipate this excess energy non-destructively through re-emission of photons as fluorescence (radiative dissipation), and by conversion of light energy into heat in the pigment bed (thermal dissipation). Previous studies have demonstrated that the interconversion of the xanthophyll cycle pigments can be detected in leaves as subtle changes in reflectance at 531 nm (Gamon et al., 1992, 1997).

Recently, researchers have shown the sensitivity of PRI for crop water stress detection over short time scales (Gamon et al., 1997; Suárez et al., 2009, 2010; Zarco-Tejada et al., 2012, 2013), whereas studies conducted over longer time scales reported contrasting results, at the leaf and canopy scales (Gamon, 2015; Magney et al., 2016; Rahimzadeh-Bajgiran et al., 2012). The studies generally observed that there are certain issues with the index, such as leaf biomass, background reflectance, sensor spectral responses, and viewing-illumination geometry effects. Therefore, different researchers proposed new formulations for the index, using alternative reference bands (Hernández-Clemente et al., 2011). Zarco- Tejada et al. (2012) obtained higher correlations in a citrus orchard with PRI515 for stomatal conductance (gs) and leaf water potential (W).

Table 2. 2. Spectral vegetation indices that has been correlated to plant water stress

Reflectance Indices		Formula	References	Plant Water Stress Indicators
Names	Abbreviations			
Xanthophyll indices				
Photochemical Reflectance Index	PRI	$\frac{(R_{570} - R_{531})}{(R_{570} + R_{531})}$	Gamon et al., 1992	Chlorophyll flourescence and Stomatal conductance.
Normalized Photochemical Reflectance Index	PRI_{norm}	$\frac{PRI}{[RDVI * \left({}^{R_{700}}/{}_{R_{670}}\right)]}$	Berni *et al.,* 2009	Chlorophyll flourescence and Stomatal conductance.
Structural indices				
Normalized Difference Vegetation Index	NDVI	$\frac{R_{800} - R_{670}}{R_{800} + R_{670}}$	Rouse et al., 1974	Stomatal Conductance, Leaf water potential
Renormalized Difference Vegetation Index	RDVI	$\frac{R_{800} - R_{670}}{\sqrt{R_{800} + R_{670}}}$	Rougean and Breon, 1995	Stomatal Conductance, Leaf water potential
Transformed Chlorophyll Absorption in Reflectance Index	TCARI	$3[(R_{700} - R_{670}) - 0.2(R_{700} - R_{550}) * (R_{700}/R_{670})]$	Haboudane et al., 2002	Stomatal Conductance, Leaf water potential

Optimized Soil Adjusted Vegetation Index	OSAVI	$\frac{(1+0.16)(R_{800} - R_{670})}{(R_{800} + R_{670}) + 0.16}$	Haboudane et al., 2002	Stomatal Conductance, Leaf water potential
	TCARI/OSAVI	$\frac{3[(R_{700} - R_{670}) - 0.2(R_{700} - R_{550}) * (R_{700}/R_{670})]}{(1+0.16)(R_{800} - R_{670})/(R_{800} * R_{670} + 0.16)}$	Haboudane et al., 2002	Stomatal Conductance, Leaf water potential
Water indices				
Normalized Difference Water Index	NDWI	$\frac{(R_{860} - R_{1240})}{R_{860} + R_{1240}}$	Gao et al., 1996	Leaf water potential
Simple Ratio Water Index	SRWI	$\frac{R_{860}}{R_{1240}}$	Zarco-Tejada et al., 2003	Leaf water potential
Water Index	WI	$\frac{R_{900}}{R_{970}}$	Zarco-Tejada et al., 2003	Leaf water potential

Where R represents the reflectances at the respective wavelengths, nm.

Panigada et al. (2014) showed a high correlation between PRI586 and EWTcanopy, for cereal crops. Berni et al. (2009a, 2009b) normalized the standard PRI using the Renormalized Difference Vegetation Index (RDVI), an index that is sensitive to canopy structure, and a red edge index that is sensitive to chlorophyll content (R700=R670). The new index (PRInorm) not only detects xanthophyll pigment changes as a function of water stress, but also normalizes for the chlorophyll content level and canopy leaf area reduction induced by stress. The PRInorm, showed an improved capacity for water stress detection (correlated with leaf stomatal conductance, gs and leaf water potential, Ψ) in comparison with other greenness and structural indices (Gago et al., 2015). Several other researchers have used the PRI and PRInorm for water stress detection as an alternative to thermal measurements, with varying degrees of success (Behmann et al., 2014; Cheng and Wang, 2014; Colombo et al., 2008; Dangwal et al., 2015; Meroni et al., 2008, 2009; Panigada et al., 2014; Peñuelas et al., 2011; Rossini et al., 2013; Suárez et al., 2009, 2010; Wang et al., 2015; Zarco-Tejada et al., 2009, 2013). Rossini et al. (2013) revealed the feasibility of mapping water stress using spectral vegetation indices, taking advantage of the high spatial resolution capabilities that are more difficult in the thermal region. The studies revealed the potential applicability of remote sensing data in precision agriculture for improving irrigation scheduling. Nevertheless, the sensitivity of PRI measured at the crop canopy level requires further investigation, including an assessment for a new index formulation for high value vegetable crops, in order to optimise yield and productivity.

2.5.1.2. Structural indices

Structural indices are based on the reflectance of leaves in the visible and near-infrared bands of the electromagnetic spectrum. The Normalized Difference Vegetation Index (NDVI) is the best known vegetation index, used as a numerical indicator of vegetation greenness (Leroux et al., 2016; Zhao et al., 2015). The NDVI is an indication of the amount of chlorophyll and fraction of green cover. It is used in irrigation studies for mapping of crop cover as a means for estimating crop coefficients (Kc) for use in the conventional FAO-56 method (Allen et al., 1998), and for irrigation scheduling (Jones, 2012). Previous studies have also shown that NDVI has a linear relationship with the basal crop coefficient for ET (Kcb), because Kcb primarily depends on the dynamics of plant canopies (cover fraction, LAI, greenness). Based on this, several researchers have used NDVI to predict Kcb for various agricultural crops (Allen et al., 2005; Choudhury et al., 1994; Irmak et al., 2011; Kamble et al., 2013; Kullberg et al., 2017; Jayanthi et al., 2000).

Roujean and Breon (1995) and Haboudane et al. (2002) showed that empirically derived NDVI products are unstable, because they are affected by soil reflectance and sun view geometry. In an attempt to improve NDVI, the Renormalized Difference Vegetation Index (RDVI), Optimised Soil Adjusted Vegetation Index (OSAVI), and Transformed Chlorophyll Absorption in Reflectance Index (TCARI), were developed to minimize soil brightness influences from spectral vegetation indices involving red and Near-Infrared (NIR) wavelengths and to reduce the variability of the photosynthetically active radiation due to the presence of diverse non-photosynthetic materials. Subsequently, TCARI/OSAVI was established (Haboudane et al., 2002) to make accurate predictions of crop chlorophyll content from hyperspectral remote sensing imagery. The ratio has been shown to be relatively insensitive to canopy cover variations, even for very low LAI values. Apart from their use in yield estimation, structural indices (NDVI, RDVI, OSAVI, TCARI, and TCARI/OSAVI) are useful in plant stress monitoring to capture the changes in canopy structures caused by water stress (Haboudane et al., 2002; Roujean and Breon, 1995; Zarco-Tejada et al., 2012), and this is due to their positive correlations with stomatal conductance and leaf water potential (Gago et al., 2015). For instance, NDVI and TCARI/OSAVI were clearly related to the stem water potential (Ψ_{stem}) and gs in vineyards cv. Tempranillo (Baluja et al., 2012). However, in Citrus orchards the indices were less correlated with gs (Zarco-Tejada et al., 2012). Usually, most structural indices are more related to plant vigor than the plant physiological status, and might correlate well in crops where the biomass proportionally increases in parallel to photosynthesis. While the studies demonstrated the feasibility of narrow-band indices obtained from hyperspectral sensors onboard UAVs for monitoring plant water stress, the results indicate that the sensitivity of the indices at the plant canopy level needs further study, before they could be adopted for precision irrigation water management.

2.5.1.3. Water indices

Typically, the water-absorption bands in the 1300–2500 nm region show the highest sensitivity to leaf water concentration in most crops (Carter, 1991). However, the absorption by water in this region is very strong, so that infrared bands are inadequate for measuring the water concentration of the plant canopies (Peñuelas and Filella, 1998). Therefore, a reflectance trough in the near-infrared region at 950–970 nm, corresponding to a weaker water absorption band has been shown to be effective for representing the total plant or canopy moisture content (Peñuelas et al., 1997). When plants are water stressed, the 970 nm trough of the reflectance spectrum tends to disappear and to shift towards lower wavelengths (Peñuelas and Filella, 1998), and this concept was used to develop a reflectance water index (WI) and simple ration water index (SRWI) (Zarco-Tejada et al., 2003). The reflectance at 900 nm is used as a reference because there is no absorption by water at this wavelength, but it is subjected to the same changes in sample structure as the reading at 970 nm. This water index has been found to be highly correlated with plant water content in several crops (Peñuelas et al., 1997; Dawson et al., 1999; Wang et al., 2015). Peñuelas et al. (1997)

observed a strong correlation between greenness and moisture content, and proposed the WI: NDVI ratio as a better indicator of canopy water content than the water index itself.

Gao (1996) used the Normalized Difference Water Index (NDWI) to monitor changes in water content of leaves using NIR (Near Infrared) and SWIF (Short Wave Infrared) at a wavelength of approximately 860 nm, and the other at 1240 nm, respectively. The SWIR reflectance reflects changes in both the vegetation water content and the spongy mesophyll structure in vegetation canopies, while the NIR reflectance is affected by leaf internal structure and leaf dry matter content but not by water content. The combination of the NIR with the SWIR removes variations induced by leaf internal structure and leaf dry matter content, thereby, improving the accuracy in retrieving the vegetation water content (Wang et al., 2015). However, Gao (1996) noted that NDWI is responsive to changes in water content of plant canopies, but is less sensitive to atmospheric aerosol scattering effects than NDVI. It is therefore, complementary to, not a substitute for NDVI. Nevertheless, previous studies have shown the relevance of water indices (WI; SRWI, NDWI, and WI/NDVI) for monitoring plant water stress in wheat and maize crops. For instance, Panigada et al. (2014) obtained a significant correlation between WI and EWTcanopy; Rossini et al. (2013) showed a high correlation between WI/NDVI and RWC; while Wang et al. (2015) obtained a good relationship between NDWI and leaf water content, and concluded that the narrow bands at 780 and 1750 nm are sensitive to the water parameters of spring wheat. The interest in reflectance indices is to use them to scale-up to satellite imagery since the use of thermal imagery is unreliable due to its poor resolution, which obtains mixed information from the plant and the soil background. The researchers showed the possibility of mapping plant water stress using hyperspectral indices, but observed that the translation of this finding in accurate irrigation scheduling requires further investigations.

2.5.2. Satellite imagery for assessing plant stress

Researchers highlighted the use of VIs (such as NDVI) derived from satellite imagery for assessing plant stress and for estimating crop evapotranspiration (ETc) and irrigation requirements (Calera et al., 2017; Vanino et al., 2018). This method relies on the relationship between VIs and crop coefficient (Kc), because Kc depends on dynamics of plant canopy cover. The major limitation on the use of this method for estimating actual crop evapotranspiration is the compromise between the revisit time and the spatial resolution of satellite sensors. Satellite images such as the Moderate-resolution Imaging Spectroradiometer (MODIS), with daily coverage have coarse spatial resolution (>250m), while the Landsat series, with medium spatial resolution (30 m) have long revisit times (16 days) (Rozenstein et al., 2018). Also, earth observation data are affected by cloud covers (Al Zayed et al., 2016), which further limits the use satellite imagery for operational applications in agriculture. Nevertheless, Sentinel-2A and 2B satellite platforms offer a combined spatial resolution of 10 m and revisit time of 5 days, which is suitable for routine crop stress assessment (Vanino et al., 2018). Investigating the spectral consistency of these Sentinel-2 data with field measurements, and assessing their suitability for estimating crop water requirements would be useful for developing operational tools to support agricultural water management.

2.5.2.1. Surface energy balance algorithms

Recent studies have highlighted the need for reliable estimates of crop water status from spectral remote sensing data at the field level with high spatial and temporal resolutions (Calera et al., 2017; Samuel et al., 2018; Rozenstein et al., 2018; Vanino et al., 2018). The surface energy balance

(SEB) algorithms have been recommended for estimating actual crop ET. The most common SEB algorithms include Surface Energy Balance Algorithm for Land (SEBAL) (Bastiaanssen et al., 1998), Surface Energy Balance System (SEBS) (Su, 2002), Simplified Surface Energy Balance Index (S-SEBI) (Roerink et al., 2000), Two Source Energy Balance (TSEB) (Norman et al., 1995), Mapping EvapoTranspiration at High Resolution with Internalized Calibration (METRIC) (Allen et al., 2007), ETLook (Pelgrum et al., 2010), and operational Simplified Surface Energy Balance ($SSEB_{op}$) (Senay et al., 2013). These algorithms utilize satellite observations in the thermal range to estimate latent heat flux as a residual of surface energy balance, hence the actual evapotranspiration. The SEB method is highly accurate for capturing actual crop status and does not need information on specific crop type or various stages of crop growth (Allen et al., 2011). Previous studies have documented the merits and demerits of each SEB models for estimating actual crop ET (Bhattarai et al., 2016; Numuta et al., 2017; Zayed et al., 2016). The SEB algorithms are generally suitable for estimating crop ET and scheduling irrigation, but are limited by cloud covers (Al Zayed et al., 2016) and poor spatial and temporal resolution of satellite observations (Bisquert et al., 2016).

2.6. Crop growth simulation models

Crop growth models are tools for estimating yields as a function of weather, soil conditions, and field management practices (Siad et al., 2019). Models range from empirical to physical based, which describe mechanisms causing a response to climate and management practices. Empirical models are generally based on regression equations to estimate crop yields. These models have no information on the mechanisms that control the outputs. In contrast, mechanistic models explain the relationships between weather parameters and crop yields, and the mechanisms that control these relationships (Foster et al., 2017). Mechanistic crop growth models, eg. AquaCrop, DSSAT, CropSyst, and APSIM (Vanuytrecht et al., 2014), use climate and soil moisture inputs to assess irrigation strategies to maximize yield.

2.6.1. AquaCrop simulation model

The AquaCrop is a crop growth model, developed by the Land and Water Division of FAO, to address food security and assess the effect of the environment on crop production (Steduto et al., 2009, Hsiao et al., 2009). AquaCrop is a multi-crop model that simulates water-limited yield under different biophysical and management conditions (Foster et al., 2009), and simulates soil evaporation and crop transpiration separately. Transpiration is used to estimate daily biomass accumulation, using a crop-specific water productivity parameter that is normalized for reference evapotranspiration, making it highly applicable to irrigation studies (Foster et al., 2017). The model relates its soil-crop-atmosphere components through its soil and water balance (Araya et al., 2010). It uses several input files for simulation, including the climatic data, ETo, crop canopy cover, and soil water conditions. The ETa values are obtained based on the determination of the appropriate values of Kc using maximum soil evaporation and crop transpiration coefficients. The basic concepts and calculation procedures of AquaCrop model are summarized in Steduto et al. (2009). Several studies have highlighted the usefulness of AquaCrop model for estimating ETa (Araya et al., 2010; Hsiao et al., 2009; Toumi et al., 2016).

2.7. Concluding remarks and future perspectives

Conventional irrigation scheduling techniques rely on soil moisture measurements, climatic data, and physiological measures of plant response to assess water stress. The approach is inadequate due to the high costs of sensors and their installation, and the difficulty with obtaining measurements, especially for heterogeneous soil and crop canopies. Plant indicators commonly used to determine crop water status are leaf water potential and stomatal conductance, but their measurements are either destructive, labour intensive or unsuitable for automation, which make it difficult for irrigators to adopt. Thus, automated techniques for monitoring crop water status that would provide non-destructive, rapid, and reliable estimates of plant water status are needed.

Spectral remote sensing data acquired from UAVs and satellite platforms have been identified as a valuable tool for monitoring plant abiotic stress to improve water and nitrogen management. Generally, most physiological studies on plant stress report low correlation (with R^2 values of 0.5 or less) between a remotely sensed parameter such as NDVI or PRI and measures of plant stress parameters such as leaf area index, stomatal conductance, and leaf water potential. This sort of precision is inadequate to allow the use of single measurements of the parameters (e.g., NDVI or PRI) for estimation of plant stress. Therefore, innovative data management techniques that would integrate data from soil-based and plant-based approaches are needed to widen the scientific knowledge on the use of crop stress parameters to schedule irrigation, and provide irrigators with advanced tools for decision making.

Even though spectral reflectance indices have been proposed for water stress detection in various crops, most of these studies focused on different species of tree and cereal crops. To our knowledge, the use of narrow-band optical indices for detecting water stress and scheduling irrigation has not been extensively investigated for high value vegetable crops in water stressed regions and environments, and growing conditions. Furthermore, since VIs for water stress detection are crop and climate specific, it is imperative to investigate the spectral VIs needed to improve the productivity and yields of vegetable crops. This potential is enormous based on recent advances in sensor technologies, image analysis and processing, computer based decision making, and in the measurement of hyperspectral indices from UAS.

Leaf spectral properties are not solely dependent on plant water status. Factors such as soil background, canopy structure, leaf thickness, leaf age, differences in surface properties of leaves, and variations in leaf angle could influence the correlation between spectral response of leaves and plant water status. Future research should focus on the integration of thermal and narrow-band hyperspectral imagery to provide more precise information about plant water status, and the real-time data analysis and detection of plant water stress using advanced data analysis techniques that would be cost-effective and commercially available to farmers.

Connecting text

The literature review in Chapter II showed spectral reflectance indices as a valuable tool for monitoring plant water status and improving irrigation water management. It is advantageous over conventional soil measurements because it takes into account the crop physiological status. However, the use of these indices for detecting water stress and scheduling irrigation has not been extensively investigated for high value vegetable crops in water stressed regions and environments, and growing conditions. Most of the studies on this concept only focused on different species of tree and cereal crops. Therefore, it was imperative to investigate the spectral reflectance indices needed to improve the productivity and yields of high-value vegetable crops. In this study, bell pepper crop, which is a widely cultivated greenhouse vegetable crop, was used as a test crop, due to its sturdy architecture. Chapter III of this thesis investigated the sensitivity of crop reflectance indices for mapping water stress in bell pepper crops grown under greenhouse conditions.

This study was published in *Agricultural Water Management*. The paper was co-authored by Dr. Chandra A. Madramootoo, my supervisor. In order to ensure consistency with the thesis format, the original draft has been modified, and the cited references are listed in the reference section. All the funding used for this study was provided by my supervisor, Dr. Chandra A. Madramootoo.

Chapter III

Crop reflectance indices for mapping water stress in greenhouse grown bell pepper

3.1. Abstract

Early detection of plant water status is essential to optimize crop water use, and to implement water savings methods such as precision irrigation. This study investigated the potential of using crop reflectance indices to detect water stress, in order to improve irrigation of bell pepper (Capsicum annuum L.), grown under greenhouse conditions. Spectral reflectance data were acquired from bell pepper plants, with five different irrigation regimes namely 100, 80, 60, 40, and 20% of plant available water, in a completely randomized design. Plant stress parameters including stomatal conductance (G_s), canopy temperature (Tc), relative water content (RWC), yield, and volumetric soil moisture content (SMC) were concurrently measured with spectral data acquisition from the plants throughout the growing season. Various reflectance indices including Normalized Difference Vegetation Index (NDVI), Renormalized Difference Vegetation Index (RDVI), Optimized Soil Adjusted Vegetation Index (OSAVI), Photochemical Reflectance Index centered at 570 nm (PRI_{570}), Photochemical Reflectance Index centered at 553 nm (PRI_{553}), normalized PRI (PRI_{norm}), Water Index (WI), and WI/NDVI were obtained from the spectral data. The relationships between these crop reflectance indices and the water stress indicators were statistically examined at the five irrigation levels. The results revealed that PRI_{553}, *WI, RDVI*, PRI_{norm}, and *WI/NDVI* were the most useful indices for detecting water stress in bell pepper plants. The findings of this study show promise of using a proximal method for assessing water stress and to improve water management of high value vegetable crops grown under greenhouse conditions.

Keywords: Crop water stress; irrigation scheduling; bell pepper plants; spectral reflectance indices; water management.

3.2. Introduction

Conventional methods of scheduling irrigation such as soil moisture monitoring are laborious, time consuming, and require large number of soil moisture sensors to account for spatial heterogeneity of soil properties (Ihuoma and Madramootoo, 2016). An alternative method of irrigation scheduling is to directly monitor the plant water status through the physiological responses of plants to water stress. Water stressed plants absorb more radiant energy than is required for their photosynthetic activities, thereby exceeding their photosynthetic demand. The plants dissipate this excess energy as chlorophyll fluorescence and heat to avoid damage to the photosynthetic pigment (Rossini et al., 2013). Also, plants undergoing water stress close their stomata to conserve water, which closes the pathway for the exchange of oxygen, water, and carbon dioxide. As a result, water stress causes a drop in photosynthetic activities, which reduces growth and development of crops (Dangwal et al., 2015). Stomatal closure also results in decreases in the transpiration rate and evaporative cooling, thereby increasing the leaf temperature. This concept was used by (Idso et al., 1981, Jackson and Center, 1981) to develop the crop water stress index (CWSI) for tracking water stress in crops, with the aid of infrared thermometers.

Recently, researchers have utilized high-resolution airborne thermal sensors to detect differences in canopy temperature for monitoring water stress in plants (Berni et al., 2009, Gonzalez-Dugo et al., 2013, Osroosh *et al*., 2015; O'Shaughnessy *et al.,* 2012), as leaf temperature is a direct indicator of plant transpiration. However, leaf temperature does not account for changes in photosynthetic pigments in water stressed crops (Zarco-Tejada et al. 2013) and is limited in estimating plant water status due to variations in environmental temperature and humidity (Chung et al., 2018). Within the past few years, studies have investigated alternative narrow-band hyperspectral indices for detecting crop water stress (Panigada et al., 2014, Rossini et al., 2013, Wang et al., 2015, Zhao et al., 2015). This approach relies on the absorption and scattering of light, which controls the spectral features of plant leaves, to provide reliable, quantitative, and timely information on crop stress in a cost-effective manner.

Previous studies have investigated several spectral vegetation indices such as Normalized Difference Vegetation Index (*NDVI*), Renormalized Difference Vegetation Index (*RDVI*), Optimized Soil Adjusted Vegetation Index (*OSAVI*), Photochemical Reflectance Index (PRI_{570}), normalized PRI (PRI_{norm}), Water Index (*WI*), *WI/NDVI*, and Normalized Water Index (*NWI*), for monitoring water stress in crops. A comprehensive review of reflectance indices for assessing plant water status and scheduling irrigation has been outlined in Ihuoma and Madramootoo (2017). However, most of the studies focused on various species of tree and cereal crops (Dangwal *et al.,* 2015; Magney et al., 2016, Panigada et al., 2014, Rossini et al., 2013), and their findings cannot be adopted for estimating water status in vegetable crops, due to differences in their physiological characteristics. While crop reflectance measurements have been widely investigated for crops grown under open field conditions, the same cannot be said for high value vegetable crops grown under greenhouse conditions. Meanwhile, reflectance indices for open field production may not be suitable for the greenhouse since plant water stress is influenced by a combination of environmental conditions, microclimate, root conditions, and plant genetic traits (Katsoulas et al., 2016). Therefore, there is need to investigate crop reflectance indices that can be applied for early assessment of plant water stress, to improve the productivity and yields of high value vegetable crops grown under greenhouses.

Most vegetable crops such as bell pepper have high water demand and are susceptible to water stress. Kirnak et al. (2003) showed that water stress adversely affects the physiological and nutritional development of bell pepper. To achieve optimal bell pepper production, supplemental irrigation is required to ensure adequate water supply during their growth cycle (Ferrara et al., 2011, Yildirim et al., 2012). However, climate change, drought, and rising water demands from non-agricultural sectors are limiting the availability of freshwater resources for irrigation. Therefore, precise irrigation scheduling is essential to optimize irrigation water use, improve crop yield, and avoid excessive irrigation that may result in yield or water loss (Afzal et al., 2017), or leaching of agricultural nutrients that would degrade soil and water. Implementation of this strategy requires information on plant water status (Ali, 2011).

The objective of this study was to investigate the feasibility of spectral vegetation indices (VIs) for detecting water stress for optimizing irrigation water management in greenhouse grown bell pepper plants. Specifically, the objectives were to: (i) evaluate and compare various spectral VIs for monitoring water stress in bell pepper plants; (ii) test different PRI formulations for detecting water stress in bell pepper plants, by changing the normalization bands from 530 nm to 570 nm; (iii) determine the relationship between VIs and water stress of bell pepper.

3.3. Materials and methods

3.3.1 Experimental design and irrigation treatments

This research was conducted in the greenhouse at Macdonald Campus of McGill University, Ste Anne De Bellevue, Quebec, Canada. The study area lies between latitude 45° 26’ 17” N and longitude 73° 56’ 17” W with an elevation of 36 m. The greenhouse with a dimension of 8 m x 7 m x 5 m, was covered with single pane tempered glass that allows 95% of light transmission. The greenhouse roof was inclined at an angle of 37° to the horizontal. Bell pepper (cultivar Red Knight) seedlings were transplanted on August 26, 2016, into 25 pots (18-L each and one plant per pot) using soil from the Horticultural Research Centre of McGill University. Each pot had a depth of

32 cm and diameter of 27 cm. The soil was a sand clay loam with sand, silt, and clay content of 48%, 22%, and 30% respectively (USDA-NRCS, 2000); field capacity of 33% and permanent wilting point of 17% by volume. The pots were placed on 330 × 150 × 150 mm bricks, which were randomly positioned in the greenhouse at a spacing of 0.6 m by 0.6 m. A water tap was affixed to the bottom of the pots so that excess water could be drained and measured with a volumetric flask. The pots were saturated and allowed to drain out for 24 hours so that the soil water content was at field capacity before the plants were transplanted.

The experiment was arranged in a completely randomised design with five (5) irrigation water treatment levels of 100, 80, 60, 40, and 20% of plant available water as treatments, because weather variables were not expected to vary significantly within the greenhouse. Irrigation applications were based on the soil's plant available water (AWC), defined as as the difference between the field capacity and permanent wilting point of the soil and soil moisture content (SMC) in each pot was continuously measured with soil moisture sensors. The water treatment levels for each treatment (100, 80, 60, 40, and 20% AWC) were used as the upper irrigation threshold while the lower irrigation threshold was set at 10% depletion of AWC for each treatment. Irrigation was initiated when the SMC in the pots depleted to its requisite moisture treatment threshold value and was terminated when the upper trigger (100, 80, 60, 40, and 20% AWC) moisture content was attained. The volume of water applied to each pot during irrigation was determined as the product of the irrigation duration and the flow rate per pot, while the equivalent irrigation depth applied at each irrigation event for each pot was determined as the product of the volumetric water content and the plant rooting depth. High quality irrigation water was applied through a drip system, with emitters placed in each pot. The drip system consisted of pressure compensating emitters, with a discharge of 2 L h^{-1}, and the flow rates were calibrated in the greenhouse. Irrigation was uniformly applied to all treatments at the beginning of transplanting, based on 100% replenishment of water in the plant root zone to field capacity for plants to be well established; thereafter, the various irrigation treatments were implemented until harvest.

Replenishment of soil water at the five water application levels was done using continuous Time Domain Reflectometers (TDR) (CS625 water content reflectometer, Campbell Scientific Inc., UT, USA) installed vertically at a depth of 30 cm in the middle of each pot, to correspond with the plant rooting depth (Jaria and Madramootoo, 2013). TDR readings were calibrated with gravimetric soil moisture measurements, and the sensors were installed with the aid of an insertion guide following the procedures articulated in the Sentek manual (Sentek Sensor Technologies, 2003). The soil moisture sensors were connected to data loggers (model CR205/6, Campbell Scientific Inc., UT, USA). The data were scanned every 5 minutes and recorded every 15 minutes. Hourly and daily data were retrieved from the TDR using a laptop computer and LoggerNet software from Campbell Scientific Inc. Fertilizer applications, pest and weed control were based on guidelines for greenhouse production provided by the technicians in the Horticulture Research Centre. Agrochemical applications were the same for all the treatments to ensure that physiological stress detected were only due to water stress and not from nutrient stress or disease attacks. The plants were fertilized biweekly with 20-20- 20 N-P-K water-soluble fertilizer, at a rate of 4 kg of N per hectare. This was changed to calcium nitrate after the first fruits were noticed and later changed to potassium nitrate when the fruits were approaching maturity.

3.3.2. Measurements

Daily air temperature, relative humidity, and vapor pressure deficit were measured using a Campbell scientific psychrometer (Campbell Scientific, Logan, UT, USA) installed in the greenhouse. Evapotranspiration (ET) in the greenhouse was estimated during the growing season based on the soil moisture approach as shown in Eq. 3.1:

$$SWC_t = SWC_{t-1} + I - D - ET \ldots\ldots\ldots\ldots\ldots\ldots\ldots\ldots (3.1)$$

where, SWC_t: Soil water content today (mm), SWC_{t-1}: Antecedent soil water content (mm), I: Irrigation depth since yesterday (mm), D: Drained water from the soil column (mm), ET: Crop evapotranspiration (mm), $SWC_t - SWC_{t-1}$: Soil water storage (ΔS).

3.3.2.1. Measurement of plant stress indicators

Leaf temperature was measured with handheld infrared thermometry set at an emissivity of 0.95 W m^{-2} (Evett et al., 2000) (Fluke 572 model, Fluke Corporation, Everett, WA). The instrument was held 30 cm above the plant canopy and directed at the leaf of the bell pepper plant with a laser point of the instrument set at an angle of 90° to the horizontal (Orta et al., 2002). Four infrared thermometer measurements were made when the plant canopy covered about 80% of the pot area. The temperature of the stressed and non-stressed plants was determined from canopy temperature data; four (north, south, east and west) viewing directions were considered and average temperatures obtained. Measurements were made between 11:00 and 15:00 hours to ensure maximum solar intensity when the sun was shining directly on the plants, as adopted by Aladenola and Madramootoo (2014). Stomatal conductance was measured during the growing period using a Li-6400 Portable Photosynthesis System (LI-COR Ltd., Lincoln, NE). Three (3) healthy, fully sunlit leaves were selected, and stomatal conductance was measured on the leaves using the Li-6400, and the averages calculated. Leaf relative water content (RWC) was measured at each stage of plant growth by selecting the youngest fully expanded leaves from one representative crop in each treatment. The leaf samples were enclosed in a sealed plastic bag and kept in a cooler at 5 °C until they reached the laboratory. Fresh weight (FW) was recorded using an analytical balance, and the samples were immersed in distilled water for 72 h, blotted and weighed to obtain the turgid weight (TW). Finally, leaf samples were dried at 72 °C in an oven, until constant dry weight (DW) was achieved. The RWC was calculated according to Eq. 3.2, as adopted in previous studies on crop water stress (Colombo et al., 2008, Wang et al., 2015). Bell pepper plants were harvested about 4 (four) times, after maturity, and the total and marketable yield were measured and recorded.

$$RWC = \frac{FW - DW}{TW - DW} 100\ (\%) \ldots\ldots\ldots\ldots\ldots\ldots\ldots (3.2)$$

3.3.2.2. Spectral data acquisition and processing

A miniature fiber optic spectrometer (Stellar Net Inc. USA), which measures reflectance in the 200–1150 nm spectral range, was used to measure canopy reflectance. The spectrum is characterized by a 0.5 nm spectral resolution and was calibrated before each reading was taken. The calibration process involved holding the probe at 45° to a white standard (reference), at a distance of about 60 mm, to optimize the integration time (typically set at 50 ms), recording dark current, and then obtaining target reflectance. All canopy spectral measurements were taken under clear sky conditions between 11:00 and 15:00 hours to ensure maximum solar intensity when the sun was shining directly on the plants, as conducted in similar studies (Zhao et al., 2017). The spectrometer was positioned at a height of 30 cm from the plant canopy so that it viewed only the plant leaves. Five leaves were measured in every pot and four scans were averaged in every measurement, considering four (north, south, east and west) viewing directions. The measurements were carried out five times (16 and 21 September; 10, 18, and 25 October 2016), during the flowering and maturity stages of the crops, when the crops are more susceptible to water stress.

Due to the absorption of atmospheric water, signal background, and light scattering effects, the spectral reflectance contains substantial interference noise (Zhao et al., 2017), which must be eliminated as it affects the smoothness of the spectral curve. The most commonly used smoothing algorithms include the moving average method, fitting polynomial method, wavelet transform and various regression smoothing methods. Based on the recommendations of previous research (Zhao et al., 2017), the 7-point weighted moving average method was used to smooth the spectral curve in this research. This algorithm enhances the smoothness of the spectral curve while keeping all the spectral details intact, to ensure the extraction of suitable wavelengths. The spectral indices used in this study were obtained from the optical reflectance measurements from each treatment and are presented in Table 3.1. The reflectance indices were divided into three (3); the xanthophyll pigment indices related to photosynthetic pigment changes, the structural/greenness indices related to the canopy structure and biomass, and the water indices related to the water content of the plant canopy.

3.3.3. Statistical analysis

The Pearson correlation ratio was used to describe the effects of irrigation levels on the stress indicators (Tc, RWC, Gs). Given that the correlation ratio η^2 is defined as:

$$\eta^2 = \frac{\sigma_{\bar{y}}^2}{\sigma_y^2}, where\ \sigma_{\bar{y}}^2 = \frac{\sum_x n_x(\bar{y}_x - \bar{y})^2}{\sum_x n_x}\ and\ \sigma_y^2 = \frac{\sum_{x,i} n_x(y_{xi} - \bar{y})^2}{n} \quad (3.3)$$

Where each observation is y_{xi} (x indicates the five irrigation levels, and i indicates an observation). n_x is the number of observations in category x, $\bar{y}_x$ is the mean of the category x and $\bar{y}$ is the mean of the whole population. The correlation ratio assumes values in the interval (0, 1) and indicates how the data variance is explained by the factor irrigation. A correlation ratio close to 1 implies that all the data variance is explained by the factor irrigation.

One-way Analysis of variance (ANOVA) was conducted on the vegetation indices and field data using PROC/GLM (General Linear Model) procedure of SAS software (version 9.3, SAS Institute, Inc. Cary, NC, USA), and significance of differences among treatments were separated using Fisher's Least Significant Difference (LSD) at a 5% probability level. The relationship between the vegetation indices (NDVI, OSAVI, RDVI, PRI_{570}, PRI_{553}, PRI_{norm}, WI, WI/NDVI) and stress indicators (Tc, RWC, Gs), total marketable yield, Irrigation Water Use Efficiency (IWUE), and soil moisture content were evaluated by Ordinary Least Square (OLS) regression analysis.

Table 3. 1. Optical indices used in this study, their formulations and references.

Names	Index	Formulation	Reference
Xanthophyll pigments			
Photochemical Reflectance Index	PRI_{570}	$(R_{570} - R_{531})/(R_{570} + R_{531})$	Gamon *et al* (1992)
	PRI_{553}	$(R_{553} - R_{531})/(R_{553} + R_{531})$	Gamon *et al* (1992)
Normalized Photochemical Reflectance Index	PRI_{norm}	$PRI/(RDVI * (R_{700}/R_{670}))$	Berni *et al (*2009)
Greenness Indices			
Normalized Difference Vegetation Index	NDVI	$(R_{800} - R_{670})/(R_{800} + R_{670})$	Rouse *et al* (1974)
Renormalized Difference Vegetation Index	RDVI	$(R_{800} - R_{670})/(R_{800} + R_{670})^{1/2}$	Rougean and Breon (1995)
Optimized Soil Adjusted Vegetation Index	OSAVI	$(1 + 0.16)(R_{800} - R_{670})/(R_{800} + R_{670} + 0.16)$	Haboudane *et al* (2002)
Water content Indices			
Water Index	WI	R_{900}/R_{970}	Penuelas *et al* (1997)
Normalized Water Index	NWI	$(R_{970} - R_{900})/(R_{970} + R_{900})$	Bandyopadhyay *et al* (2014)
	WI/NDVI	WI/NDVI	Penuelas *et al* (1997)

Where R represents the reflectance values at the indicated wavelengths in nm.

3.4. Results

3.4.1. Crop evapotranspiration and soil water content

Daily mean temperature, relative humidity, and vapor pressure deficit in the greenhouse ranged from 19 to 28 °C, 60 to 86%, and 0.31 to 1.51 kPa, respectively, during the plant growing season. The total seasonal ET_c was approximately 135 to 222 mm, and the total water applied for each treatment ranged from 45 to 168 mm, as shown in Table 2. The difference between the ETc and total water applied represents water storage in the pot. The ET_c increased generally with irrigation water amount and was higher during the flowering and maturity stages of plant growth, as these corresponded to the periods when the crops required more water for their physiological development. Daily volumetric soil water content for various irrigation treatments are shown in Fig. 3.1. The soil water content generally decreased with decreasing water application, with 100 and 20% AWC resulting in the highest and lowest values of soil water content, respectively. Soil water contents for 20, 40, and 60% AWC were relatively low throughout the growing season. The 80% AWC was not statistically different from full irrigation treatment (100% AWC) but was significantly different from other treatments.

3.4.2. Effects of irrigation on marketable yield

The effects of irrigation treatments on marketable yield of the plants are shown in Fig. 3.2. The total marketable yield ranged from 0.40 to 0.59 kg plant^{-1}, for 20 and 100% AWC treatments, respectively. The highest mean marketable yield was obtained from 100% AWC treatment (0.59 kg plant^{-1}), while the least marketable yield was obtained from 40% AWC treatment (0.40 kg plant^{-1}). The average yield from the full irrigation treatment (100% AWC) was statistically different from the yield obtained from the 40 and 20% AWC, but not significantly different from the yield obtained from 80 and 60% AWC, which implies that water stress below 60% AWC treatment caused an evident decrease in crop yield.

Table 3. 2. Water applied (mm) for bell pepper plants per growth stage for different treatments.

Treatments (% of AWC)	Days	100	80	60	40	20
Initial stage	20	24	22	20	18	16
Flowering stage	30	48	38	29	19	10
Maturity stage	30	60	48	36	24	12
Senescence stage	25	36	29	22	14	7
Total	105	168	137	107	76	45

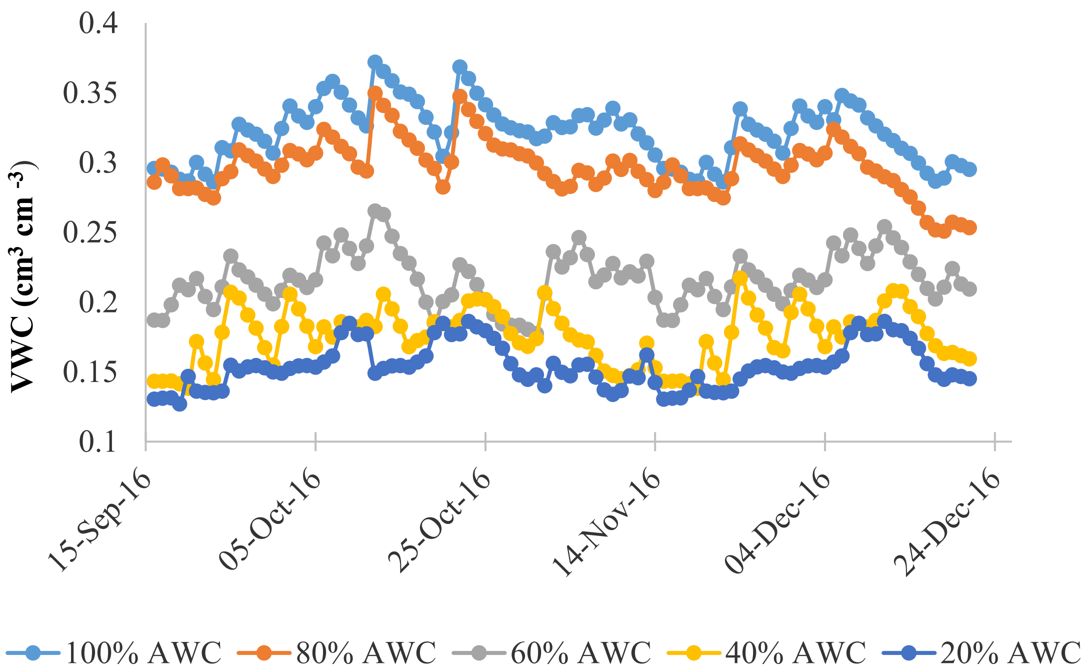

Fig. 3. 1. Variation of soil moisture content during the growing season

3.4.3. Water stress indicators

The mean of all the measured stress indicators generally decreased as irrigation water application decreased (Table 3.3). The leaf temperature showed the highest correlation ratio ($\eta^2 = 0.93$), which implies that irrigation treatments explained most of the Tc variance. The results show that 100 and 20% AWC had the average lowest and highest leaf temperatures. The 100% AWC was not statistically different from the 80% AWC but was significantly different from the 60, 40, and 20% AWC. This indicates that water stress affected the leaf temperature of the plants. The stomatal conductance had a high value of correlation ratio ($\eta^2 = 0.82$), indicating that the variance in Gs was explained by the irrigation treatments administered in the study. Leaf relative water content was weakly affected by the irrigation levels ($\eta^2 = 0.42$), compared to the Tc and Gs. There is a linear relationship between the leaf temperature and stomatal conductance, with $R^2 = 0.86$ ($p < 0.0001$). This indicates that stomatal conductance increased linearly with decreases in leaf temperature. Also, the RWC is linearly correlated with Tc, having an $R^2 = 0.51$ ($p < 0.01$).

3.4.4. Crop spectral reflectance

The spectral signatures of the plant leaves obtained from the spectrometer from various treatments are shown in Fig. 3.3(a). The plant canopy reflectance varied among various water treatment regimes and displayed similar trends throughout the entire growing season. The spectral signature follows a similar pattern for each of the treatments, with the 100 AWC and 20% AWC recording the highest and lowest reflectance values in the visible spectral range (400 – 700 nm), respectively. The spectral reflectance curves show peaks near 550 and 668 nm, and trough near 680 nm. The stressed crops exhibited higher reflectance values within the visible spectral range as shown in Fig.

3(b). The measured values of canopy reflectance were used to calculate the spectral vegetation indices shown in Table 3.1.

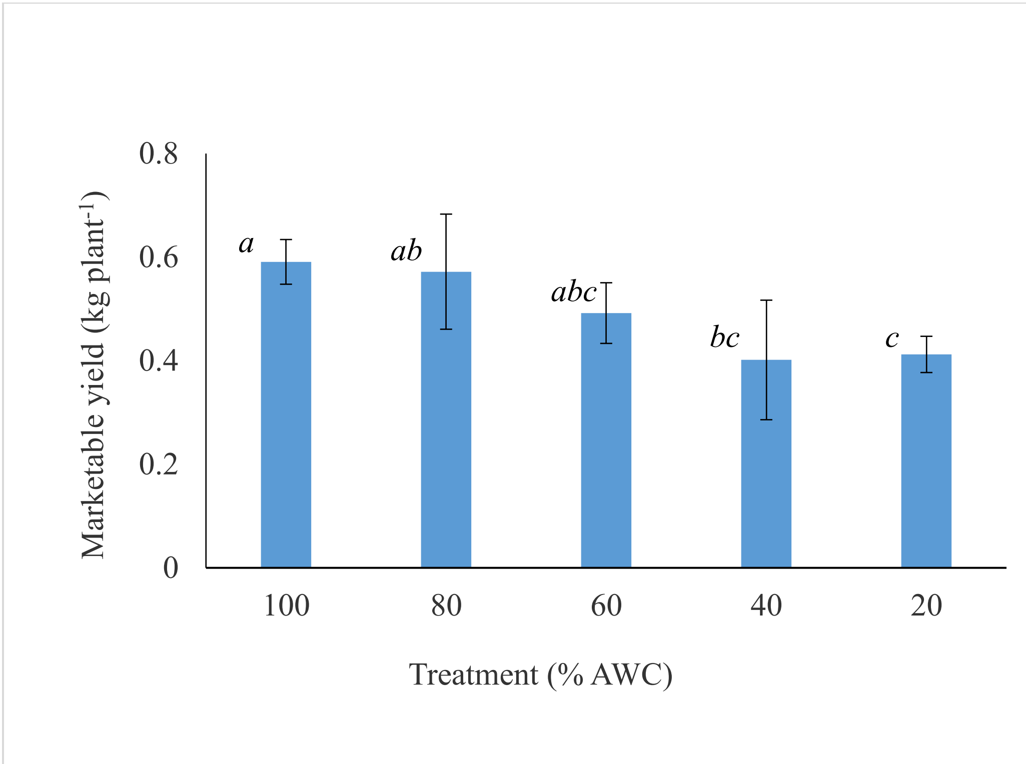

Fig. 3. 2. Effects of irrigation treatments on marketable yield (kg $plant^{-1}$) of bell pepper

Table 3. 3. Descriptive statistics (mean, standard deviation, and correlation ratio (η^2) of bell pepper grouped by the irrigation treatment levels (100, 80, 60, 40, and 20% AWC). Where Tc: leaf temperature (°C), Gs: stomatal conductance (mmol m^2 s^{-1}), RWC (%); leaf relative water content.

Stress indicators	100% AWC	80% AWC	60% AWC	40% AWC	20% AWC	η^2
Tc	16.08 ± 0.18^{d}	16.17 ± 0.34^{cd}	17.32 ± 0.17^{bc}	17.95 ± 0.23^{ab}	18.32 ± 0.28^{a}	0.93
Gs	0.41 ± 0.06^{a}	0.31 ± 0.07^{ab}	0.21 ± 0.01^{bc}	0.17 ± 0.01^{bc}	0.16 ± 0.03^{c}	0.82
RWC	61.99 ± 6.73^{a}	61.69 ± 6.83^{a}	59.67 ± 7.55^{ab}	53.52 ± 2.81^{bc}	49.67 ± 2.56^{c}	0.42

$^{a\text{-}c}$ Means followed by the same letter within a column are not significantly different at p = 0.05.

Reported values are averages of five replicates.

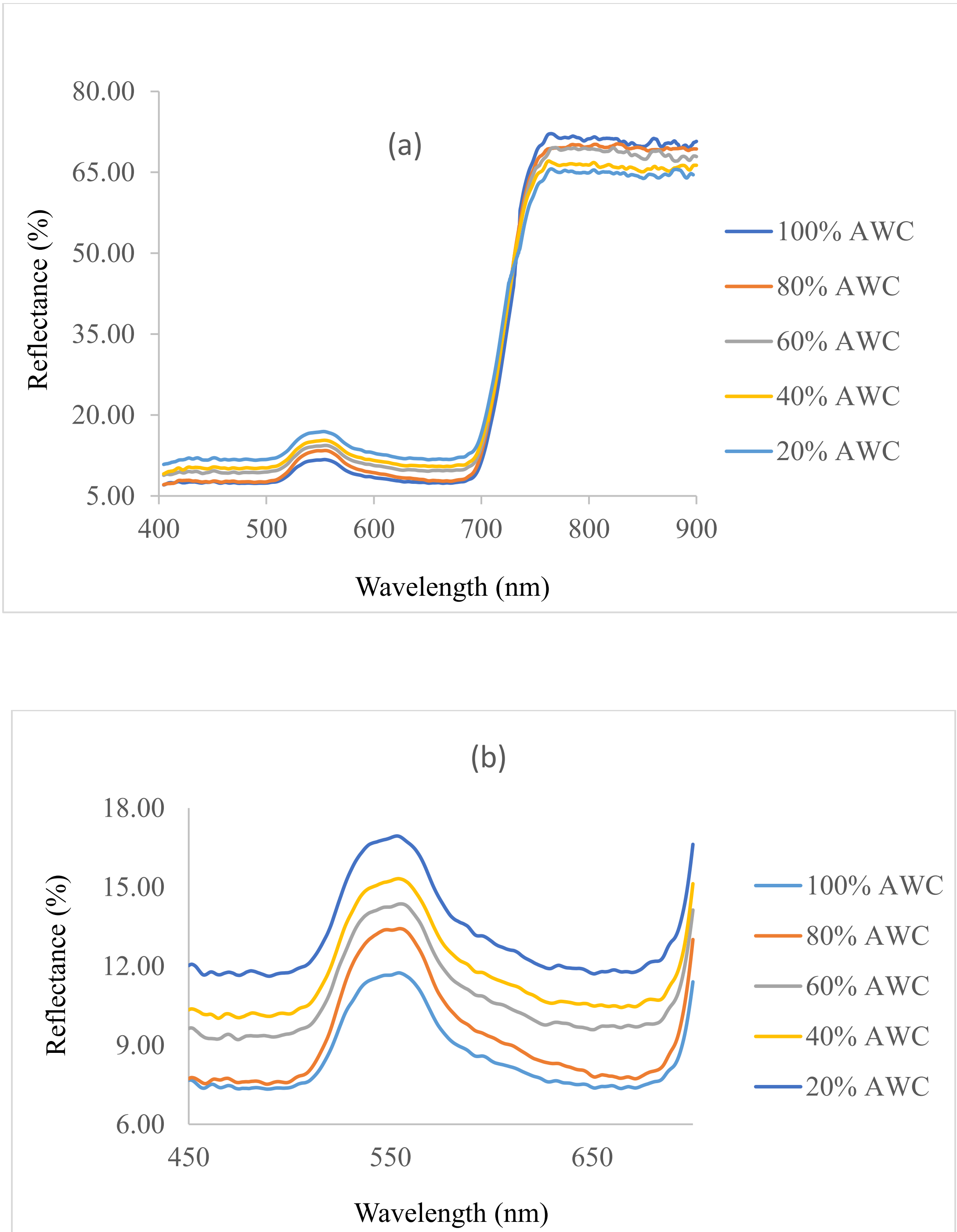

Fig. 3. 3. (a) Examples of spectral signatures of the plant canopy for different treatments (b) Spectral reflectance curves in the visible spectral range.

3.4.5. Crop reflectance indices

The reflectance indices identified for monitoring water stress in this study were distinctly correlated with canopy temperature, stomatal conductance, relative water content, yield, and volumetric soil water content. The relationship between various reflectance indices and canopy temperature (Tc) obtained from the different water treatment levels is shown in Fig. 3.4. Analysis of the results revealed that all the crop reflectance indices considered in this experiment were significantly correlated with Tc. However, the PRI_{553}, WI/NDVI, and PRI_{norm} showed the most significant correlation with Tc, ($R^2 = 0.82$, $p < 0.001$; 0.80, $p < 0.001$; and 0.73, $p < 0.001$; respectively). The greenness indices, NDVI, RDVI, and OSAVI were significantly related to Tc, ($R^2 = 0.5$, $p < 0.01$; 0.62, $p < 0.001$; and 0.63, $p < 0.01$; respectively).

Fig. 3.5 shows the relationship between various vegetation indices and stomatal conductance (Gs) of the plants. The result showed the correlation between Gs and WI, NDVI, and RDVI ($R^2 = 0.52$, $p < 0.01$; 0.51, $p < 0.01$; and 0.73, $p < 0.001$; respectively). The OSAVI and WI/NDVI were weakly correlated with Gs ($R^2 = 0.32$, $p < 0.05$; and 0.42, $p < 0.05$; respectively). Similarly, PRI_{norm} and PRI_{553} showed significant correlations with Gs ($R^2 = 0.70$, $p < 0.001$; and 0.62, $p < 0.001$; respectively), and PRI_{570} was correlated with Gs ($R^2 = 0.42$, $p < 0.01$).

The coefficient of determination of the linear relationships between all the reflectance indices and stress parameters are summarized in Table 3.4. The results show that the water indices (WI/NDVI and WI) showed the strongest correlation with crop yield ($R^2 = 0.76$, $p < 0.001$; and 0.69, $p < 0.001$; respectively). Also, there were significant correlations between the greenness indices and crop yield ($R^2 = 0.53$, $p < 0.01$; 0.62, $p < 0.001$; and 0.62, $p < 0.01$; for NDVI, RDVI, and OSAVI, respectively). The PRI_{553} and PRI_{570} showed weak correlations with crop yield ($R^2 = 0.41$, $p < 0.01$;

and 0.30, $p < 0.05$; respectively), while the PRI_{norm} showed a strong correlation with crop yield ($R^2 = 0.62$, $p < 0.01$). The structural indices showed no significant correlation with the RWC of bell pepper.

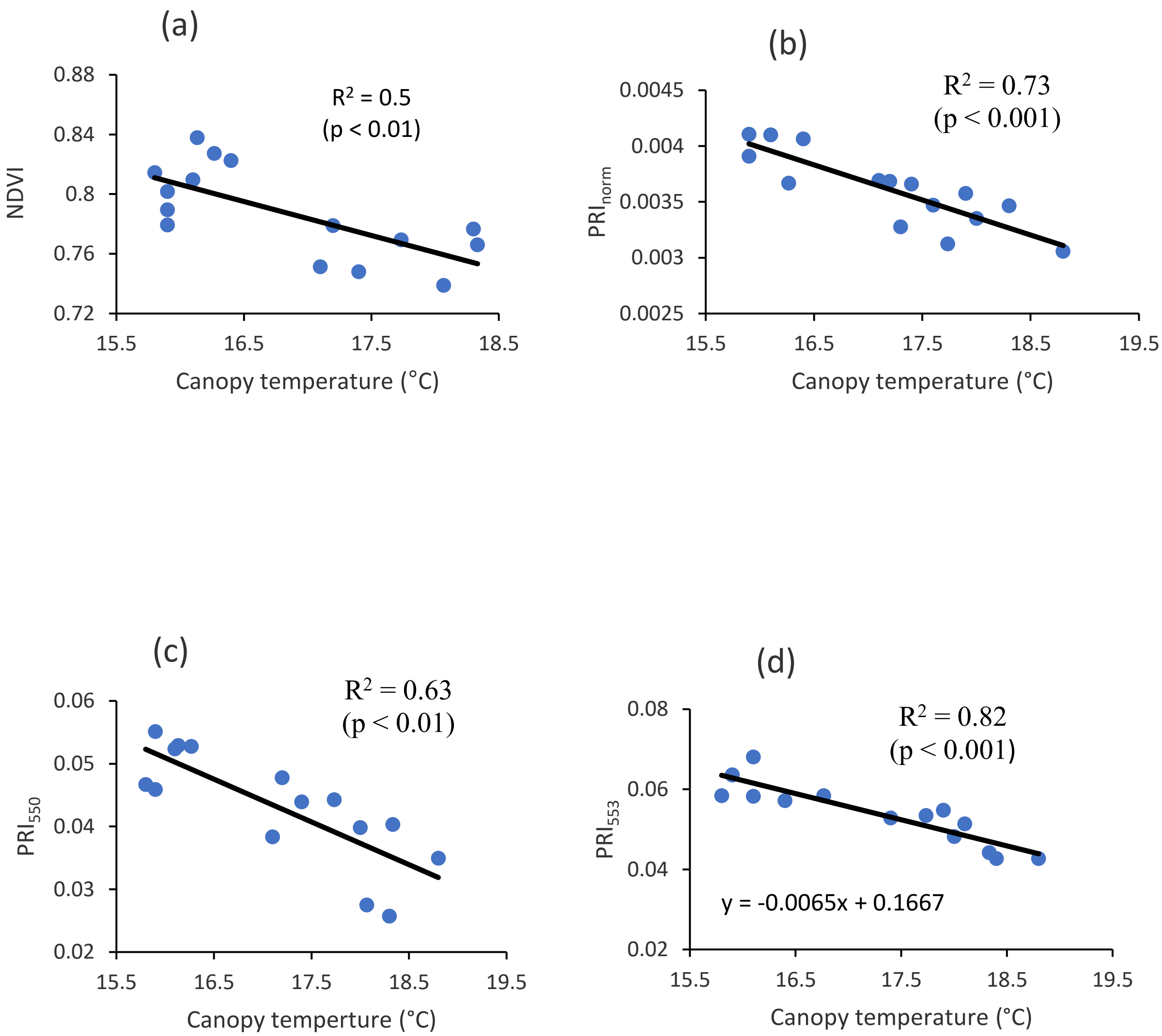

Fig. 3. 4. Relationship between (a) NDVI (b) PRI_{norm} (c) PRI_{550} (d) PRI_{553} and canopy temperature (Tc) obtained from the various treatments.

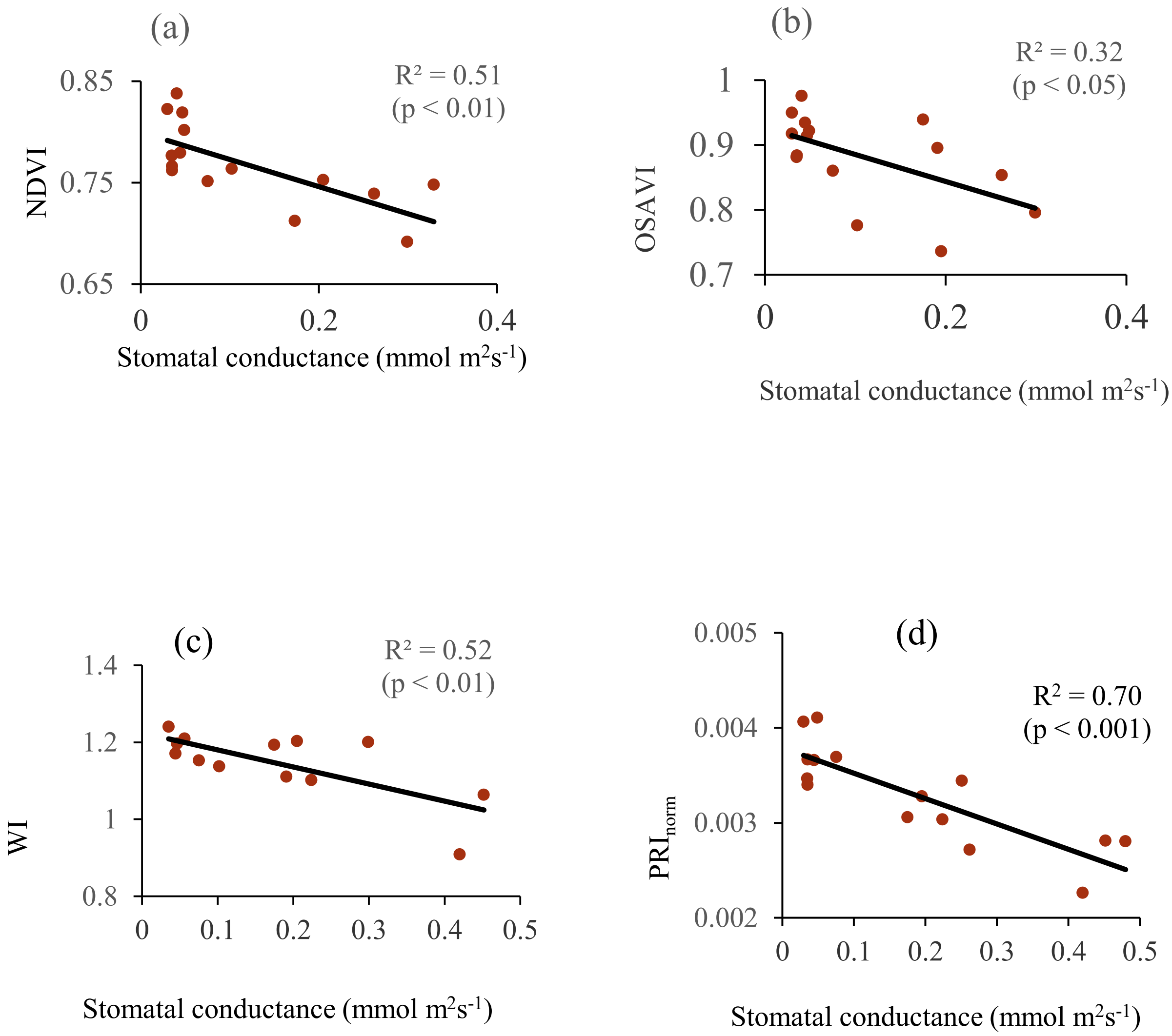

Fig. 3. 5. Relationship between (a) NDVI, (b) OSAVI, (c) WI, and (d) PRI_{norm} and stomatal conductance.

Specifically, PRI with reference wavelength of 553 nm (PRI_{553}) showed a good correlation with water stress indicators considered in this experiment, with $R^2 = 0.72$, $p < 0.05$; 0.62, $p < 0.001$; 0.82, $p < 0.001$; 0.41, $p < 0.001$, for RWC, Gs, Tc, and yield, respectively. The water index showed a strong correlation with the plant stress parameters ($R^2 = 0.89$, $p < 0.01$; 0.52, $p < 0.01$; 0.66, $p < 0.01$; and 0.69, $p < 0.001$; for RWC, Gs, Tc, and yield, respectively). The WI/NDVI was significantly correlated with RWC, Gs, Tc, and yield, with $R^2 = 0.69$, $p < 0.05$; 0.43, $p < 0.05$;

0.80, $p < 0.001$; 0.76, $p < 0.001$; respectively. NDVI, RDVI, OSAVI, and PRI_{norm} were not significantly correlated with RWC, while the PRI_{570}, PRI_{550}, PRI_{553}, WI, and WI/NDVI were correlated with the RWC, with $R^2 = 0.44$, $p < 0.05$; 0.30, $p < 0.01$; 0.72, $p < 0.05$; 0.89, $p < 0.01$; and 0.69 $p < 0.05$, respectively. Table 4 also showed that the NDVI, RDVI, OSAVI, PRI_{570}, PRI_{550}, PRI_{norm}, PRI_{553}, WI, and WI/NDVI were correlated with crop ET, with $R^2 = 0.47$, $p < 0.001$; 0.62, $p < 0.001$; 0.43, $p < 0.5$; 0.61, $p < 0.01$; 0.56, $p < 0.01$; 0.73, $p < 0.001$; 0.63, $p < 0.01$; 0.61, $p < 0.01$; and 0.77, $p < 0.001$, respectively.

There was no significant difference between 100 and 80% AWC for most of the indices. However, all the reflectance indices showed significant differences when the soil moisture content depletes below 40% AWC, which implies that the indices detected changes in plant water status. Table 3.5 shows the correlations between various indices. Indices of the same group tend to show higher statistical significance with each other. Apart from NDVI, other structural indices, RDVI and OSAVI, were significantly correlated with each other, while NDVI was only correlated with PRI_{norm}. The xanthophyll pigment indices all showed significant correlations with each other, and with the xanthophyll and water indices. Based on the results shown in Table 3.4, the PRI_{553} showed the best potential for detecting water stress in greenhouse-grown bell pepper plants with $R^2 = 0.82$ ($P < 0.001$).

Table 3. 4. Coefficient of determination (R^2) of the linear relationship RWC (%), Gs (mmol m^2 s^{-1}), ETc (mm day^{-1}), Tc (°C), and Yield (kg $plant^{-1}$), and vegetation indices computed from the hyperspectral sensor.

	RWC (%)	Gs (mmol m^2s^{-1})	Tc (°C)	ETc (mm day^{-1})	Yield (kg $plant^{-1}$)
NDVI	*N.S*	0.51^{**}	0.50^{**}	0.47^{***}	0.53^{**}
RDVI	*N.S*	0.73^{***}	0.62^{***}	0.62^{***}	0.62^{***}
OSAVI	*N.S*	0.32^{*}	0.63^{**}	0.43^{*}	0.62^{***}
PRI_{570}	0.44^{*}	0.42^{**}	0.72^{***}	0.61^{**}	0.32^{*}
PRI_{550}	0.30^{**}	0.58^{**}	0.63^{**}	0.56^{**}	0.56^{*}
PRI_{norm}	*N.S*	0.70^{***}	0.73^{***}	0.73^{***}	0.62^{**}
PRI_{553}	0.72^{*}	0.62^{***}	0.82^{***}	0.63^{**}	0.41^{**}
WI	0.89^{**}	0.52^{**}	0.66^{**}	0.61^{**}	0.69^{***}
WI/NDVI	0.69^{*}	0.43^{*}	0.80^{***}	0.77^{***}	0.76^{***}

$* P < 0.05$; $** p < 0.01$; $*** p < 0.001$; N.S = Not significant.

3.5. Discussions

3.5.1. Effects of water stress on yield

The irrigation treatments implemented in this experiment caused moderate to severe water stress on the plants, and this caused a reduction in photosynthetic efficiency of the leaf pigments, as reflected in reduced yields of the stressed plants. The lowest crop yield was obtained from the 40% AWC and resulted in a yield loss of 32% compared to the optimum yield. This indicates that the depletion of soil water content to 40% AWC caused severe water stress that adversely affected the crop yield. Water application at 60% AWC resulted in a yield loss of 17% compared to the optimum yield, and this justifies the need for supplemental irrigation.

3.5.2. Effects of irrigation treatment on crop reflectance

The stressed plants exhibited high reflectance values within the visible spectrum. Usually, plant pigments absorb radiance in the visible spectral range but reflect most radiance in the near-infrared (NIR) range. This spectral reflectance pattern is affected by plant stress due to reduced efficiency of the photosynthetic pigments, leading to increased reflectance in the visible band and decreased reflectance in the NIR band. Based on this concept, structural indices (such as NDVI) were calculated, and have been used by researchers to estimate biomass, leaf area index, and yield of various crop species (Jones et al., 2004, 2007, Rossini et al., 2013, Panadiga et al., 2014, Huang et al., 2014, Leroux et al., 2016). Recent studies utilize NDVI to map crop cover for estimation of crop coefficients (Kc) used in the conventional FAO-56 Penman-Monteith equation (Allen et al., 1998), and for irrigation scheduling (Jones, 2012). NDVI has also shown a linear relationship with the basal crop coefficient for ET (Kcb) because Kcb mainly depends on the dynamics of plant canopies (greenness, biomass, and LAI). Several other researchers have used NDVI to predict Kcb for several other crops (Allen et al., 2005, Irmak et al., 2011, Kamble et al., 2013, Kullberg et al., 2017), which makes it useful for estimating crop water requirements and scheduling irrigation.

3.5.3. Effects of water stress on crop reflectance indices

An evaluation of the reflectance indices for detecting water stress in bell pepper revealed that the PRI_{553} had the best correlation with leaf temperature and stomatal conductance, making the index a valuable tool for monitoring water stress in bell pepper plants. Basically, water-stressed plants close their stomatal leading to increased leaf temperature, to dissipate excess excitation energy, detected as changes in leaf xanthophyll pigment. Eq. 3.4 showed an inverse relationship between plant water stress levels and PRI_{553}, a xanthophyll pigment index, with water stress decreasing as the PRI index plant increases. This result agrees with previous studies that used the xanthophyll pigment indices to detect water stress (Berni et al., 2009, Dangwal et al., 2015, Leroux et al., 2016, Panigada et al., 2014, Rossini et al., 2013, Suárez et al., 2010, Zarco-Tejada et al., 2013, Zhao et al., 2015). The relationship between PRI and water stress can be explained by the role of the xanthophyll pigments in dissipating excess heat that occurs when plants are stressed and the functional interaction between eco-physiological indicators of water stress in plants. At the beginning of water stress, RWC decreases, stomata close, and Tc increases concurrently with a reduction in photosynthesis pigment activities (Prasad et al., 2008), which is detected by variations in PRI. The PRI_{570}, proposed in previous studies to minimize structural effects (Hernández-Clemente et al., 2011, Zarco-Tejada et al., 2012) showed weak correlations with RWC and Gs in this study, and therefore not suitable for monitoring water status in bell pepper plants. The strong correlation between the PRI_{norm} and Gs implies that water stress-induced changes in

Table 3. 5. Relationship between various vegetation indices obtained from the spectrometer. Correlation coefficients are significant at $p < 0.05$.

	NDVI	RDVI	OSAVI	PRInorm	PRI550	PRI553	PRI570	WI	NWI	WI/NDVI
NDVI	1									
RDVI	-0.15	1								
OSAVI	0.18	0.68	1							
PRI_{norm}	0.40	0.31	0.61	1						
PRI_{550}	-0.30	0.48	0.69	0.31	1					
PRI_{553}	0.12	0.62	0.61	0.26	0.55	1				
PRI_{570}	0.05	-0.45	-0.74	-0.56	-0.80	-0.54	1			
WI	-0.18	0.30	0.48	-0.01	0.45	0.39	-0.61	1		
NWI	0.14	0.37	0.78	0.69	0.69	0.25	-0.80	0.27	1	
WI/NDVI	-0.13	0.71	0.63	0.49	0.53	0.57	-0.75	0.41	0.46	1

xanthophyll pigment. Previous studies showed the improved capacity of PRI_{norm} to detect water stress because it is more sensitive to dynamic changes in vegetation compared to other greenness indices (Evain et al., 2004, Garbulsky et al., 2011, Zarco-Tejada et al., 2013).

Again, the physiological processes of bell pepper plants were differently affected by water stress during the plant's growth stages. The diurnal course of Tc is strongly related to the regulation of the stomatal opening and other aspects of crop physiology (Gonzalez- Dugo et al., 2014). In non-stressed plants, Tc reduced as the day progressed due to the increased evaporative demand causing the transpiration rate to also increase. In this experiment, water stress significantly affected leaf temperature with the non-stressed and fully-stressed treatments recording the least and highest Tc values, respectively. This affirms the assertion that water stress leads to a reduction in transpiration, thereby causing an increase in leaf temperature compared to non-stressed plants (Idso et al., 1982). This concept has been adopted by several researchers who used crop water stress index (CWSI) to evaluate water stress in various crops (Aladenola and Madramootoo, 2014, Jones, 2010, Nielson and Gardner, 1988, Osroosh et al., 2015, O'Shaughnessy et al., 2012, Payero and Irmak, 2006, Sezen et al., 2014). Their studies demonstrated that Tc is sensitive to water stress and relies on stomatal closure as an early indicator of water deficits.

The irrigation treatments resulted in changes in canopy structure, detected by the variations in the structural indices with different water treatment levels. The significant relationship between the greenness indices and Gs shows that water stress adversely affected the leaf pigment structures, leading to variations in NDVI and RDVI among various treatments. This may be the effect of accumulated water stress on plant physiology, and the structural indices detected these changes in plant leaves. Rinaldi et al. (2014) obtained a significant correlation between NDVI and plant biomass and yield, which is consistent with this study. Other studies obtained a good correlation between NDVI and plant water content (Genc et al., 2011, Kim et al., 2010, Marino et al., 2014). Koksal (2011) attributed these findings to the effects of water stress on the crop canopy that may have caused changes in leaf structure and composition. Gago et al. (2015) demonstrated that the greenness indices are more related to the plant biomass than its dynamic physiological status. In this study, good correlations between plant water status and structural indices were obtained during the late maturity stage of the plants. By then the effects of water stress on the plants were already established. This presents a limitation on the use of structural indices for monitoring plant water stress and scheduling irrigation.

Most of the indices investigated in this study showed a strong correlation with crop yield, apart from PRI_{570} and PRI_{533}, as shown in Table 3.4. Previous researchers reported a high correlation between NDVI and biomass, chlorophyll, leaf area, and yield (Jones et al., 2007, Koksal, 2011, Liu et al., 2004).

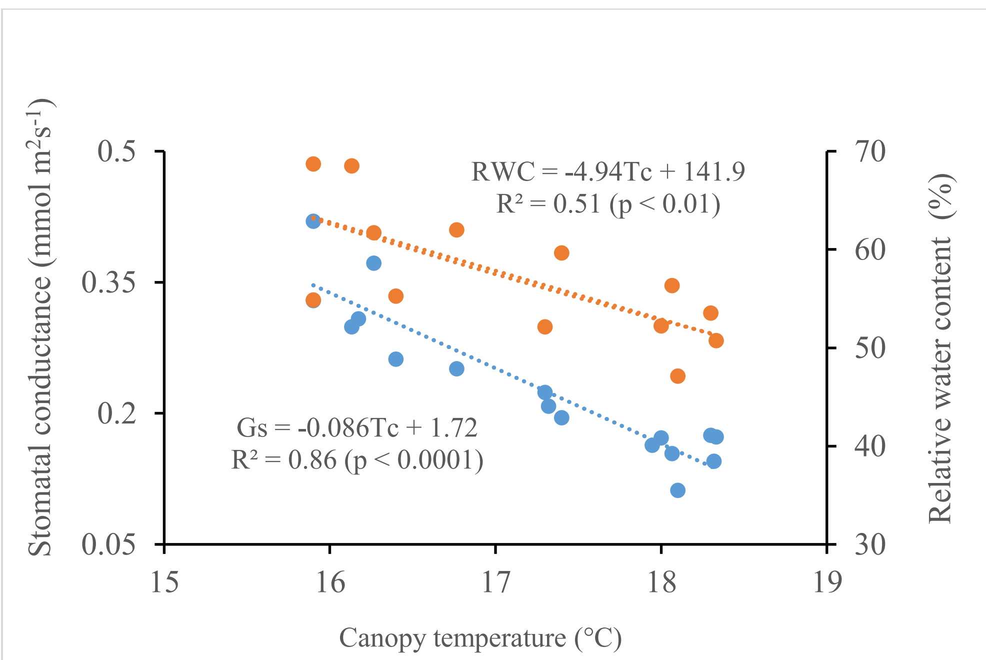

Fig. 3. 6. Relationship between stomatal conductance (mmol m^2s^{-1}), RWC (%) and leaf temperature (°C) of the bell pepper plants.

Jones et al. (2004) explained that although NDVI may be a good indicator of nitrogen content and biomass, it provides a medium estimate of plant water content. Usually, NDVI is not significantly correlated with stomatal conductance, which is affected by variations in environmental conditions such as vapor pressure deficit and air temperature, but it is strongly correlated to leaf area index (LAI) (Aguilar et al., 2012, Magney et al., 2016). The relationship between NDVI and LAI could be explored to monitor the effects of water stress on crop yield and provide appropriate information on the spatial and temporal variations in water stress levels and plant water requirements for precise irrigation water management. The significant correlation between PRI_{norm} and crop yield indicates that the index (PRI_{norm}) captured the effect of water stress on the photosynthetic pigment of the plant, which could have been responsible for the reduced crop yield of the stressed plants. The index generates a normalization that considers the chlorophyll content using the red edge index (R_{700}/R_{670}), which is sensitive to chlorophyll content and canopy leaf area reduction (RDVI) induced by stress. Also, the significant correlation between most of the reflectance indices and crop ET is indicative of the potential usefulness of the indices for improving agricultural water management, as crop ET is one of the best indicators of water stress.

The correlation between WI/NDVI and Tc indicates that the index detected changes in plant canopy structure induced by water stress. In most plants, the water index reflects water absorption in the mesophyll pigment and tends to increase as leaf RWC increases. Previous studies had observed significant relationships between WI and RWC (Amatya et al., 2012, Genc et al., 2011, Jones et al., 2004, Kittas et al., 2016), and this supports the use of water index for predicting plant water status. In this study, the crop reflectance indices and RWC were not significantly correlated. This is because bell pepper, like most isotropic crops, tends to maintain a stable leaf water status under a declining soil moisture condition and changing evaporative demand. However, the strong correlation between Tc and Gs showed in Fig. 3.6, indicates that Gs is a better indicator of water status in bell peppers than RWC.

3.6. Conclusions

The present study evaluated the sensitivity of spectral vegetation indices for monitoring water stress in greenhouse-grown bell pepper plants. The results indicated that water stress adversely affected crop yield, with the yield decreasing as irrigation water decreases. Generally, irrigation applications below 80% available water content caused a significant decrease in crop yield. The spectral vegetation indices were sensitive to different water stress levels in bell pepper plants. The results of this study indicate that the photochemical reflectance indices centered at 553 nm (PRI_{553}), water index (WI), renormalized difference vegetation index (RDVI), normalized photochemical reflectance index (PRI_{norm}), and the ratio of water index to normalized difference vegetation index (WI/NDVI) were the most useful indices for detecting water stress in bell pepper plants. Though it was challenging to select a single index as the best indicator of water status, the PRI_{553} showed strong correlations with all stress indicators. Previous studies suggested the use of photochemical reflectance indices centered at 570 nm (PRI_{570}) for monitoring water status of various plant species cultivated under open field conditions, but the findings of this experiment demonstrated that the PRI_{553} was better than the PRI_{570} when correlated to all water stress indicators in the greenhouse. Nevertheless, it is important to note that leaf biophysical and biochemical effects on the physiochemical reflectance index during the growing season could affect the use of the index for detecting water stress. Therefore, the integration of several crop reflectance indices using advanced data management tools are required to improve crop water stress monitoring and optimize irrigation water management.

It is recommended that future research should focus on the integration of thermal and spectral vegetation indices to precisely estimate plant water status. Real-time analysis of these data, which could be integrated into a crop water stress model, would provide a vital tool for greenhouse crop growers to aid in decision making and optimization of agricultural water use. It is further recommended that prospective irrigation scheduling models test and validate the above-mentioned spectral indices for irrigation management.

Connecting text

Following the literature review in Chapter II, it was imperative to investigate the feasibility of spectral reflectance indices in a wide range of vegetable crops. In this study, tomato crop, which is another widely cultivated high-value vegetable crop, was used as a test crop because tomatoes are highly sensitive to water stress. Thus, Chapter IV of this thesis examined the feasibility of spectral vegetation indices for monitoring water stress in greenhouse-grown tomato crops.

This study was published in *Computers and Electronics in Agriculture.* The paper was co-authored by Dr. Chandra A. Madramootoo, my supervisor. The original draft of this paper has been modified to ensure consistency with the thesis format. All the cited references are listed in the reference section. The funding used for this study was provided by my supervisor, Dr. Chandra A. Madramootoo.

CHAPTER IV

Sensitivity of spectral vegetation indices for monitoring water stress in tomato plants

4.1. Abstract

Innovations in irrigation water management are required to optimize agricultural water use in water-stressed regions of the world, and the physiological response of plants to water stress is an important criterion. Remotely sensed plant stress indicators, based on the visible and near-infrared spectral regions, provide an alternative to traditional field measurements of plant stress parameters, as this provides information about the spatial and temporal variability of crops and soil. The present study is a proof of concept on the feasibility of using narrow-band hyperspectral derived indices for monitoring water stress in tomato plants (Solanum Lycopersicum L.). Spectral reflectance data were acquired from tomato plants, with five different irrigation regimes namely 100, 80, 60, 40, and 20% of plant available water, in a completely randomized design. Also, plant water stress indicators including canopy temperature (Tc) and relative leaf water content (RWC), as well as volumetric soil moisture content (SMC) were concurrently measured with spectral data acquisition. Normalized Difference Vegetation Index (NDVI), Renormalized Difference Vegetation Index (RDVI), Optimized Soil Adjusted Vegetation Index (OSAVI), Photochemical Reflectance Index centered at 570 nm (PRI_{570}), normalized PRI (PRI_{norm}), Water Index (WI), and Normalized Water Index (NWI) were computed from the spectral data. The relationships between canopy reflectance and water stress indicators were analyzed at different water stress levels. The result showed that the PRI centered at 550 nm wavelength (PRI_{550}), WI, OSAVI, and WI/NDVI were the most sensitive indices to distinguish water stress levels in tomato plants. This study provides an insight into the feasibility of using spectral vegetation indices to monitor water stress in tomato crops for precision irrigation water management.

Keywords: Crop water stress; precision irrigation; tomato plants; spectral vegetation indices; hyperspectral data.

4.2. Introduction

Current irrigation scheduling techniques depend mainly on in-situ soil moisture measurements, weather-related variables, and physiological measurements of plant response to crop water stress (Ihuoma and Madramootoo, 2017). However, these methods are time-consuming, labor-intensive, and are limited in accounting for variability in soil and crop canopy conditions. Idso *et al*. (1978) stated that irrigation scheduling can be improved by monitoring the plant water status directly, rather than depending solely on soil water content measurements or estimates of evapotranspiration. Water stress induces stomatal closure, which reduces the transpiration rate, thus decreasing evaporative cooling and increasing leaf temperature. The increase in leaf temperature was earlier suggested (Idso et al., 1981, Jackson and Center, 1981) as a method of tracking water stress using infrared thermometers. More recently, high-resolution airborne thermal sensors flown over orchard crops detected differences in canopy temperature linked to water stress levels (Zarco-Tejada *et al*., 2012). The concept has been used in practice to monitor crop water stress and schedule irrigation of crops with great success as shown by Gonzalez-Dugo *et al*. (2014) and O'Shaughnessy *et al.* (2012).

However, various physiological concerns necessitated the investigation of alternative narrow-band hyperspectral indices for detecting crop water stress (Dangwal *et al.,* 2015). For instance, an increase in evaporative demands as a result of high vapor pressure deficits may induce a continuous decline in stomatal conductance, even when the plants were well watered (Zarco-Tejada *et al.,* 2012). Again, leaf temperature, though a direct indicator of plant transpiration, did not directly account for other physiological changes such as photosynthetic pigment changes or non-stomatal reductions of photosynthesis under water stress conditions (Zarco-Tejada *et al.,* 2013). Therefore, remotely sensed stress indicators that are based on visible and near-infrared spectral regions, which have high spatial and spectral resolutions that are difficult to obtain in the thermal regions, are of interest. The interest in reflectance indices is to use them to scale-up to satellite imagery since the use of thermal imagery may be limited by its poor resolution and mixed information obtained from the plant and the soil background (Gago *et al*., 2015).

Several optical reflectance indices such as Photochemical Reflectance Index (PRI_{570}), Normalized Difference Vegetation Index (NDVI), Renormalized Difference Vegetation Index (RDVI), normalized PRI (PRI_{norm}), Optimized Soil Adjusted Vegetation Index (OSAVI), Water Index (WI), WI/NDVI, and Normalized Water Index (NWI) have been investigated for predicting plant water status. A comprehensive review of the reflectance indices for monitoring crop water stress and scheduling irrigation has been detailed by Ihuoma and Madramootoo (2017) and Katsoulas et al. (2016).

In spite of these studies, a general agreement on the use of spectral vegetation indices (VIs) for crop water stress monitoring is yet to be reached due to numerous confounding factors (such as canopy structure, soil background, leaf thickness, and leaf surface properties) affecting the VIs at plant canopy levels. Narrow-band optical indices for detecting water stress and scheduling irrigation has been extensively investigated for tree and cereal crops grown under open field conditions (Dangwal et al., 2015; Elvanidi et al., 2017; Magney et al., 2016; Panigada et al., 2014; Rossini et al., 2013). However, there is little reported work on high-value vegetable crops grown under greenhouse conditions (Ihuoma and Madramootoo, 2019). The findings of the open field studies are not applicable for irrigation scheduling in greenhouse-grown vegetables (Katsoulas et al., 2016), because the VIs threshold for monitoring plant water status is crop and climate-specific. Therefore, it is essential to assess spectral VIs for supporting precision irrigation to improve yields of greenhouse-grown vegetable crops.

The objective of this study was to investigate the possibility of using VIs to detect water stress for optimizing irrigation water use efficiency in tomato crops grown under greenhouse conditions. Specifically, the objectives were to: (i) evaluate and compare various spectral VIs for monitoring water stress in tomato plants; (ii) test different PRI formulations for detecting water stress in tomato plants, by changing the normalization bands from 530 nm to 570 nm; and (iii) determine the relationship between VIs and tomato water stress.

4.3. Materials and methods

4.3.1. Experimental design and irrigation treatments

This study was carried out in the greenhouse at the Macdonald Campus of McGill University, Ste Anne De Bellevue, Quebec, Canada. The study area lies at latitude 45.438 °N and longitude 73.938 °W with an elevation of 36 m. The greenhouse has a dimension of 32 x 7 x 5 m and was covered with single pane tempered glass, which allows about 95% of light transmission. The greenhouse roof was inclined at an angle of 37° to the horizontal. The cover material is not expected to influence the leaf spectral measurements and results, due to its high transmissivity. According to Shamshiri et al. (2018), change in a light quality of about 10% would have no influence on plant biochemistry and photosynthetic activities. Ventilation in the greenhouse was regulated through automatically controlled vents (Argos Electronics, Athens, Greece), two side roll-up windows, and a flap roof window. Heating was provided via aboveground PVC pipes and a fan coil located at a height of 2.6 m. Climate set points were; 24/14°C for temperature (day/night), a relative humidity of 78%, and CO_2 partial pressure 500 μbar.

Picus tomato (Solanum Lycopersicum L.) seedlings, 42-days old, were transplanted on August 6, 2016, into 25 pots (18-L each and one plant per pot) using soil from the Horticultural research center of McGill University; the plants were harvested on December 24, 2016. Each of the pots has a depth of 32 cm and a diameter of 27 cm. The soil was a sandy clay loam with sand, silt, and clay content of 48, 22, and 30% respectively (USDA-NRCS, 2000); field capacity of 33% and permanent wilting point of 17% by volume. The pots were placed on 330 × 150 × 150 mm bricks, which were randomly positioned at the center of the greenhouse at a spacing of 0.6 m by 0.6 m, to minimize variabilities from the greenhouse materials (such as doors, ceiling, light source or walls). A tap was fixed to each of the pots so that excess water can drain out. The pots were saturated and allowed to drain out for 24 hours so that the soil water content can be at field capacity before crops were transplanted. Drained water was collected by means of a measuring cylinder placed under each tap.

The experiment was arranged in a completely randomized design with five (5) water treatment levels of 100, 80, 60, 40, and 20% of plant-available water. Irrigation applications were based on the plant available water (AWC), and the soil moisture content in each pot was continuously measured with soil moisture sensors. The upper irrigation threshold was set as the water treatment level in each treatment (100, 80, 60, 40, and 20% AWC) and a lower irrigation threshold was at 10% AWC depletion for each treatment. Irrigation events commenced when soil moisture content for each pot depleted to its lower moisture threshold (10% AWC) and was terminated when the upper threshold was reached, as shown by the soil moisture sensors. The irrigation scheduling process for each plot was done throughout the growing season. The volume of water applied during each irrigation event to each pot was determined as the product of the irrigation duration and the flow rate per pot, while the equivalent irrigation depth applied at each irrigation event for each pot was determined as the product of the volumetric water content and the plant rooting depth. Irrigation water was applied through a drip system, with emitters placed in each pot. The drip system consists of pressure compensating emitters, with a discharge of 2 L/h, and the flow rates were calibrated in the greenhouse. The water application in each pot was regulated using a water control valve attached to each dripper. When the required moisture content for each pot was achieved, irrigation was terminated for that pot by turning off the valve. Irrigation was uniformly applied to all treatments at the beginning of transplanting, based on 100% replenishment of water in the plant root zone to field capacity for plants to be well established; thereafter, variable rate irrigation was applied until harvest.

Soil water contents at the five water treatment levels were replenished using continuous Time Domain Reflectometers (TDR) (CS625 water content reflectometer, Campbell Scientific Inc., UT) installed vertically at a depth of 30 cm in each pot, to correspond with the plant rooting depth (Jaria and Madramootoo, 2013). TDR readings were calibrated in the greenhouse with gravimetric soil moisture measurements, and the sensors were installed with the aid of an insertion guide following the procedures articulated in the Sentek manual (Sentek Sensor Technologies, 2003). The soil moisture sensors were connected to solar-powered data loggers (model CR205/6, Campbell Scientific Inc.). The data was scanned every 5 minutes and recorded every 15 minutes¸ hourly and daily and was retrieved from the CR205/6 using a computer and Campbell Scientific Inc. LoggerNet software. Fertilizer applications were based on guidelines for greenhouse-grown tomatoes at the Macdonald campus of McGill University. The plants were fertilized biweekly with 20-20- 20 N-P-K water-soluble fertilizer, at a rate of 4 kg of N hectare^{-1}. This was changed to calcium nitrate after the first fruits were noticed and were later changed to potassium nitrate when the fruits were approaching maturity. Fertilizer application was the same for all the treatments to avoid nutrient stress.

4.3.2. Measurements

Daily air temperature, relative humidity, and vapor pressure deficit were measured in the greenhouse using a Campbell scientific psychrometer (Campbell Scientific, Logan, UT) installed about 1 m above the plant canopy. Evapotranspiration (ET) in the greenhouse was estimated during the growing season based on the soil moisture approach as shown in Eq. 4.1:

$$SWC_t = SWC_{t-1} + I - D - ET \dots\dots\dots\dots\dots\dots\dots\dots (4.1)$$

where, SWC_t: Soil water content today (mm), SWC_{t-1}: Antecedent soil water content (mm), I: Irrigation depth since yesterday (mm), D: Drained water from the soil column (mm), ET: Crop evapotranspiration (mm), $SWC_t - SWC_{t-1}$: Soil water storage (ΔS).

4.3.2.1. Spectral data acquisition and processing

A miniature fiber optic spectrometer (Blue-wave, Stellar Net Inc., FL, USA), which measures reflectance in the 200–1150 nm spectral range, was used to measure canopy reflectance. The spectrum is characterized by a 0.5 nm spectral resolution and was calibrated before each reading was taken. The calibration process involved holding the probe at 45° to a white standard (reference), at a distance of about 64 mm, to optimize the integration time (typically set at 50 ms), recording dark current, and then obtaining target reflectance. All canopy spectral measurements were taken under clear sky conditions between 10:00 and 15:00 hours to ensure maximum solar intensity when the sun was shining directly on the plants, as adopted in a similar study (Zhao *et al.,* 2017). The spectrometer was positioned at a height of 30 cm from the plant canopy so that it viewed only the plant canopy. Five leaves were measured in every pot and four scans were averaged in every measurement, considering four (north, south, east and west) viewing directions.

The spectral data acquisition was conducted five times (16 and 21 September; 10, 18, and 25 October 2016), during the plant growing season and the data were used for spectral data calculation and estimation of vegetation indices.

Due to the absorption of atmospheric water, signal background, and light scattering effects, the spectral reflectance contains substantial interference noise (Zhao et al., 2017), which must be eliminated as it affects the smoothness of the spectral curve. The most commonly used smoothing algorithms include the moving average method, fitting polynomial method, wavelet transform and various regression smoothing methods. The 7-point weighted moving average method was used to smooth the spectral curve in this research, as adopted by Zhao et al. (2017).

The spectral indices used in this study were obtained from the optical reflectance measurements from each treatment and are presented in Table 4.1. The reflectance indices used in this study were divided into three (3); the xanthophyll pigment indices related to photosynthetic pigment changes, the structural/greenness indices related to the canopy structure and biomass, and the water indices related to the water content of the plant.

4.3.2.2. Measurement of plant stress indicators

Leaf temperature was measured with handheld infrared thermometry set at an emissivity of 0.95 W m^{-2} (Fluke 572 model, Fluke Corporation, Everett, WA). The instrument was held about 1.5 m above ground level and directed at the leaf of the tomato plant with a laser point of the instrument set at an angle about 30° to the horizontal (Orta *et al.*, 2002). Four infrared thermometer measurements were made when the plant canopy covered about 80% of the pot area. The temperature of the stressed and non-stressed plants was determined from canopy temperature data; four (north, south, east and west) viewing directions were considered and average temperature values obtained. Measurements were made between 11:30 h and 14:00 h to ensure maximum solar intensity when the sun was shining directly on the plants. Relative water content (RWC) compares the water content of a leaf with the maximum water content at full turgor and was considered as an indicator of water status (Colombo *et al.,* 2011). Leaf sampling was conducted on each treatment with the collection of the youngest fully expanded leaf from each plant. The leaf samples were enclosed in a sealed plastic bag and kept in a cooler at 5 °C until they reached the laboratory. Fresh weight (FW) was recorded using an analytical balance, and the samples were immersed in distilled water for 72 h, blotted and weighed to obtain the turgid weight (TW). Finally, leaf samples were dried at 72 °C in an oven, until constant dry weight (DW) was reached. The RWC was calculated according to Eq. 4.2, as adopted by similar studies on crop water stress (Wang *et al.,* 2015).

$$RWC = \frac{FW - DW}{TW - DW} 100\ (\%) \dots \dots \dots \dots \dots \dots \dots .. (4.2)$$

4.3.3. Statistical analysis

Statistical analyses were carried out on vegetation indices (NDVI, OSAVI, RDVI, PRI_{570}, PRI_{550}, PRI_{norm}, WI, and NWI), stress indicators (Tc, RWC, and SMC), total marketable yield, Irrigation Water Use Efficiency (IWUE) and water applied for each treatment using a regression analysis and PROC/GLM (General Linear Model) procedure of SAS software (version 9.3, SAS Institute, Inc., Cary, NC, USA). One-way analysis of variance (ANOVA) was conducted, and the significance of differences among treatments was separated using Fisher's Least Significant Difference (LSD) at a 5% probability level. The values of vegetation indices were related to values of RWC, T_c, SMC, and yield of each of the treatments using linear regression.

Table 4. 1. Optical indices used in this study, their formulations and references

Names	Index	Formulation	Reference
Xanthophyll pigments			
Photochemical Reflectance Index	PRI_{570}	$(R_{570} - R_{531})/(R_{570} + R_{531})$	Gamon *et al* (1992)
	PRI_{550}	$(R_{550} - R_{531})/(R_{550} + R_{531})$	Gamon *et al* (1992)
Normalized Photochemical Reflectance Index	PRI_{norm}	$PRI/(RDVI * (R_{700}/R_{670}))$	Berni *et al (*2009)
Greenness Indices			
Normalized Difference Vegetation Index	NDVI	$(R_{800} - R_{670})/(R_{800} + R_{670})$	Rouse *et al* (1974)
Renormalized Difference Vegetation Index	RDVI	$(R_{800} - R_{670})/(R_{800} + R_{670})^{1/2}$	Rougean and Breon (1995)
Optimized Soil Adjusted Vegetation Index	OSAVI	$(1 + 0.16)(R_{800} - R_{670})/(R_{800} + R_{670} + 0.16)$	Haboudane *et al* (2002)
Water content Indices			
Water Index	WI	R_{900}/R_{970}	Penuelas *et al* (1997)
Normalized Water Index	NWI	$(R_{970} - R_{900})/(R_{970} + R_{900})$	Bandyopadhyay *et al* (2014)
	WI/NDVI	WI/NDVI	Penuelas *et al* (1997)

where R represents the reflectance values at the indicated wavelengths in nm.

4.4. Results

4.4.1. Crop evapotranspiration and applied irrigation water

Mean daily air temperature, humidity, and vapor pressure deficit in the greenhouse ranged from 19 to 28 °C, 60 to 86%, and 0.31 to 1.51 kPa, respectively, during the growth period. The crop evapotranspiration was higher during the flowering and maturity stages of plant growth, as these correspond to the periods when the crops need more water for their physiological development. The ET_c increased generally with irrigation water amount and the total seasonal ET_c ranged from approximately 197 to 321 mm. The total water applied for each treatment ranged from 73 to 230 mm during the growth period, as shown in Table 4.2. The difference between the ETc and total water applied represents water storage in the pot.

4.4.2. Soil water content

Volumetric soil water content for the various water treatment levels are presented in Fig. 4.1. A comparison of different water stress conditions showed that soil water content was low in high stressed conditions. Soil water content generally decreased with decreasing water application, with 100 and 20% AWC resulting in the highest and lowest values of soil water content, respectively. Soil water content remained relatively low for 20, 40, and 60% AWC treatments due to insufficient supplementary irrigation, while the soil water content for 100% AWC treatment was kept at a high level during the growing season. The 100% AWC treatment was not significantly different from the 80% AWC treatment but reached the highest yield.

Table 4. 2. Water applied (mm) for tomato plants per growth stage for different treatments

		Treatments (% of AWC)				
Growth stages	Days	100%	80%	60%	40%	20%
Initial	30	48.00	45.12	42.24	39.36	36.48
Flowering	40	62.40	49.92	37.44	24.96	12.48
Maturity	45	72.00	57.60	43.20	28.80	14.40
Senescence	30	48.00	38.40	28.80	19.20	9.60
Total	145	230.40	191.04	151.68	112.30	72.90

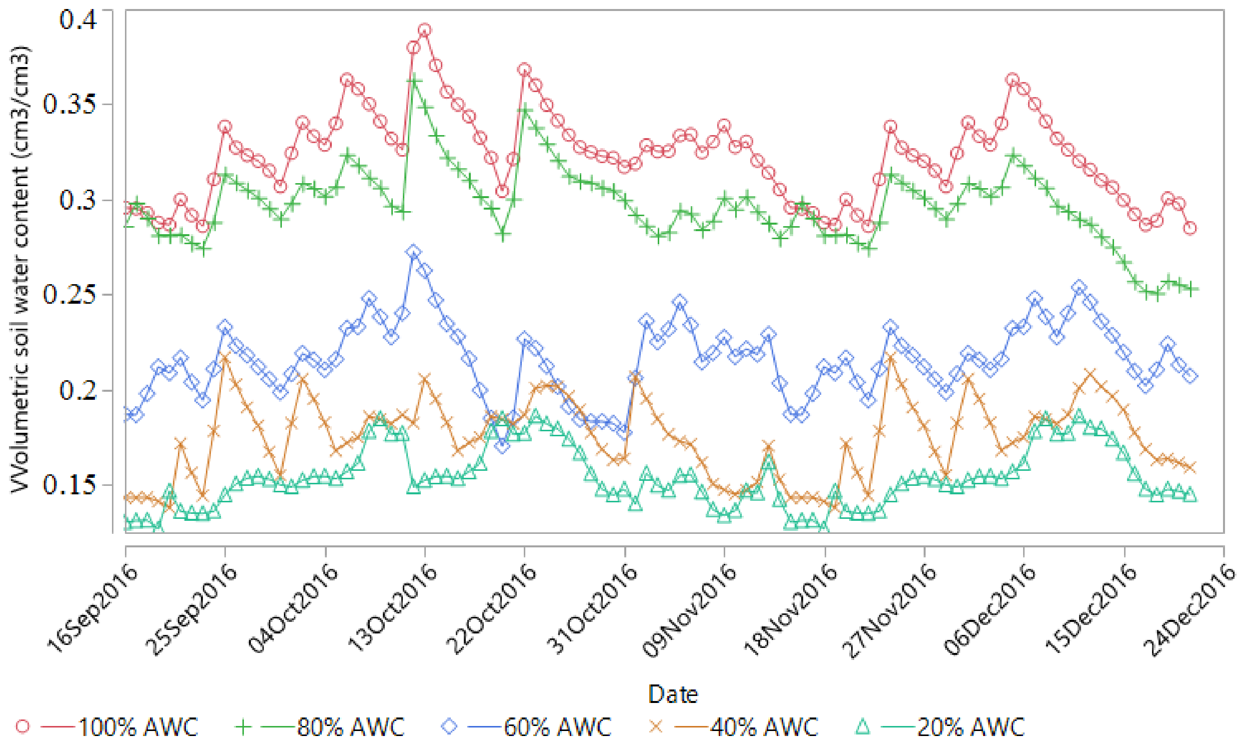

Fig. 4. 1. The volumetric soil moisture content at various treatment levels during the growing season.

4.4.3. Yield and irrigation water use efficiency

The effects of the irrigation treatments on marketable yields and Irrigation Water Use Efficiency (IWUE) are shown in Table 4.3. The total marketable yield ranged from 0.46 to 2.28 kg plant^{-1}, for 20 and 100% AWC treatments, respectively. The highest mean marketable yield was obtained from 100% AWC treatment (1.83 kg plant^{-1}) while the least mean marketable yield was obtained from 20% AWC treatment (0.40 kg plant^{-1}). The average yield from the full irrigation treatment (100% AWC) was statistically different from the yields obtained from the 60, 40, and 20% AWC treatments, but not significantly different from the yield obtained from 80% AWC. This indicates that water stress caused significant declines in crop yield, at $p < 0.05$.

Table 4. 3. Effects of irrigation treatments on Marketable yield (kg plant^{-1}) and Irrigation Water Use Efficiency (kg m^{-3})

Treatments (% AWC)	Marketable yield (kg plant^{-1})	Depth of Irrigation water applied (m^{-3} m^{-2})	IWUE (kg m^{-3})
100	1.83^{a}	0.23	17.72^{ab}
80	1.52^{ab}	0.19	17.83^{a}
60	1.06^{bc}	0.15	15.63^{bc}
40	0.68^{cd}	0.11	13.57^{cd}
20	0.40^{d}	0.07	12.18^{d}

$^{a\text{-}d}$Means followed by the same letter within a column are not significantly different at $p = 0.05$. Reported values are averages of five replicates.

The IWUE was calculated as the ratio between marketable yield (kg plant^{-1}) and the total volume of water applied (m^{3}). The highest IWUE value (17.83 kg m^{-3}) was recorded with 80% AWC, as shown in Table 4.3, but this is not statistically different from the IWUE value obtained from 100% AWC. Both the 100% and 80% AWC values were different from the other water treatments. Water stress less than 80% AWC treatment caused an evident decrease in crop yield, as shown in Table 4.3. The IWUE is important for most crops as it indicates the optimal use of water in agriculture (Rinaldi *et al.,* 2015).

4.4.4. Crop reflectance

Examples of the spectral signature of the plant canopy obtained from the crop reflectance values, which was measured with a portable spectrometer, are presented in Fig. 4.2(a). The leaf reflectance in the five water treatments showed similar trends during the entire growth stage and varied among irrigation treatments. However, the spectral response for water stress was more evident in the

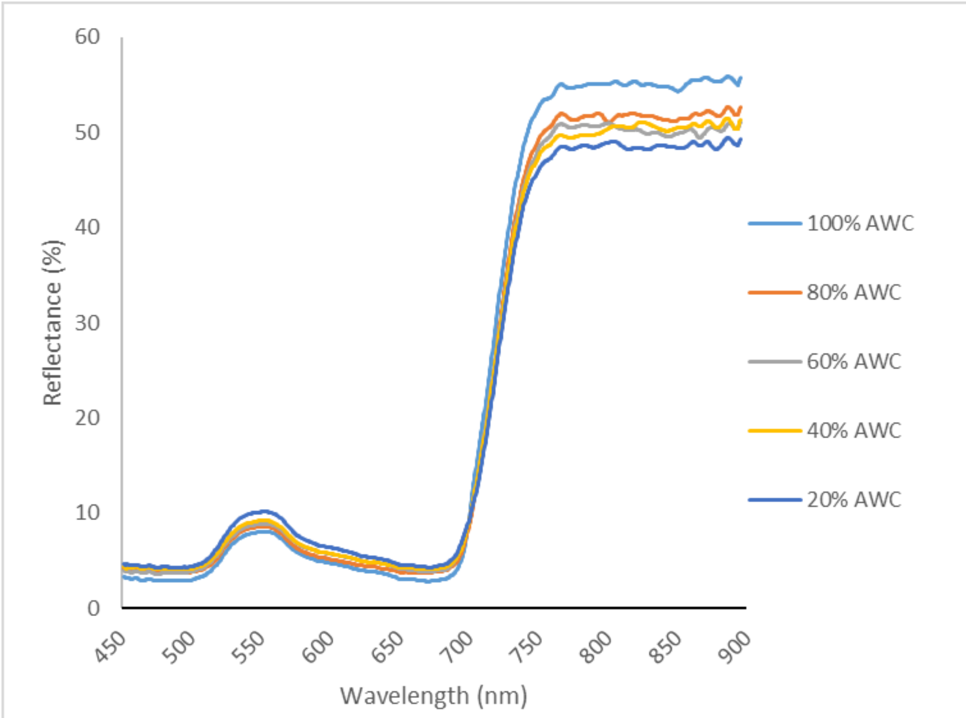

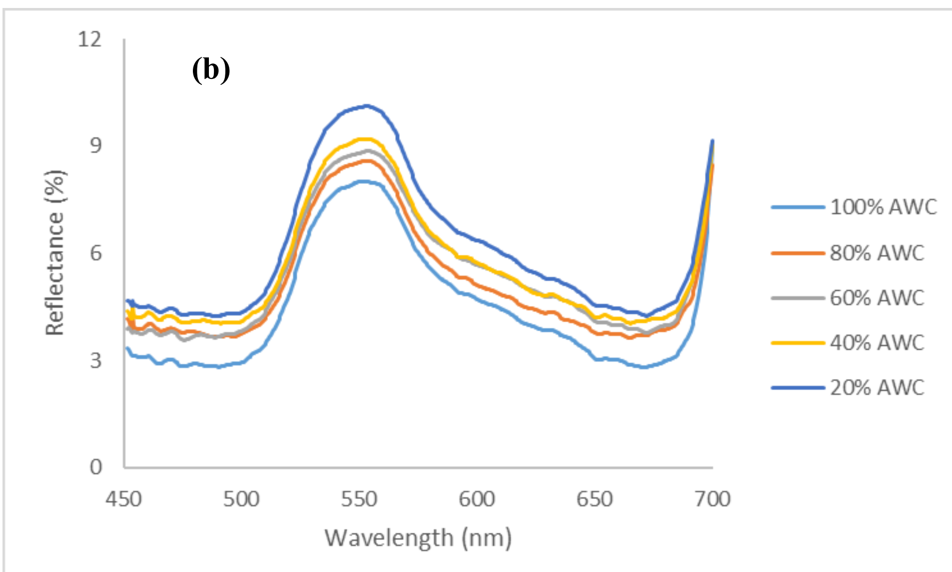

Fig. 4. 2. Examples of the spectral signature of tomato plants under different water stress conditions (a) 450 – 900 nm; (b) 450 – 700 nm.

flowering and early maturity stages, because the plants are more sensitive to water stress at these stages. Thus, hyperspectral reflectance in the flowering and early maturity stages was used to identify the water stress levels. The spectral reflectance curves show peaks near 550 nm and 668 nm, and trough near 680 nm, and follow a similar pattern for each of the treatments, with the 100% AWC and 20% AWC recording the lowest and highest reflectance values in the visible spectral range (400 – 700 nm), respectively, as shown in Fig. 4.2(b).

The measured values of leaf reflectance were used for the calculation of spectral vegetation indices presented in Table 4.1. The response of various vegetation indices to water stress in tomato plants is shown in Fig. 4.3. Statistical analysis of the indices revealed that PRI_{550}, WI, OSAVI, WI/NDVI were significantly related to water stress in tomato plants, while NDVI, RDVI, and PRI_{norm} showed no significant differences among various water stress levels. There is no significant difference between 100% AWC and 80% AWC for most of the indices, as shown in Fig. 4.3. However, there was a significance difference when the AWC depletes below 20%, in all the reflectance indices. This shows that the identified indices successfully detected high water stress in the plants.

4.4.5. Testing spectral vegetation indices

Plant water stress detection using optical reflectance indices were tested using the reflectance indices specified in Table 4.1. The selected indices were separately correlated to canopy temperature, relative water content, yield, and soil water content, which were concurrently measured at the time of spectral data acquisition. From the results, the structural indices (NDVI, OSAVI, RDVI) were significantly correlated with Tc ($R^2 = 0.51$, $p < 0.01$; 0.40, $p < 0.05$; 0.59, $p < 0.05$; respectively), and with RWC ($R^2 = 0.41$, $p < 0.05$; 0.48, $p < 0.05$; 0.61, $p < 0.01$; respectively).

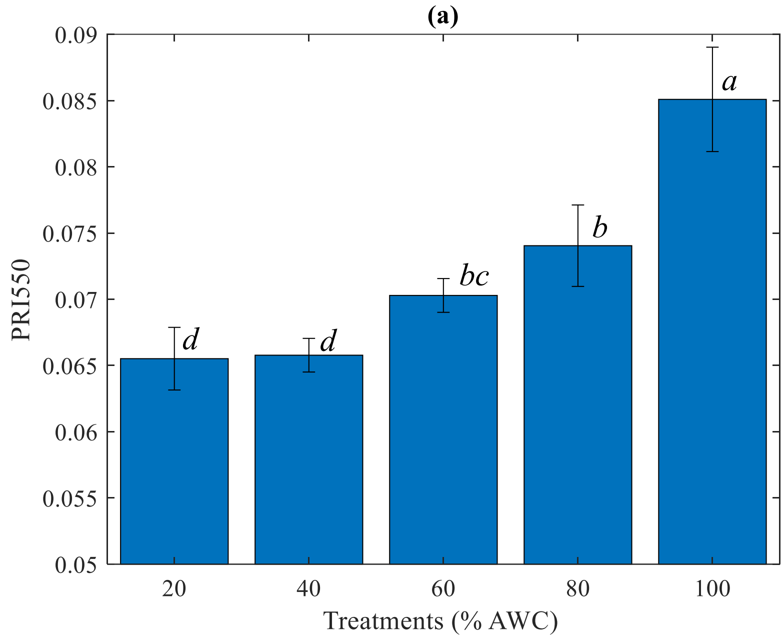

(a)
PRI550
0.09
0.085
0.08
0.075
0.07
0.065
0.06
0.055
0.05
20
40
60
80
100
Treatments (% AWC)
d
d
bc
b
a

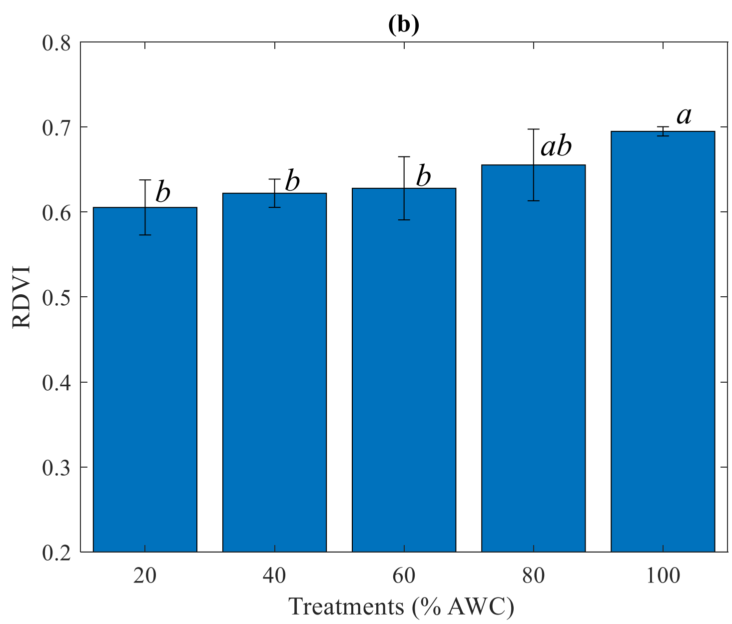

(b)
RDVI
0.8
0.7
0.6
0.5
0.4
0.3
0.2
20
40
60
80
100
Treatments (% AWC)
b
b
b
ab
a

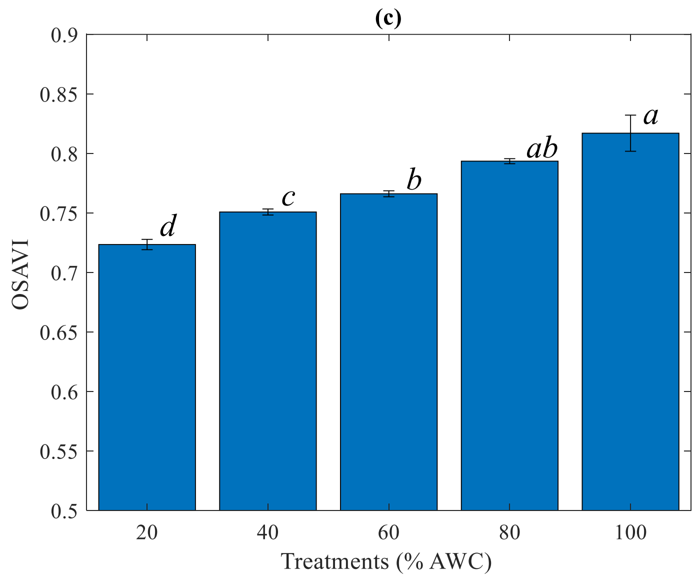

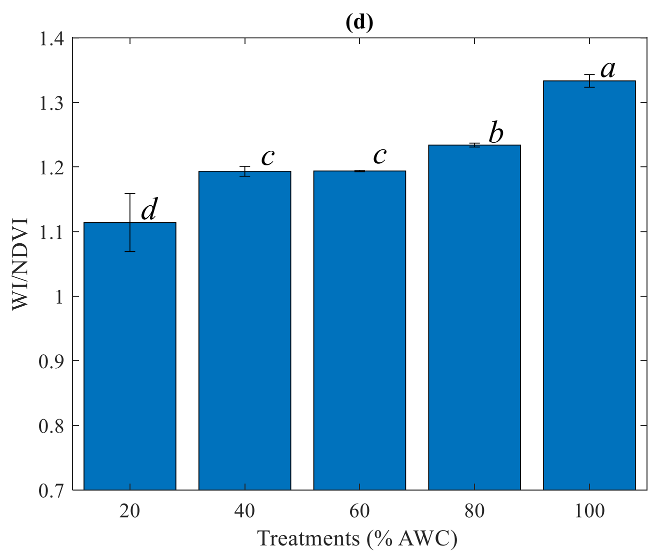

Fig. 4. 3. Responses of various vegetation indices (a) PRI_{550}, (b) RDVI, (c) OSAVI, and (d) WI/NDVI) to water treatments in tomato plants. [a-d] Means followed by the same letter are not significantly different at p = 0.05. Reported values are averages of five replicates.

Table 4.4 summarized the coefficient of determination of the linear relationship between vegetation indices and plant stress parameters, under different water stress levels. The results indicate that the correlations between structural indices and crop yield were significant ($R^2 = 0.65$, $p < 0.001$; and 0.60, $p < 0.001$; for OSAVI and RDVI, respectively). The results of the relationships between spectral vegetation indices and volumetric water content indicated that NDVI, OSAVI, and RDVI were significantly related to volumetric soil moisture content ($R^2 = 0.89$, $p < 0.05$; 0.88, $p < 0.01$; and 0.86, $p < 0.05$; respectively).

The xanthophyll pigment indices correlated differently with the various stress parameters. Fig. 4.4 shows the relationship between vegetation indices and canopy temperature obtained from the various treatments. The PRI_{550} showed significant correlation with all the measured plant stress indicators, with $R^2 = 0.66$, $p < 0.01$; 0.69, $p < 0.001$; 0.81, $p < 0.05$; and 0.67, $p < 0.0001$; for the RWC, Tc, SWC, and yield, respectively. The PRI_{570} was weakly correlated to all the measured stress parameters, with $R^2 = 0.21$, 0.38, 0.47, and 0.39 for the RWC, Tc, SWC, and yield, respectively. However, the correlation between PRI_{570} and the measured water stress indicators were not statistically significant at $p < 0.05$, as shown in Table 4.4. The PRI_{550} showed the highest correlation with crop yield ($R^2 = 0.67$, $p < 0.0001$), which indicates that water stress adversely affected the photosynthetic activities of the plants, leading to reduced crop yield. The PRI_{norm} showed high correlation with relative water content ($R^2 = 0.86$, $p < 0.0001$), as shown in Fig. 4.5, which indicates high sensitivity to plant water stress and implies that water stress-induced changes in xanthophyll pigment. The index generates a normalization that considers the chlorophyll content using the red edge index (R_{700}/R_{670}), which is sensitive to chlorophyll content, and canopy leaf area reduction (RDVI) induced by stress. Also, the index showed a good correlation with soil moisture content ($R^2 = 0.82$, $p < 0.05$), but was less correlated with Tc ($R^2 = 0.31$, $p < 0.05$) and yield ($R^2 = 0.35$, $p < 0.05$).

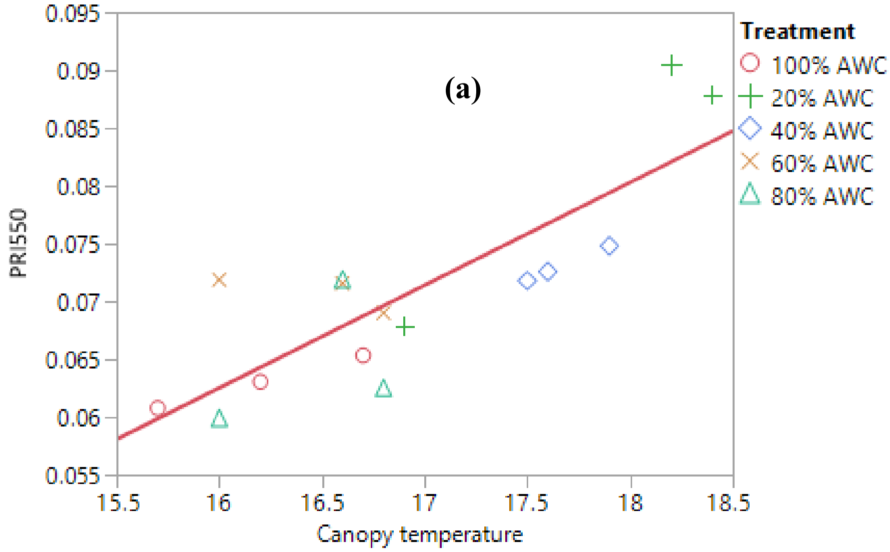

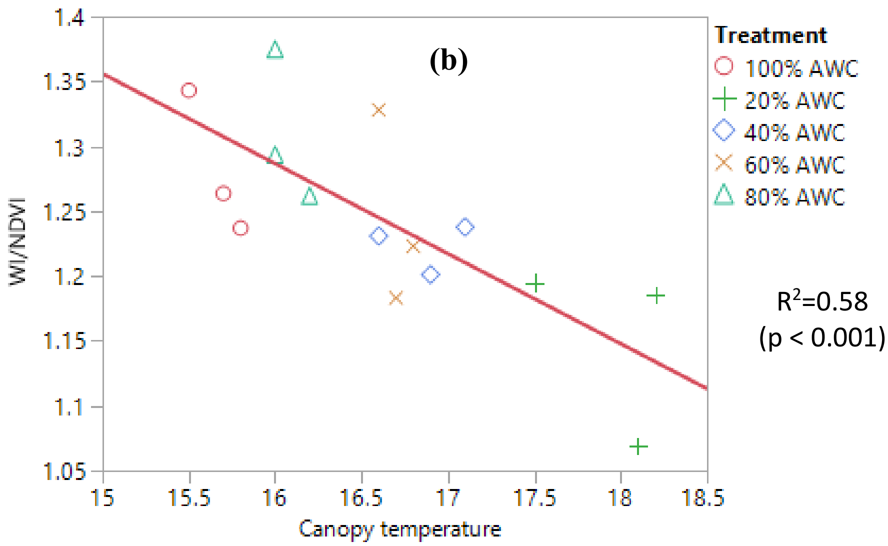

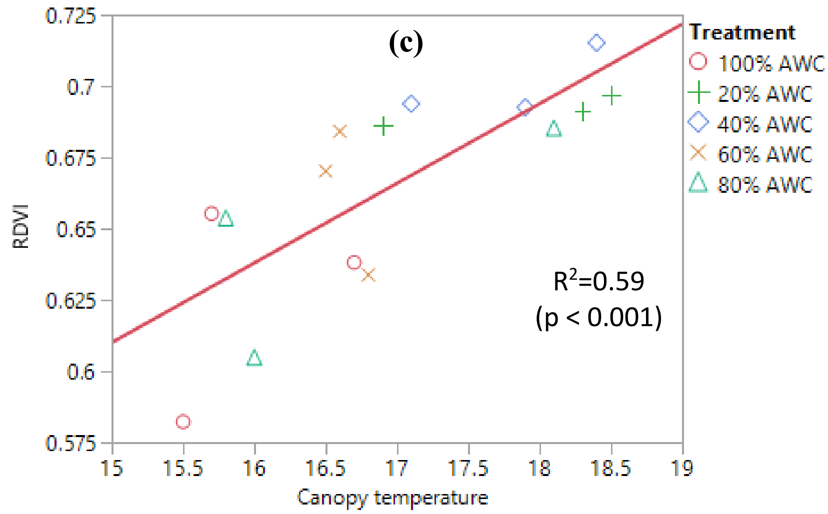

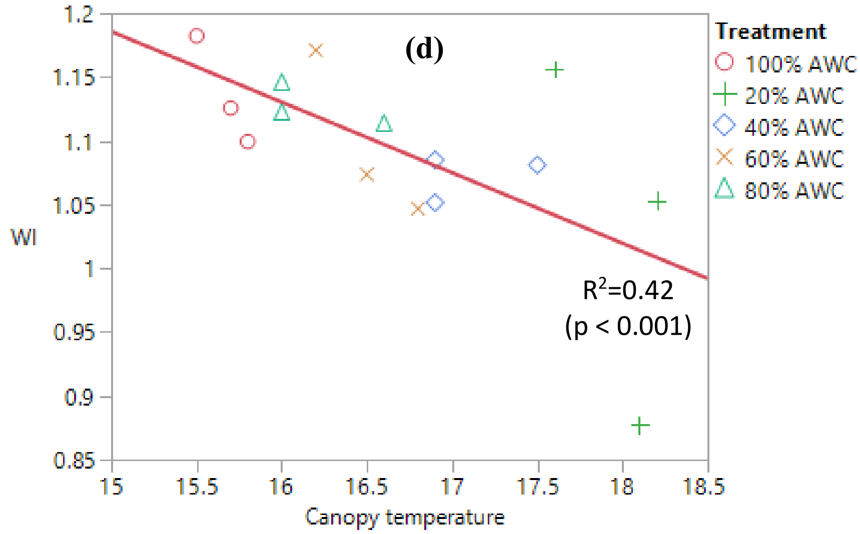

Fig. 4. 4. Relationship between (a) PRI_{550} (b) WI/NDVI (c) RDVI (d) WI and canopy temperature (°C) obtained from the various treatments.

Table 4. 4. Coefficient of determination (R^2) of the linear relationship RWC (%), Tc (°C), Yield (kg/plant), and SMC (%), and vegetation indices (VIs) computed from the hyperspectral sensor. The highest significant index for each variable is in bold print.

VIs	RWC (%)	Tc (°C)	SMC (%)	Yield (kg/plant)
NDVI	0.41*	0.51**	0.89*	0.44**
RDVI	0.61**	0.59**	0.86*	0.6***
OSAVI	0.48*	0.41*	0.88**	0.65***
PRI_{570}	0.21*	0.38*	0.47*	0.39*
PRI_{550}	0.66**	0.69***	0.79*	0.67****
PRI_{norm}	0.86****	0.31*	0.82*	0.35*
WI	0.69**	0.42*	0.51*	0.39*
WI/NDVI	0.55*	0.58***	0.39*	N. S
NWI	0.43*	0.59***	0.82*	0.64***

*Where * p < 0.05, ** p < 0.01, *** p < 0.001, **** p < 0.0001, and N. S = not significant.*

The water index was correlated to RWC and yield, with $R^2 = 0.69$ and 0.59 respectively, at $p < 0.05$; but was weakly correlated to Tc, with $R^2 = 0.42$, $p < 0.05$ (Table 4). The WI/NDVI showed significant correlation with RWC ($R^2 = 0.54$, $p < 0.05$), Tc ($R^2 = 0.58$, $p < 0.001$), but was not significantly related to SMC and crop yield (Table 4).

Fig. 4.6 showed that the various treatment levels had significant differences in Tc, with the non-stress and fully-stressed treatments recording the least and highest Tc values. Consequently, the magnitude of Tc was greater in non-irrigated plants. RDVI showed a significant correlation with Tc ($R^2 = 0.59$, $p < 0.01$), and this could imply that changes in canopy structure occurred as a result of water stress. Fig. 4.6 also revealed that the RWC was significantly different among the various water treatment levels. The non-stressed and fully-stressed treatments recorded the highest and lowest RWC. Again, the PRI_{550} had a significant positive correlation with RWC ($R^2 = 0.67$, $p < 0.01$). However, the renormalized PRI (PRI_{norm}) showed the best correlation with RWC ($R^2 = 0.86$, $p < 0.0001$), indicating a correlation with xanthophyll pigments and the carotenoid content. The correlation between the leaf relative water content and canopy temperature was analyzed, and the result is shown in Fig. 4.7. The analysis showed a strong correlation between the leaf relative water content and canopy temperature, with $R^2 = 0.93$ ($p < 0.0001$). The graph revealed that leaf relative water content increased linearly with decreasing leaf temperature.

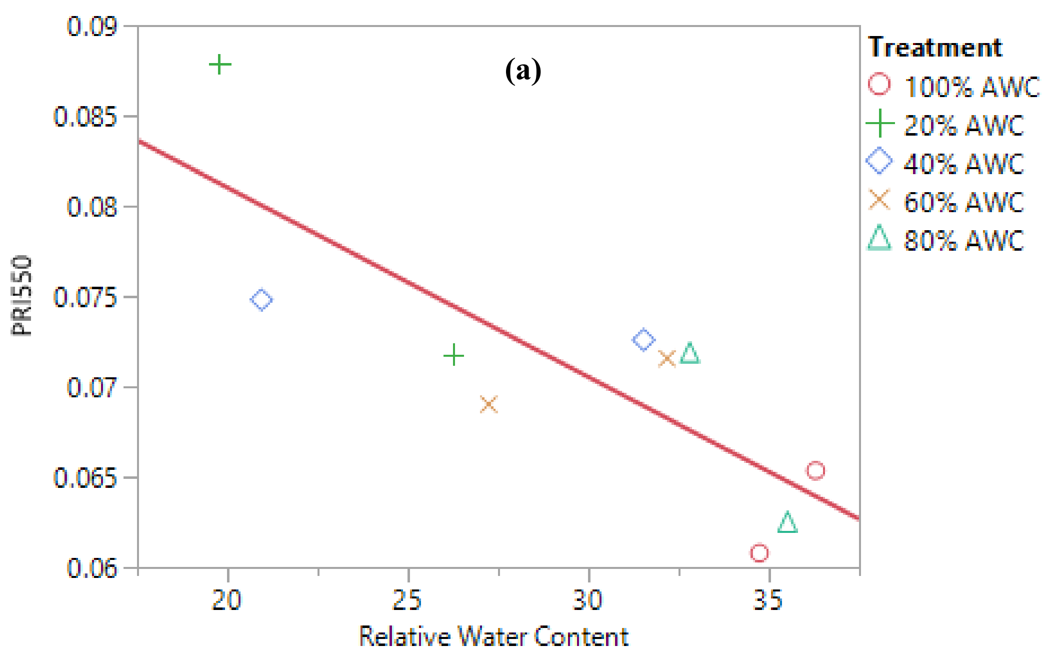

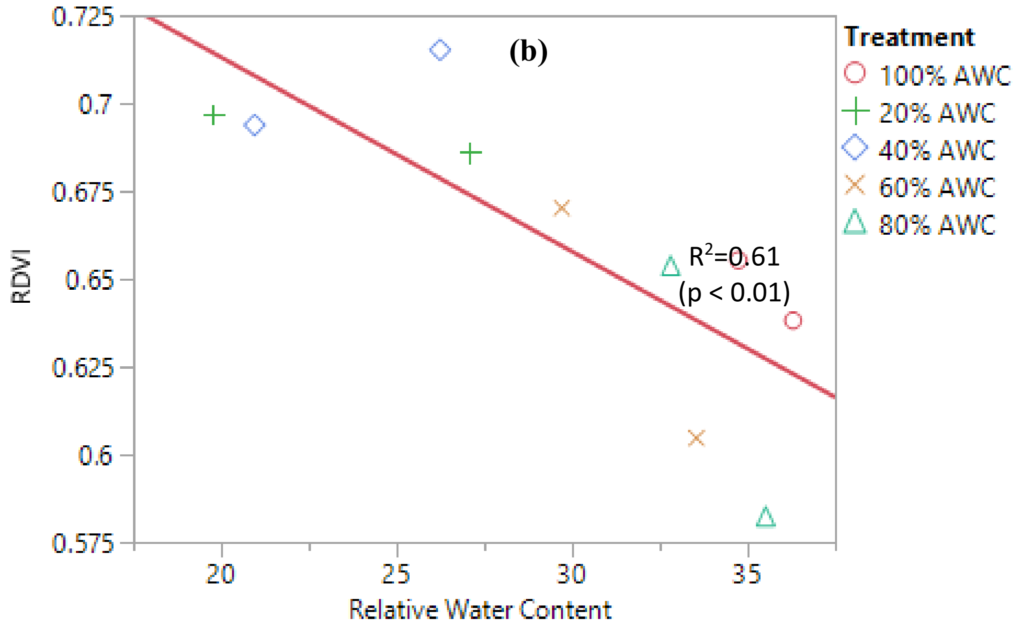
(b)
RDVI
0.725
0.7
0.675
0.65
0.625
0.6
0.575
20
25
30
35
Relative Water Content
R2=0.61
(p < 0.01)
Treatment
100% AWC
20% AWC
40% AWC
60% AWC
80% AWC

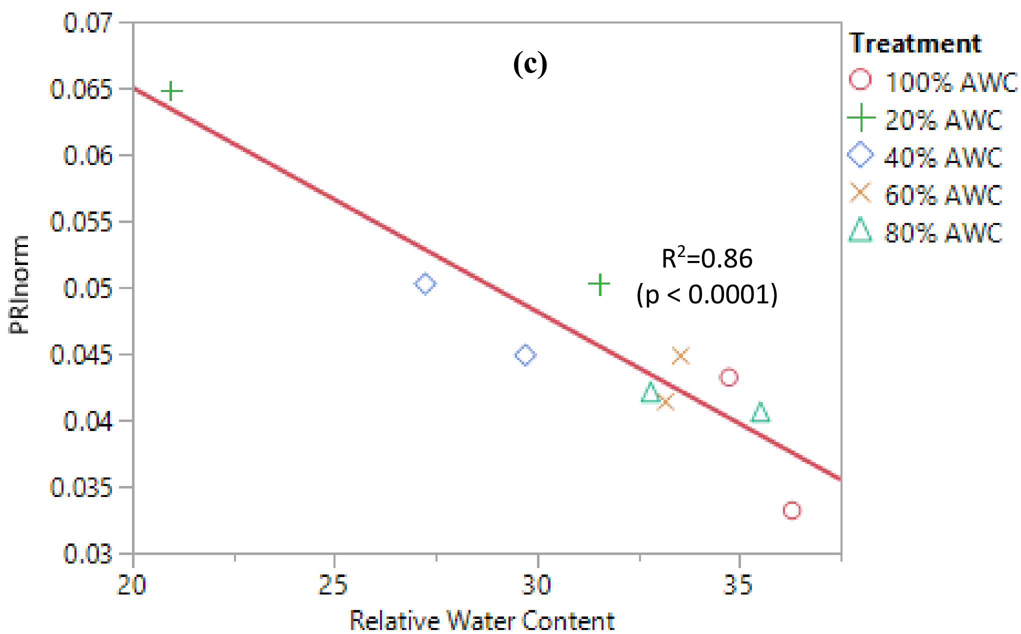
(c)
PRInorm
0.07
0.065
0.06
0.055
0.05
0.045
0.04
0.035
0.03
20
25
30
35
Relative Water Content
R2=0.86
(p < 0.0001)
Treatment
100% AWC
20% AWC
40% AWC
60% AWC
80% AWC

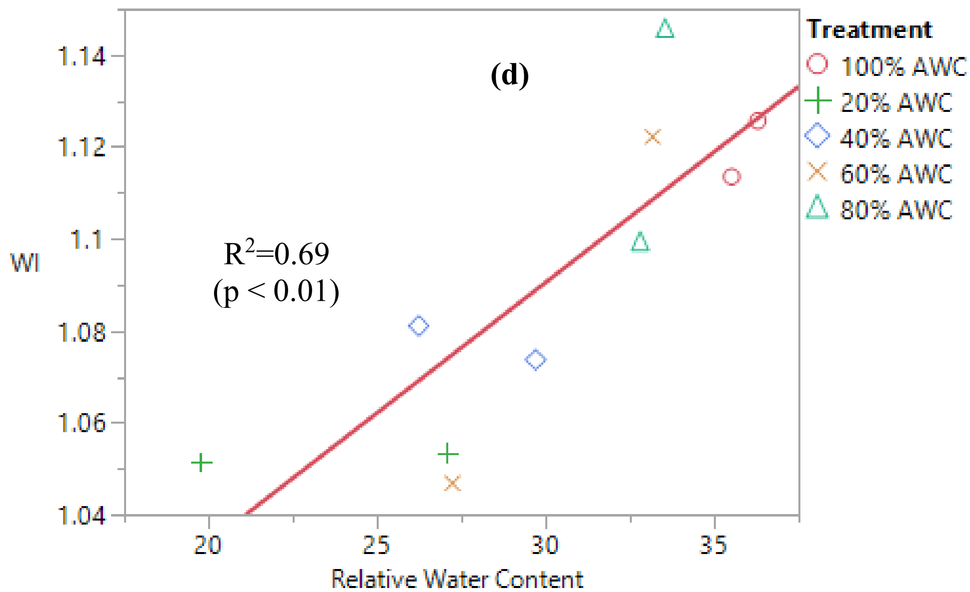

Fig. 4. 5. Relationship between (a) PRI_{550} (b) RDVI (c) PRI_{norm} (d) WI, and relative water content (%) obtained from the various treatments.

4.5. Discussions

4.5.1. Effects of water stress on yield and IWUE

The analysis of the results showed that there were no significant differences in yield and IWUE for 80% and 100% AWC treatments. Though the 100% AWC treatment reached the highest yield, the 80% AWC treatment recorded the highest IWUE. The study implies that the 80% AWC is best suited for optimizing water use of tomato plants, and could be adopted in water-scarce regions, where optimization of water is paramount. The result is consistent with the findings of Hartz *et al.* (2005), which indicated that tomatoes can tolerate a moderate degree of stress, with about 20-30% depletion in available soil moisture in the plant root zone without significant yield loss. Soil moisture depletion levels during the entire growth periods of tomato plants should remain below 30% of available soil moisture content to avoid yield loss. The most severe water stress (20% AWC) resulted in a yield loss of 61%, compared to the highest yield. Water application at 60%

AWC resulted in a yield loss of 30% compared to the highest yield, and this justifies the application of supplementary irrigation to water-stressed plants. Again, prolonged water stress may alter the plant physiological and biochemical processes leading to nutrients deficiency to the crop (Silva et al., 2011). However, the soil nutrient content was regularly replenished during the experiment to ensure that the results of this study are the single effect of water stress and not the combined effect of nutrients and water stress. The findings of this study are in tandem with the findings of similar studies (Jaria and Madramootoo, 2013; Petropoulos et al., 2019) that water stress adversely affected physiological and photosynthetic activities of tomato plants.

4.5.2. Effects water treatment on spectral reflectance

The stressed plants showed increased reflectance values within the visible range, and this is consistent with the fact that healthy plants absorb more visible light for photosynthesis, thereby having lower reflectance values. The reflectance in the blue and red regions of the VIS region, shown in Fig. 4.2 (b), were significantly high at high water stress levels, which suggests that the leaf water deficit reduces photosynthetic pigment concentration. The result indicates that the reflectance in the VIS region is largely influenced by primary photosynthetic pigments.

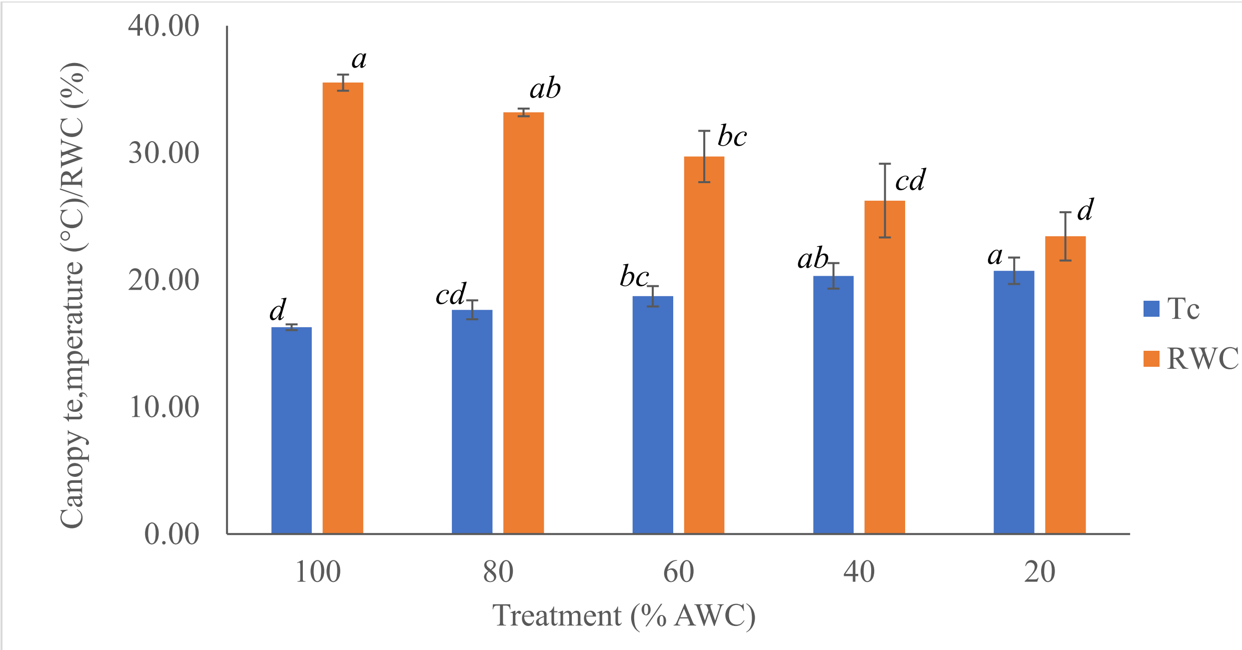

Fig. 4. 6. Effects of water treatments on the canopy temperature, Tc (°C), and leaf relative water content, RWC (%) in tomato plants.

[a-d] Means followed by the same letter are not significantly different at $p = 0.05$. Reported values are averages of five replicates.

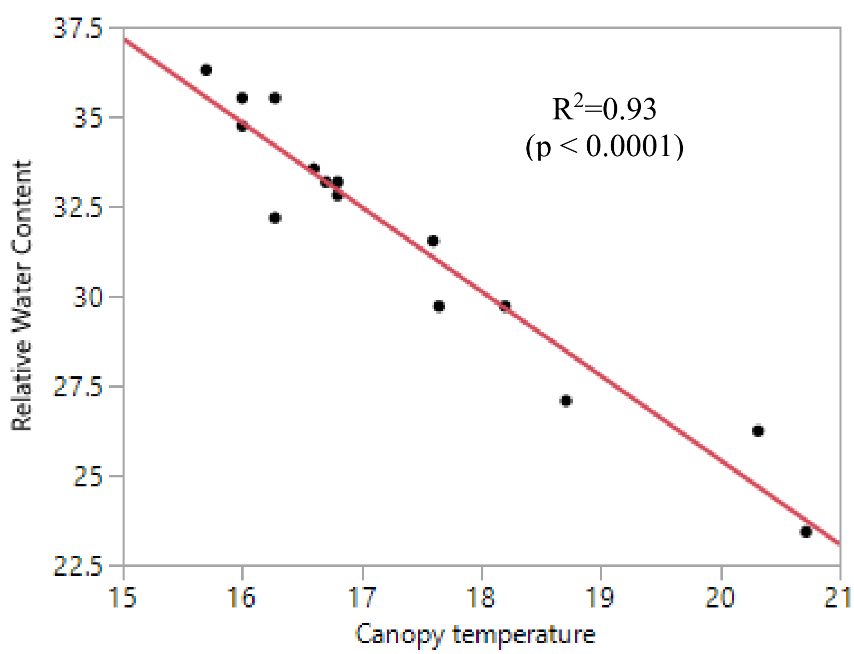

Fig. 4. 7. Regression of relative water content (%) on canopy temperature (°C) of tomato plants

The results of this study indicated that the irrigation treatments implemented in this experiment triggered a moderate to severe water stress on the plants, as reflected in the yields of the stressed and non-stressed plants. Plants irrigated with reduced amounts of water responded with stomatal closure, detected by an increase in Tc. When plants are water-stressed, osmotic adjustment may prevent dehydration of leaf cells for some time, thus not instantly affecting the plant turgor pressure. However, if plants can no longer cope with water stress, they will become dehydrated leading to a decrease in leaf cell turgor detected as a reduction of leaf RWC (Rossini *et al.,* 2013). Generally, water-stressed plants have increased leaf temperature (Idso *et al*., 1981) and reduced leaf water content compared to non-stressed plants. Therefore, leaf relative water content has been used to indicate plant water stress and schedule irrigation (Colombo *et al.,* 2011; Wang *et al.,* 2015), especially for strongly isohydric crops (such as tomatoes), which maintain a constant leaf water status over a wide range of evaporative demand (Limpus, 2009).

4.5.3. Effects of water stress on vegetation indices

An evaluation of various VIs for detecting water stress in tomato based on Tc revealed that the PRI_{550} had the best correlation with canopy temperature. This result agrees with previous studies, which confirmed the sensitivity of PRI to water stress (Berni *et al.,* 2009, Zarco-Tejada *et al.,* 2013). Generally, water treatments affected leaf physiological processes in a different way during the growing season. The results reveal that the PRI_{550} was best related to all the indicators of water stress measured in this study (RWC, Tc, and yield). This can be explained by the functional relationship between these eco-physiological indicators of water stress. At the beginning of water stress, RWC decreases, stomata close and Tc increases concurrently with a decline of photosynthesis (Prasad *et al.,* 2008). The PRI_{570}, proposed in a previous study (Zarco-Tejada *et* *al.,* 2012), showed weaker correlations with all the leaf physiological indicators tested in this study. This indicates that the index is not suitable for detecting water stress in greenhouse-grown tomato plants.

Although some recent studies demonstrated that PRI can also be related to water potential and stomatal conductance, canopy temperature generally showed the highest correlations. The link between PRI and Tc is likely due to the role of the xanthophyll pigments in dissipating excess heat arising under stressed conditions. Specifically, PRI with reference wavelength of 550 nm (PRI_{550}) showed the best correlation with water stress indicators and performed better than PRI_{570} (reference wavelength of 570 nm), which has been used by several researchers, for estimating xanthophyll pigment changes under water stress conditions (Gamon *et al.,* 1997; Suarez *et al*., 2009; Wang *et al.,* 2015). However, the results by these researchers showed the sensitivity of PRI_{570} for detecting crop water stress over short time scales, whereas studies conducted over longer time scales reported contrasting results, at the leaf and canopy scales (Gamon, 2015; Magney e*t al*., 2016). The result of this research is consistent with the original study on photochemical reflectance indices by Gamon *et al* (1992), which reported a reference wavelength of 550 nm for monitoring crop water stress.

The irrigation treatments executed in this experiment might have induced structural and morphological changes (e.g. changes in canopy structure, shape, leaf thickness) in the plants, detected by the variations in the structural indices with different water treatment levels. This could be the effect of prolonged water stress on the plants that affected the plant structure and physiological parameters. Previous researchers reported a high correlation between the structural indices and biomass, chlorophyll, leaf area index, and yield (Koksal, 2011; Rinaldi *et al.,* 2014). Jones (2004) explained that although NDVI may be a good indicator of nitrogen content and biomass, and it provided an approximate estimate of plant water status. Several studies showed that NDVI obtained a good correlation with plant water content (Genc *et al.,* 2011; Kim *et al.,* 2010), but this was not the case in this study. In their study, Kittas *et al.* (2016) explained that NDVI had a better correlation with soil moisture content in greenhouse tomatoes, which is consistent with the findings of this study. Amatya *et al.* (2012) showed that NDVI in potato had a high correlation with soil water content, as obtained in this experiment. Variations in soil moisture content affect the vegetation vigor, yield, and biomass production of plants, hence the highly significant correlations between the structural indices and soil moisture content. Usually, NDVI is not related to variations in environmental conditions such as VPD and air temperature, but it is strongly correlated to LAI and weakly correlated to stomatal conductance (Magney *et al.,* 2016).

The good correlation between water indices and RWC indicates that the indices increase with increasing RWC. This implies that water stress affected water absorption in the mesophyll pigment of the plants. Typically, the reflectance trough in the near-infrared region at 900 – 970 nm corresponds to the water absorption band, but the 970 nm trough disappears and shifts towards lower wavelengths when the plants are water-stressed (Penuelas *et al.,* 1997). The findings of this study are consistent with previous studies (Genc *et al.,* 2011; Katsoulas *et al.*, 2016), which observed significant correlations between water indices and plant water content in several crops. This shows the possibility of mapping plant water status using reflectance indices for improving irrigation management. In all the reflectance indices that showed a significant correlation with water stress indicators, there was a significant difference in these indices whenever the AWC depletes below 20%, which indicates that this method can be used for crop water stress detection under normal and extreme water stress conditions.

4.6. Conclusion

The work presented in this paper assessed the feasibility of using spectral vegetation indices to detect water stress in tomato plants. Water deficit induced in this experiment adversely affected crop yield, with yield decreasing as irrigation water decreased. Irrigation application below 80% AWC treatment caused significant yield loss of 30 – 60%. This study showed that PRI_{550}, WI, OSAVI, and WI/NDVI were the most sensitive indices to distinguish water stress levels in greenhouse-grown tomato plants.

Though previous studies suggested the use of PRI_{570} for monitoring water status of various field crops, the results found in this experiment have shown that PRI_{550} was better than PRI_{570} for detecting water stress in the greenhouse-grown tomatoes. It is important to note that leaf biophysical and biochemical effects on PRI during the growing season would affect the use of the index for measuring crop water stress. Nevertheless, monitoring crops using hyperspectral sensors may provide automated techniques for rapid, non-destructive, and reliable estimates of plant water status. Analyzing these features in real-time and providing qualitative and quantitative information to the growers can help them optimize agricultural water use for increased crop yield.

Based on the findings of this study, it was difficult to select a single index for precise estimation of plant water status. Therefore, innovative data management techniques that would integrate various vegetation indices are needed to widen the scientific knowledge on crop stress monitoring and provide irrigators with precise indices for scheduling irrigation. Also, future research efforts should be geared towards the integration of thermal and narrow-band hyperspectral indices to provide more precise information about plant water status, and advanced data analysis techniques that would provide irrigators with an easily accessible and cost-effective tool for decision making.

Connecting text

The previous two chapters demonstrated the feasibility of spectral vegetation indices for monitoring water stress in greenhouse-grown vegetable crops. However, the findings of the greenhouse studies might not be suitable for open field conditions because these indices are affected by microclimatic conditions. Also, most growers are confronted with both water and nitrogen stress management, and it is important to assess vegetation indices for monitoring both water and nitrogen stress under field conditions. Chapter V of this thesis evaluated narrow-band reflectance indices for detecting the combined effects of water and nitrogen stress in field tomato crops. Tomato was used as a test crop in the field study because the greenhouse experiment revealed that tomatoes are more sensitive to abiotic stress than bell peppers.

The manuscript from this study, narrow-band reflectance indices for mapping the combined effects of water and nitrogen stress in field-grown tomato crops, has been published in *Biosystems Engineering*. The manuscript was co-authored by Dr. Chandra A. Madramootoo, my supervisor. The cited references are listed in the reference section. All the funding used for this study was provided by my supervisor, Dr. Chandra A. Madramootoo.

CHAPTER V

Narrow-band reflectance indices for mapping the combined effects of water and nitrogen stress in high-value vegetable crops

5.1. Abstract

This study assessed the use of reflectance indices for detecting the combined effects of water and nitrogen stress in tomatoes *(Solanum Lycopersicum L.).* Spectral reflectance data were acquired from tomato plants, subjected to three water and three nitrogen treatments. Irrigation water was applied in amounts of 100, 70, and 30% of full replenishment of root zone soil water to field capacity. Nitrogen application was 100, 70, and 30% of crop nutrient requirement. The treatments were replicated five times in a randomized complete block design. Plant stress indicators, including leaf temperature (Tc), relative water content (RWC), yield, and leaf chlorophyll content (LCC) were measured at the same time of leaf reflectance data, during the growing season. Reflectance indices including Normalized Difference Vegetation Index (NDVI), Renormalized Difference Vegetation Index (RDVI), Optimized Soil Adjusted Vegetation Index (OSAVI), Photochemical Reflectance Index centered at 550 nm (PRI_{550}), normalized PRI (PRI_{norm}), Transformed Chlorophyll Absorption in Reflectance Index (TCARI), Water Index (WI), and WI/NDVI were obtained from the reflectance data. The results showed that the PRI_{550}, PRInorm, and WI were the most sensitive indices for distinguishing crop water stress, while RDVI, PRI_{norm}, and TCARI had the best correlation with nitrogen stress indicators. PRI_{norm} was the most sensitive index for detecting the combined effect of water and nitrogen stress. This study provided more insights into the usefulness of leaf spectral features for assessing crop abiotic stress. Measuring these indices with hyperspectral sensors provides a rapid, non-destructive, and reliable approach for estimating crop stress.

Keywords: Plant stress; leaf reflectance indices; high-value vegetable crops; irrigation; crop stress.

5.2. Introduction

Early identification and prediction of plant nitrogen and water stress are required to ensure sustainable agricultural management. Traditional plant and soil-based methods of estimating plant nitrogen and water status, which involves the augering of soil and removal of plant leaves, are invasive and destructive. These methods often do not represent the heterogeneity of soil and crop parameters at large spatial scales (Ihuoma and Madramootoo, 2019a). Monitoring crop abiotic stress can be improved using plant-based methods, which are considered better stress indicators because they integrate soil properties, climatic conditions, and crop management factors (Tremblay et al., 2012).

Spectral reflectance data provide near real-time and non-destructive methods for monitoring crop health status (Liang et al., 2013; Lohr et al., 2016; Steidle Neto et al., 2017; Zhao et al., 2010). This approach combines available ground and remotely sensed data to provide relevant information to support decision-making. The use of remote sensing in agriculture is based on the interaction between specific plant traits with electromagnetic radiation (Ihuoma and Madramootoo, 2017). Other researchers (Bandyopadhyay et al., 2014; Katsoulas et al., 2016) associated reflectance in the green and red bands with water and nutrient stress due to the link between leaf spectral reflectance and leaf chlorophyll concentration.

Water stressed plants experience stomata closure, leading to decreased CO_2 assimilation and reduced photosynthetic rate. Thus, absorbed light energy cannot be used for electron transport to drive the photosynthetic process, and part of the absorbed light energy is reflected, dissipated as heat, or re-emitted as chlorophyll fluorescence (Katsoulas et al., 2016). Similarly, nutrient stress affects the rate of photosynthesis as well as leaf spectral reflectance, since the nutrient is a major component of chlorophyll and photosynthetic enzymes. Vegetation indices are mostly derivatives of reflectance bands from visible, infrared and other regions of the reflectance spectrum. These reflectance bands can be measured using multispectral and hyperspectral sensors (Gago et al., 2015), and have been utilized to monitor plant physiological status. Therefore, a better understanding of various reflectance indices is required to improve the detection of plant stress and optimize water and fertilizer management in agriculture.

Reflectance indices for assessing crop stress can be classified into three major categories (Table 5.1); xanthophyll pigment, structural, and water indices (Gago et al., 2015; Ihuoma and Madramootoo, 2017). The xanthophyll pigments include the Photochemical Reflectance Index centered at 550 nm (PRI_{550}) and 570 nm (PRI_{570}) and the normalized PRI (PRI_{norm}). These indices are sensitive to changes in carotenoids through the de-epoxidation of the xanthophyll pigments (Magney et al., 2016), and are useful for indicating plant water and nutrient stresses (Panigada et al., 2014). The structural indices include the Normalized Difference Vegetation Index (*NDVI*), Renormalized Difference Vegetation Index (*RDVI*), Optimized Soil Adjusted Vegetation Index (*OSAVI*), and Transformed Chlorophyll Absorption in reflectance Index (TCARI). These indices are related to plant vigor and give a good indication of leaf chlorophyll content and fraction of green cover (Leroux et al., 2016). Previous studies also showed the use of other vegetation indices, such as normalized difference vegetation index on greenness (GNDVI), green vegetation index (GVI = NIR/green), and red vegetation index (RVI = NIR/red) for assessing plant stress (Gianquinto et al., 2011 and Padilla, et al., 2015).

The water indices, including Water Index (*WI*), Normalized Water Index (*NWI*), and *WI/NDVI*, correspond to the water absorption band observed in the near-infrared region (900 – 970 nm). The water indices have been utilized to monitor water status in different plants (Ihuoma and Madramootoo 2019b; Panigada et al., 2014; Rossini et al., 2013; Wang et al., 2015). A detailed review of spectral reflectance indices for assessing crop water and nitrogen stresses has been documented in previous studies (Corti et al., 2017; Gago et al., 2015; Ihuoma and Madramootoo, 2017; Katsoulas et al., 2016).

Most of the studies on spectral vegetation indices focused on either water or nitrogen stress detection. However, the use of optical reflectance indices for mapping the combined effects of water and nitrogen stress for high-value vegetable crops has not been widely investigated. Since most farmers are confronted with both water and nitrogen stress management, it is imperative to assess narrow-band reflectance indices for more precise identification and classification of plant stress to support precision agriculture. The threshold values of these reflectance indices obtained from optical sensors could be used in designing fertigation systems for optimal use of water and nitrogen in the field. The objective of this study was to ascertain the best vegetation indices for detecting the combined effects of water and nitrogen stress in vegetable crops during their various growth stages. Tomato was used as a test crop due to its high sensitivity to water and nitrogen stress.

5.3. Materials and methods

5.3.1. Study area and experimental design

The study was conducted between June and October 2017 at the Horticultural Research Station of McGill University, to evaluate the sensitivity of narrow-band vegetation indices to combined effects of water and nitrogen stress in field-grown tomato crops. The study area lies at latitude

Table 5. 1. Optical indices used in this study, their formulations and references

Names	Abbreviations		
Xanthophyll indices			
Photochemical Reflectance Index	PRI_{570}	$(R_{570} - R_{531})/(R_{570} + R_{531})$	Gamon et al. (1992)
	PRI_{550}	$(R_{550} - R_{531})/(R_{550} + R_{531})$	Gamon et al. (1997)
Normalized Photochemical Reflectance Index	PRI_{norm}	$PRI_{550}/(RDVI * (R_{700}/R_{670}))$	Berni et al. (2009)
Structural indices			
Normalized Difference Vegetation Index	NDVI	$(R_{800} - R_{670})/(R_{800} + R_{670})$	Rouse et al. (1974)
Renormalized Difference Vegetation Index	RDVI	$(R_{800} - R_{670})/(R_{800} + R_{670})^{1/2}$	Rougean and Breon (1995)
Transformed Chlorophyll Absorption in Reflectance Index	TCARI	$3[(R_{700} – R_{670}) – 0.2(R_{700} – R_{550})*(R_{700}/R_{670})]$	Haboudane et al. (2002)
Optimized Soil Adjusted Vegetation Index	OSAVI	$(1 + 0.16)(R_{800} - R_{670})/(R_{800} + R_{670} + 0.16)$	Haboudane et al. (2002)
	TCARI/OSAVI	TCARI/OSAVI	Haboudane et al. (2002)
Water content indices			
Water Index	WI	R_{900}/R_{970}	Penuelas et al (1997)
	WI/NDVI	WI/NDVI	Penuelas et al (1997)

Where R represents the reflectance values at the respective wavelengths, nm.

45°43’80’’ N and longitude 73° 93’80’’ W with an elevation of 36 m. The experimental plot was a 6 x 10 m^2 field and the experimental design involved three water treatments and three nitrogen treatments. External sources of variabilities are not expected to be significant within this small plot, thus; the study was designed as a randomized complete block with a 3 x 3 factorial arrangement of treatments. The nine treatment combinations were replicated five times to give a total of 45 tomato plants (9 treatments with 5 replicates each). Irrigation water was applied in amounts of 100, 70, and 30% of full replenishment of soil water in the root zone to field capacity. Fertilizer was dissolved in water and manually applied to each plant based on guidelines for field-grown tomatoes at the horticultural research station of McGill University. The plants were fertilized biweekly with 20-20-20 N-P-K water-soluble fertilizer, at a rate of 4 kg of N ha^{-1}, as adopted in our previous study (Ihuoma and Madramootoo, 2019b). Applying N at this rate throughout the growing season will amount to a total rate of 54 kg of N ha^{-1}, which represents the crop seasonal N requirement. Studies have demonstrated that N deficiency had a significant adverse effect on tomato marketable yield (Frias-Moreno et al., 2014). Therefore, to induce mild to severe nitrogen stress, N applications were 100, 70, and 30% of crop nitrogen requirement, corresponding to 54, 38, and 16 kg N ha-1. 100% application rate was the control while the 70% and 30% application rates were the N stressed treatments.

Tomato *(Solanum Lycopersicum L.)* cv. Picus VF/TSWV seedlings, 42-days old, were transplanted on June 12, 2017, and harvested on October 3, 2017. Picus variety was chosen because it is a popular and widely cultivated fresh market vegetable crop. The plants were transplanted on beds, with a row spacing of 1.8 m and plant spacing of 0.6, covered with plastic mulch. The planting density was 9260 plants per hectare. Irrigation water was applied through a drip system, consisting of pressure compensating emitters with a discharge of 2 L/h, and the flow rates were calibrated in the field. The soil was composed of clay, silt, and sand with contents of 65, 15, and 20%, respectively (USDA-NRCS, 2000). Field capacity (FC) was 45% and the permanent wilting point was 27% by volume. The water application in each treatment was regulated using a water control valve attached to each dripper. The water treatment level for each treatment (100, 70, and 30% FC) was used as the upper irrigation threshold, while a lower irrigation threshold was set at 20% depletion of the upper limit for each treatment. The plants were irrigated whenever the soil moisture content for each treatment was depleted by 20% of the upper limit. Irrigation was terminated when the upper trigger moisture content (100, 70, and 30% FC) was reached, as determined by Time Domain Reflectometers (TDR) (CS625 water content reflectometer, Campbell Scientific Inc., UT). TDR probes, consisting of 30 cm probes, were installed vertically with the aid of an insertion guide to correspond with the plant rooting depth (Jaria and Madramootoo, 2013). TDR readings were calibrated in the field with gravimetric soil moisture measurements. The soil moisture sensors were connected to solar-powered data loggers (model CR205/6, Campbell Scientific Inc.). The data were scanned every 5 minutes and recorded every 15 minutes, hourly, and daily and was retrieved from the datalogger using a computer and Campbell Scientific Inc. LoggerNet software.

The volume of water applied during each irrigation event to each treatment was determined as the product of the irrigation duration and the flow rate. The equivalent irrigation depth applied at each irrigation event for each treatment was determined as the product of the total available water holding capacity of the soil and the management allowable deficit (20% of the upper limit of each treatment). Water and fertilizer were uniformly applied to all treatments at the beginning of transplanting, based on 100% replenishment of nutrient and water in the plant root zone to field capacity for plants to be well established; thereafter, the water and fertilizer treatments were effected until harvest.

5.3.2. Measurements

Daily weather variables (maximum and minimum air temperature, relative humidity, solar radiation, rainfall, and wind speed) were obtained using a Campbell Scientific automatic weather station (Campbell Scientific, Logan, UT, USA) installed about two metres above the crop canopy in the field. Data from the weather station was scanned every 5 minutes and recorded every 15 minutes¸ hourly and daily. These data were used to calculate daily reference evapotranspiration (ETo) using the FAO 56-Penman-Monteith equation (Allen et al., 1998). Daily and seasonal crop evapotranspiration (ETc) was estimated as the product of ETo and the crop coefficient (Kc). Kc varies predominately with specific crop characteristics (Allen et al., 1998). In this study the Kc values were obtained from the Ontario Ministry of Agriculture, Food and Rural Affairs (OMAFRA, 2016).

5.3.3. Spectral data acquisition and processing

Spectral data acquisition was conducted using a miniature fiber optic spectrometer (Stellar Net Inc. USA), which measures reflectance in the 200–1150 nm spectral range. The spectrometer has a 0.5 nm spectral resolution and was calibrated by holding the probe at 45° to a reference white standard at a distance of about 60 mm. The integration time was optimized by setting it to 50 ms, dark current was recorded, and target spectral reflectance was obtained. The canopy spectral data acquisition was undertaken under clear sky conditions between 11:00 and 15:00 hours when the sun was shining directly on the plants, to ensure maximum solar intensity, as implemented by Ihuoma and Madramootoo (2019b). Measurements were taken from each of the 45 plants by placing the spectrometer at a height of about 30 cm above the plant canopy to view only a plant leaf at a time. Four leaves were measured in every plant and averaged to represent the plant, as adopted by Ihuoma and Madramootoo (2019b). The values for the five replicates of each treatment were averaged to represent each treatment combination. All the reflectance measurements and stress indicators were obtained from the same leaf samples to ensure that leaf reflectance measurements can be associated with the stress indicators. The measurements were conducted five times (18^{th} and 30^{th} July; 9^{th} and 26^{th} August; and 18^{th} September 2017), during the plant growing season. The 7-point weighted moving average method was used to enhance the smoothness of the spectral curve, eliminating interference noise from signal background and light scattering effects (Zhao et al., 2017). The mean of the optical reflectance measurements obtained from each treatment was used to calculate the spectral reflectance indices studied (Table 5.1).

5.3.4 Measurement of plant stress indicators

A portable infrared thermometer set at an emissivity of 0.95 W m^{-2} was used to measure the leaf temperature (Fluke 572 model, Fluke Corporation, Everett, WA). The thermometer was held 30 cm above the plant canopy with its laser pointer directed at the plant leaves at an angle of 90° to the horizontal. Four leaf temperature measurements were taken from each plant considering four viewing directions (north, south, east, and west) and average temperature values were recorded to represent each plant. The values for the five replicates of each treatment were averaged to represent each treatment combination. All the measurements were conducted between 11:00 and 15:00 hours, when the sun was shining directly on the plants, ensuring maximum solar intensity. Leaf relative water content (RWC) was measured from each plant following the procedures of Colombo et al. (2011) and Wang et al. (2015). Leaf chlorophyll content (LCC) was measured with a handheld chlorophyll meter (SPAD-502, Minolta Camera Co., Japan) on four selected leaves from each plant, and the average reading was recorded to represent the plant. The values for the five replicates of each treatment were averaged to represent each treatment combination. SPAD measurements were converted to LCC (mg g^{-1}) using the tomato-specific model proposed by Jiang et al. (2017). ETc is also an indicator of plant stress and was calculated using the FAO 56-Penman-Monteith equation method as previously explained. Also, the average fruit yield from each treatment combination was measured, recorded, and classified into marketable and non-marketable yield.

5.3.5 Statistical analysis method

The effects of water and nitrogen on stress indicators (Tc, RWC, yield, and LCC) were described using the Pearson correlation ratio, defined in Eq. 5.1. The correlation ratio indicates how the stress factors explain the data variance and assumes values between 0 and 1; a correlation ratio close to 1 suggests that the stress levels could explain the data variance.

$$\eta^2 = \frac{\sigma_{\bar{y}}^2}{\sigma_y^2}, where\ \sigma_{\bar{y}}^2 = \frac{\sum_x n_x(\bar{y}_x - \bar{y})^2}{\sum_x n_x}\ and\ \sigma_y^2 = \frac{\sum_{x,i} n_x(y_{xi} - \bar{y})^2}{n} \quad \text{..............................} (5.1)$$

where η^2 is the correlation ratio, y_{xi} represents each observation (x indicates the stress levels, and i indicates an observation), n_x indicates the number of observations in x, $\bar{y}_x$ represents the mean of x and $\bar{y}$ is the population mean.

Statistical analyses were carried out on vegetation indices (NDVI, OSAVI, RDVI, TCARI, PRI_{550}, PRI_{norm}, WI, TCARI/OSAVI, and WI/NDVI), and plant stress indicators (leaf temperature, leaf relative water content, crop yield, and leaf chlorophyll content) using the PROC/GLM (General Linear Model) procedure of SAS software (version 9.3, SAS Institute, Inc., Cary, NC, USA). Two-way (factorial) analysis of variance (ANOVA) was conducted on the data, and the significance of differences among treatments was separated using Fisher's Least Significant Difference (LSD) at a 5% probability level. The values of vegetation indices were related to values of RWC, Tc, LCC, and yield of each treatment combination using linear regression.

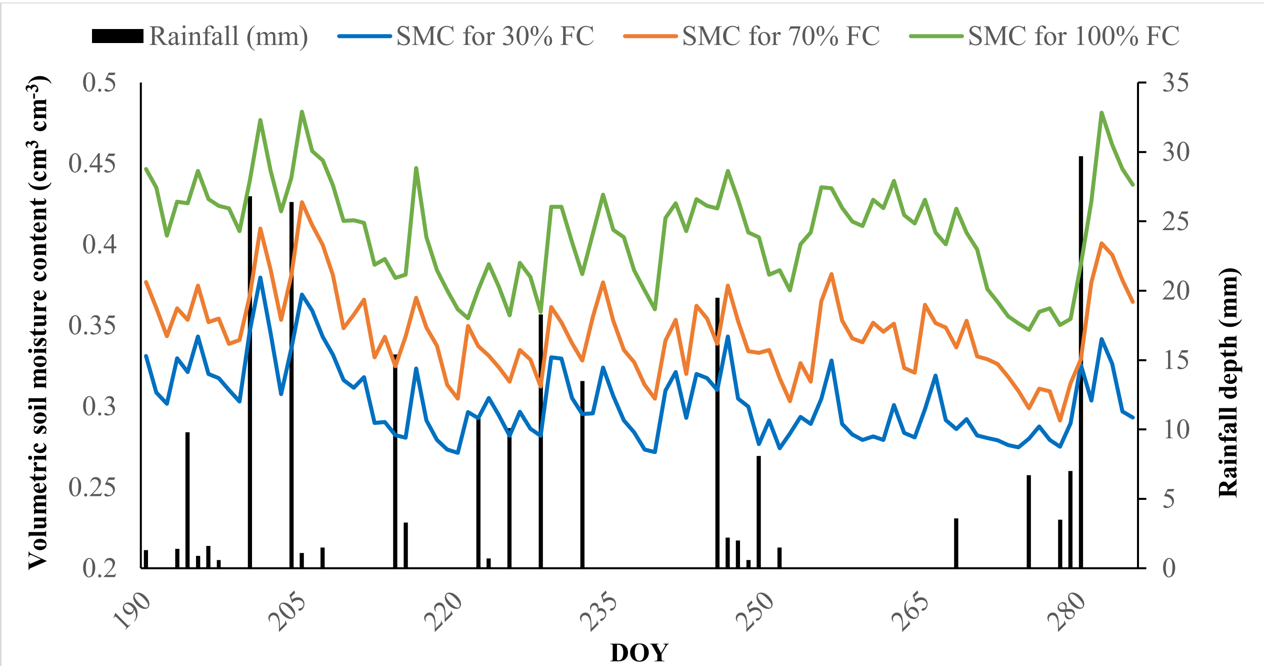

Fig. 5. 1 Rainfall (mm) and average volumetric soil moisture content ($cm^3\ cm^{-3}$) for various treatments during the growing season.

5.4. Results

5.4.1. Crop evapotranspiration and soil water content

Daily mean temperature, relative humidity, and vapor pressure deficit in the field ranged from 5 to 31 °C, 66 to 77%, and 0.30 to 1.03 kPa, respectively, during the plant growing season. Daily volumetric soil water content for various irrigation treatments, as well as rainfall amounts, are shown in Fig. 5.1. The soil water content was affected by both rainfall and irrigation events but generally decreased with decreasing water application, with 100 and 30% FC resulting in the mean highest and lowest values of soil water content, respectively, during the growing season.

However, there were significant differences in soil moisture content for the 100, 70, and 30% FC treatments, except on days with high rainfall events. The total seasonal crop evapotranspiration (ETc) and irrigation water varied from 79 to 263 mm and 139 to 406 mm for water-stressed and non-water stressed treatments, respectively, as shown in Table 5.2. The ETc was higher during the flowering and maturity stages of plant growth, which corresponded to the periods when the crop required more water for its vegetal growth and physiological development.

5.4.2. Water and nitrogen stress indicators

The descriptive statistics (mean, standard deviation, and correlation ratio) of tomato plants grouped by irrigation and fertilizer treatment levels are presented in Table 5.3. The mean of leaf relative water content generally decreased with decreasing irrigation treatment levels, with 100 and 30% FC recording the highest and lowest RWC, respectively. The results also show that 100 and 30% FC recorded the lowest and highest leaf temperatures, respectively, while the nitrogen treatment levels had no effect on the Tc and RWC. The Tc and RWC showed a high correlation ratio, with $\eta^2 = 0.85$ and 0.94, respectively, which indicates that the irrigation treatments explained most of the variance in Tc and RWC. The mean of nitrogen stress indicator (leaf chlorophyll content) also decreased with decreasing nitrogen treatment levels. The LCC showed a high correlation ratio, with $\eta^2 = 0.79$, which indicates that the nitrogen treatments explained most of the variance in LCC. The yield was used to assess the interaction effects of the water and nitrogen stress on the plants and the result shows that both water and nitrogen stress affected the yield of the tomato plants, with a correlation ratio of 0.82. The interaction of 100% water and 100% nitrogen treatments recorded the highest yield (66.2 ± 2.6 Mg ha^{-1}), while the 30% water and 30% nitrogen treatments had the least yield (31.9 ± 8.6 Mg ha^{-1}). The tomato yields interact with water and nitrogen treatments according to Eq. 5.2. There is a linear relationship between water stress indicators (Tc and RWC, with $R^2 = 0.80$ $p < 0.0001$) and nitrogen stress indicators (Yield and LCC, with $R^2 = 0.66$ $p < 0.0001$).

$$Y = 1.85 + 0.035(N) + 0.022(W) \ldots\ldots\ldots\ldots\ldots\ldots\ldots\ldots\ldots\ldots. (5.2)$$

Where Y = yield, Mg ha^{-1}, N = fertilizer application rate, kg N ha^{-1}, and W = soil water content, % FC.

Table 5. 2. Crop evapotranspiration (mm) and Irrigation water applied (mm) to tomato plants per growth stage for different treatments.

		Irrigation water applied			Crop evapotranspiration		
Treatments (% FC)	Days	100%	70%	30%	100%	70%	30%
Initial stage	20	92	74	45	21	15	6
Flowering stage	30	65	45	19	81	57	24
Maturity stage	30	166	116	50	113	79	34
Senescence stage	25	83	58	25	48	34	14
Total	105	406	293	139	263	185	78

Table 5. 3. Descriptive statistics (mean, standard deviation, and correlation ratio (η^2) of tomato plants grouped by the irrigation and fertilizer treatments. Where Tc: leaf temperature (°C), RWC leaf relative water content (%), LCC: leaf chlorophyll content (mg g^{-1}), and Yield (Mg ha^{-1}).

Stress indicators	N1W1	N1W2	N1W3	N2W1	N2W2	N2W3	N3W1	N3W2	N3W3	η^2
Tc	24.41 ± 0.68^{d}	26.63 ± 0.82^{cd}	28.31 ± 0.72^{a}	24.95± 0.52^{d}	26.79± 0.55^{bc}	28.55 0.63^{a}	25.58± 0.43^{cd}	26.79± 0.39^{bc}	27.87± 0.35^{ab}	0.85
RWC	56.46 ± 2.68^{a}	43.11 ± 0.59^{de}	32.11 ± 0.77^{f}	55.09± 1.05^{ab}	49.93± 0.91^{bc}	40.28± 0.79^{e}	57.60± 5.51^{a}	48.11± 1.20^{cd}	37.45± 0.78^{ef}	0.94
LCC	1.61± 0.21^{abc}	1.67± 0.23^{a}	1.65± 0.28^{ab}	1.41± 0.21^{cd}	1.43± 0.17^{cd}	1.46± 0.21^{bcd}	1.32± 0.24^{d}	1.27± 0.19^{d}	1.29± 0.18^{d}	0.79
Yield	66.2± 2.6^{a}	51.2± 3.2^{bc}	44.9± 3.0^{bc}	54.7± 1.9^{b}	46.3± 3.3^{bc}	41.5± 4.1^{cd}	45.6± 3.8^{bc}	43.1± 3.7^{c}	31.9± 8.6^{d}	0.82

Treatments with the same letters are not statistically significant. N represents Nitrogen treatment and W represents water treatments.

5.4.3. Correlation analysis between vegetation indices and stress indicators

Table 5.4 shows the coefficient of determination (R^2) of the linear relationships between RWC (%), Tc (°C), yield (Mg ha^{-1}), and leaf chlorophyll content (mg g^{-1}), and vegetation indices computed from the spectrometer. The results show that NDVI, RDVI, PRI_{550}, PRI_{norm}, and WI/NDVI were significantly correlated with yield (R^2 = 0.72, 0.86, 0.77, 0.74, and 0.71, respectively; $p < 0.0001$). TCARI, PRI_{norm}, WI/NDVI, and TCARI/OSAVI showed the best correlation with LCC (R^2 = 0.71, 0.78, 0.67, and 0.64, respectively; $p < 0.0001$). Similarly, PRI_{550}, PRI_{norm}, and WI were strongly correlated with RWC (R^2 = 0.77, 0.68, and 0.69, respectively; $p < 0.0001$), while PRI_{norm} and WI were best correlated with Tc (R^2 = 0.65 and 0.83, respectively; $p < 0.0001$). While the structural indices showed a strong correlation with yield and LCC, the xanthophyll pigment and water indices were best correlated with RWC and Tc. However, the PRI_{norm} showed a good correlation with all the measured stress indicators, with R^2 = 0.68, 0.65, 0.74, and 0.78; $p < 0.0001$, for RWC, Tc, yield, and LCC, respectively.

Table 5.5 shows the statistical tests of the effects of nitrogen and water treatments and their interactions on various vegetation indices. The result shows that apart from WI for nitrogen treatment, and TCARI and TCARI/OSAVI for water treatment, all the other indices were significantly affected by both water and nitrogen treatments. However, further statistical analysis in Table 5.4 shows that the structural indices (NDVI, RDVI, TCARI, and TCARI/OSAVI) performed better in detecting the effects of nitrogen stress on the plants, while the xanthophyll pigments (PRI_{550} and PRI_{norm}) and water indices (WI and WI/NDVI) were better in detecting the effects of water stress on the plants. The PRI_{norm} was the only index subject to the interactive effects of nitrogen and water stress in the plants. So PRI_{norm} allows the detection of both water and nitrogen stress in tomato crops.

Table 5. 4. Coefficient of determination (R^2) of the relationships between RWC (%), Tc (°C), Yield (Mg ha^{-1}), and leaf chlorophyll content (mg g^{-1}), and vegetation indices computed from the spectrometer for tomato plants.

VIs	RWC (%)	Tc (°C)	Yield (Mg ha^{-1})	LCC (mg g^{-1})
NDVI	0.28	0.49	0.72	0.58
RDVI	0.43	0.58	0.86	0.55
OSAVI	0.36	0.37	0.45	0.40
TCARI	0.32	0.46	0.52	0.71
PRI_{550}	0.77	0.56	0.77	0.30
PRInorm	0.68	0.65	0.74	0.78
WI	0.69	0.83	0.42	*N.S*
WI/NDVI	0.44	0.38	0.71	0.67
TCARI/OSAVI	0.51	0.49	0.39	0.64

$P < 0.0001$, N.S = not significant

5.5. Discussion

5.5.1. Effects of water and nitrogen stress on yield

The water and nitrogen treatments implemented in this study triggered a moderate to severe stress on the plants, which reduced the leaf photosynthetic efficiency and crop yields of stressed plants. The lowest crop yield was obtained from the 30% treatment combination (N3W3) and resulted in a yield loss of 51% compared to the highest yield obtained from the 100% treatment combination (N1W1). Water treatments had more effects on tomato yields in this experiment as indicated by the average yield for moderately water-stressed (N1W2) and nitrogen-stressed (N2W1) treatments (54.7 and 51.2 Mg ha^{-1}, respectively). This result is in tandem with the findings of previous studies (Zhang et al., 2017 and Jaria and Madramootoo, 2013), which observed that depletion of soil water content below 30% FC induced severe water stress that significantly reduced the yield of tomato plants. The result justifies the need for adequate application and management of agricultural inputs to enhance the productivity of high-value vegetable crops.

Again, interaction effects of prolonged water and nitrogen stress might have induced structural and morphological changes in the plants, such as changes in leaf structure, shape, and leaf thickness observed towards the end of the growing season. The variations in plant structure and physiological parameters may be responsible for the significant differences in structural indices (NDVI, RDVI, and OSAVI) observed in the stressed and non-stressed treatments. Rinaldi et al. (2014) reported a significant correlation between structural indices and plant yield, biomass, leaf area index, and chlorophyll content, which is consistent with the results of this study.

Table 5. 5. Statistical tests of the effects of nitrogen and water treatments and their interactions on various vegetation indices.

VIs	Nitrogen Treatment	Water Treatment	Nitrogen * Water Treatment
NDVI	<0.0001	<0.0001	N.S
RDVI	<0.0001	<0.0001	N.S
OSAVI	0.0393	<0.0001	N.S
TCARI	<0.0001	N.S	N.S
PRI_{550}	0.0004	<0.0001	N.S
PRInorm	<0.0001	<0.0001	0.0020
WI	N.S	<0.0001	N.S
WI/NDVI	<0.0001	0.0152	N.S
TCARI/OSAVI	<0.0001	N.S	N.S

Where N.S = Not significant

5.5.2. Effects of water and nitrogen stress on reflectance indices

The experiment carried out in this study showed that PRI_{550} and WI had the best correlation with water stress indicators (relative water content and leaf temperature, respectively). This result agrees with the findings of Suarez et al. (2009), which suggested that leaf xanthophyll pigments are sensitive to water stress. The correlation between PRI and water stress indicators can be explained by the interactions among the eco-physiological indicators of plant water stress, as explained in Ihuoma and Madramootoo (2019b). Previous studies obtained suitable relationship between PRI_{570} and water stress indicators such as leaf temperature, stomatal conductance, and xylem water potential (Stagakis et al., 2012; Hernández-Clemente et al., 2011; Zarco-Tejada et al., 2012, 2013), and proposed the index for early detection of water stress in various crops. Conversely, this study has shown that PRI_{550} is best suitable for water stress detection. A similar result was obtained by the same authors (Ihuoma and Madramootoo, 2019b) for greenhouse-grown tomatoes. It was expected that the PRI_{550} threshold for water stress detection will be different for greenhouse and field-grown tomatoes, due to the differences in climatic conditions. However, the results suggest that the PRI_{550} is not significantly affected by changes in weather variables. The findings of the greenhouse and field experiments conducted over a 2-year period revealed the feasibility of PRI_{550} for monitoring water stress in tomato crops to support agricultural water management.

The relationship between WI and RWC indicates that the WI increased as RWC increased, which implies that water stress affected the absorption of water in the plant mesophyll pigment. This agrees with the findings of Genc et al. (2011) and Katsoulas et al. (2016), which recorded significant correlations between water index and leaf water content in various field crops. Water-stressed plants closed their stomata to reduce the transpiration rate and dehydration of leaf cells, and this led to increased leaf temperature. Rossini et al. (2013) observed that under extreme water stress conditions, the plants will become dehydrated, leading to a decrease in cell turgor pressure of the leaves. This explains the reduction of leaf relative water content observed in water-stressed treatments compared to non-stressed treatments. Similarly, nitrogen stress affected the leaf photosynthetic activities because plants under stress were exposed to a greater amount of radiant energy than they required for photosynthesis. In such conditions, the plants dispel the excess energy as heat (through the interconversion of light energy in the xanthophyll pigment) and chlorophyll fluorescence to avoid damage to their tissues (Rossini et al., 2013). The study further shows the potential of vegetation indices for monitoring the water status of field-grown tomato crops for optimizing agricultural water use.

Similarly, the results showed that the RDVI, PRI_{norm}, and TCARI had the best correlation with nitrogen stress indicators (yield and leaf chlorophyll content). The result is in agreement with previous studies (Koksal, 2011; Rinaldi et al., 2014), which reported a strong correlation between the structural indices and chlorophyll content and yield. This study detected reduction in leaf chlorophyll content in stressed treatments compared to non-stressed treatments, indicating that the nitrogen treatments affected the leaf chlorophyll composition, as reported in similar studies (Jiang et al., 2017; Evanidi et al., 2018; Padilla et al., 2015; Ronga et al., 2018). The leaf spectral reflectance data, which is affected by leaf chlorophyll content, provides useful information for timely assessment of crop nitrogen status to ensure optimal management of nitrogen.

Gianquinto et al. (2011) reported a contrasting result and identified NIR/R_{560} and GNDVI as the best indicators of yield and leaf chlorophyll content in processing tomatoes. In this study, NDVI and RDVI also showed good correlations with yield and chlorophyll content. Studies have been published to show that structural indices are strongly correlated to leaf area index, chlorophyll content, and yield (Aguilar et al., 2012; Magney et al., 2016). Thus, proximal sensing of these indices may contribute to improving nitrogen management of tomato crops with positive effects on productivity.

NDVI is also useful for predicting crop canopy cover for estimating basal crop coefficients (K_{cb}) (Ihuoma and Madramootoo, 2017). The relationship between NDVI and K_{cb} is possible due to the link between crop phenological development and K_{cb}. Gago et al. (2015) observed that K_{cb} depends mainly on the dynamics of plant canopy parameters. The K_{cb} is an important parameter used with the conventional FAO-56 Penman-Monteith equation (Allen et al., 1998) for estimating crop evapotranspiration (ETc). Estimates of ETc enable the assessment of crop water needs used for scheduling irrigation (Jones, 2012).

Though NDVI significantly relates to plant vigor when the canopy cover increases proportionally to photosynthesis, it saturates at LAI values > 4 (NDVI is not sensitive to variability in LAI above 4) and is affected by background soil reflectance. The results showed that the TCARI was best correlated to LCC, making it a suitable index for the detection of nitrogen status in field-grown tomato plants, with the potential for optimizing nitrogen management.

5.5.3. Combined effects of nitrogen and water stress on reflectance indices

Based on the results found in this study, the PRI_{norm} showed the best correlation with all the water and nitrogen stress indicators investigated. The results indicate that PRI_{norm} is highly sensitive to both nitrogen and water stress and implies that stress caused changes in xanthophyll pigment and the carotenoid content of tomato leaves. This is probably due to the ability of PRI_{norm} to detect the changes in xanthophyll pigment as a result of water stress, and also normalizes for the reduction in leaf area and leaf chlorophyll content induced by nitrogen stress. Similar studies identified the robustness of PRI_{norm} for early detection of water stress in various crops (Behmann et al., 2014; Berni et al., 2009; Dangwal et al., 2015). This study has revealed the feasibility of PRI_{norm} for monitoring the combined effects of water and nitrogen stress in tomato crops. Operationalizing this concept for practical application in crop stress management requires more data points to generate response surface curves of PRI_{norm} versus water and nitrogen application rates. With the PRI_{norm}, more precise estimates of water and nitrogen rates can be obtained from the surface response to support decision making in fertigation management.

5.4. Conclusion

This study assessed the use of reflectance indices for detecting the combined effects of water and nitrogen stress in tomato plants. A comparison of various reflectance indices and their relationship with stress parameters showed that the normalized photochemical reflectance index (PRI_{norm}) was the most sensitive index for detecting the combined effect of water and nitrogen stress. The photochemical reflectance index centered at 550 nm (PRI_{550}), normalized photochemical reflectance index (PRI_{norm}), and water index (WI) were the most sensitive indices to crop water status, while the renormalized difference vegetation index (RDVI), normalized photochemical reflectance index (PRI_{norm}), and the transformed chlorophyll absorption in reflectance index (TCARI) had the best correlation with nitrogen stress indicators. This study confirmed the use of narrow-band vegetation indices to simultaneously estimate water and nitrogen status in tomato crops. Measuring these indices with hyperspectral sensors provides a timely and non-invasive technique for assessing plant stress and improving precision agriculture. Future studies should assess the proposed indices for estimating other physiological characteristics and stress effects in other high-value vegetation crops. The indices could also be evaluated for actual fertigation management in the field.

Connecting text

This chapter scaled up the results of the greenhouse and field findings to larger commercial farms using the vegetation indices to estimate irrigation water requirements from remotely sensed images. The study assessed the suitability of multispectral images acquired from unmanned aerial vehicle, Planetscope and Sentinel-2 satellite platforms for assessing crop coefficient and evapotranspiration. Sentinel-2 data were used to predict crop evapotranspiration (ETc) and the results were compared with ETc estimated from the FAO 56 Penman-Monteith module of the AquaCrop model. Then, ETc was coupled with field soil moisture measurements to estimate irrigation requirements.

The manuscript from this study, integration of satellite imagery and spatially-variable soil moisture data for estimating irrigation water requirements in high value processing crops, is ready for submission to *Remote Sensing and Environment*. The manuscript is co-authored by Dr. Chandra A. Madramootoo, my supervisor, and Dr. Margaret Kalacska, Applied Remote Sensing Laboratory, Department of Geography, McGill University. All the cited references are listed in the reference section and all the funding used for this study was provided by my supervisor, Dr. Chandra A. Madramootoo.

CHAPTER VI

Integration of satellite imagery and spatially-variable soil moisture data for estimating irrigation water requirements in high value processing crops

6.1. Abstract

Remotely sensed plant parameters account for spatio-temporal heterogeneity of crops and are advantageous for estimating crop evapotranspiration (ETc) and irrigation water requirements (IWR). This study compared the suitability of multispectral images acquired from Unmanned Aerial Vehicles (UAV), PlanetScope, and Sentinel-2A & 2B satellite platforms for estimating ETc and IWR of processing tomato crops (*Lycopersicon esculentum* Mill. cultivar Heinz H9553) on a farm in southern Canada. The field was divided into three (3) blocks and irrigation scheduling consisted of 100, 80, and 60% of full replenishment of water in the root zone to field capacity, corresponding to three irrigation regimes for the plants. Plants were selected from each of the three sections of the field, using a systematic grid sampling technique, and were georeferenced for identification in the acquired images. Normalized difference vegetation indices (NDVI) derived from the remote sensing platforms were evaluated for estimating crop coefficient. Sentinel-2 data were used to predict crop evapotranspiration (ETc), and the results were compared with ETc estimated from the FAO 56 Penman-Monteith module of the AquaCrop model. ETc maps from Sentinel-2 were combined with soil moisture data to predict irrigation water requirement. Results indicate that ETc values estimated from satellite platform were accurately predicted from AquaCrop model. The estimated IWR (165 and 199 mm in 2017 and 2018 growing seasons, respectively) were lower than the actual amount of water applied by the farmer (342 and 416 mm in 2017 and 2018 growing seasons, respectively), which suggests that the field was over-irrigated. The findings of this study have further revealed the usefulness of Sentinel-2 imagery for mapping

crop water requirements at field scale and indicates a progress towards the development of remotely sensed approach for implementing precision irrigation.

Keywords: Crop evapotranspiration, precision irrigation, remotely sensed images, Sentinel-2 imagery.

6.2. Introduction

Reliable estimate of crop evapotranspiration (ETc) at field level is essential to better manage irrigation and improve water use efficiency. The crop coefficient (Kc) for estimating ETc, defined as the ratio of ETc to the reference evapotranspiration (ETo) (Allen et al., 1998), has been shown to vary between growing seasons and sites (Kumar et al., 2015). This variability can be attributed to spatial heterogeneity in soil and crop parameters (Rozenstein et al., 2018). Standard FAO 56 Penman-Monteith Kc values are specific to each crop and reflect the plant canopy development due to agronomic practices during the growing season (Vanino et al., 2018). Kc values for various crops in different parts of the world have been documented by Allen et al. (1998). However, variations in weather conditions affect crop water-use patterns, resulting in inaccurate estimate of ETc, when the recommended FAO Kc values are used (Allen et al., 2007; Kumar et al., 2015). These limitations affect suitable estimate of ETc and crop irrigation water requirements (IWR), for optimizing agricultural water management.

Recent advances in agricultural remote sensing present an opportunity to monitor crop fields and provide reliable information about plant biophysical parameters (Gago et al., 2015; Jones and Vaughan, 2010) for improved irrigation water management. Multispectral and hyperspectral sensors onboard Unmanned Aerial Vehicles (UAV) can provide high resolution images of croplands, with short revisit time, for mapping crop physiological status (Turner et al., 2012; Gago et al., 2013). Data from these sensors provide a reliable estimate of Kc, which is possible due to the relationship between crop phenological development and Kc. Previous studies showed linear relationship between Kc and vegetation indices derived from spectral data in the visible and near-infrared spectral regions, such as the Normalized Difference Vegetation Index (NDVI), the Renormalized Difference Vegetation Index (RDVI), the Optimised Soil Adjusted Vegetation Index (OSAVI) (Campos et al., 2016; Gago et al., 2015; Ihuoma and Madramootoo, 2017). Monitoring actual crop physiological development, which influences crop evapotranspiration fluxes, facilitates the estimation of crop irrigation water requirements. However, the cost of UAVs and sensors are typically high, especially when several flights are needed for regular field monitoring during the growing season.

Therefore, researchers are shifting interests to the use of satellite imagery for estimating ETc and managing irrigation water (Calera et al., 2017; Vanino et al., 2018). The major limitations for adoption of satellite imagery for precision agriculture are the poor spatial and temporal resolution of satellite sensors (Bisquert et al., 2016). Also, the trade-off between the spatial resolution of the image and the satellite revisit time poses a major challenge to the use of the various satellite platforms. For example, the Landsat series has a relatively good spatial resolution (30 m) but has long revisit time (16 days) making it unsuitable for regular agricultural field assessment. The Moderate-resolution Imaging Spectroradiometer (MODIS) with daily coverage cannot be adopted for precise crop stress monitoring at field level due to its coarse spatial resolution (> 250 m).

Satellite resolution is further reduced by cloud cover, thus limiting the use of this imagery for assessing crop stress parameters. High resolution satellite sensors that are commercially available such as the GeoEye, Worldview series, PlanetScope, QuickBird, and RapidEye are too costly for routine crop monitoring since their imagery are not open to the public. Thus, despite established relationships between Kc and remotely derived vegetation indices, lack of cheap and high spatial and temporal resolution imagery presents a major limitation on the use of remote sensing for advancing precision agriculture.

Other researchers described the potential of satellite observations for predicting actual crop evapotranspiration over large agricultural fields. This approach is based on estimates of latent heat flux (hence, actual crop evapotranspiration) from surface energy balance (SEB) algorithms such as Surface Energy Balance Algorithm for Land (SEBAL) (Bastiaanssen et al., 1998) and Mapping EvapoTranspiration at High Resolution with Internalized Calibration (METRIC) (Allen et al., 2007). Again, the use of SEB methods for detecting crop water stress is limited by poor spatial and temporal resolution of thermal observations at field levels (Vanino et al., 2018; Bhattarai et al., 2016; Numuta et al., 2017; Al Zayed et al., 2016).

However, the launching of Sentinel-2A and 2B, which offers a reasonable compromise between the spatial resolution and revisit time, has greatly enhanced the prospects of routine monitoring of crop parameters. The multispectral sensors onboard Sentinel-2 captures data at 10, 20, and 60 m spatial resolution over 13 spectral bands, with a revisit time of five days (Vanino et al., 2018). The data provides rich information for describing crop reflectance and crop parameters such as biomass, leaf area index, yield, and leaf chlorophyll content (Laurent et al., 2014; Verrelst et al., 2015).

This study focused on the: (i) comparison of spectral data obtained from satellite platforms (Sentinel-2A & 2B and PlanetScope) and unmanned aerial vehicles for estimating crop coefficient (Kc); (ii) determination of crop evapotranspiration of processing tomato crop based on Sentinel-2 imagery; (iii) integration of ETc from Sentinel-2 and spatially-variable soil moisture data to predict irrigation water requirements. The hypothesis is that integration of soil and crop canopy data from satellite images would provide a more reliable estimate of crop water requirements. The AquaCrop simulation model was used to validate the ETc predicted from sentinel-2 imagery. AquaCrop computes Kc using maximum soil evaporation and crop transpiration coefficients, making it a reliable method of estimating actual crop evapotranspiration (Steduto et al., 2009; Toumi et al., 2016). The findings of this study will be useful for developing near real-time method to monitor crop water needs for implementing precision irrigation on large vegetable fields.

6.3. Materials and methods

6.3.1. Study area

The study area, shown in Fig. 6.1, is in Leamington, Southern Ontario, Canada, and lies between latitude 42° 05' 08" N and longitude 82° 33' 05" W, at an average altitude of 187 m above sea level. The local climate is classified as humid with hot summers, dry and cold winters. The growing season for field processing tomatoes extends from mid-May to September with an average maximum and minimum daily temperatures of 25 °C and 15 °C, respectively. The soil is predominantly loamy sand with sand, silt, and clay content of 86, 8, and 6%, respectively; average bulk density of 1450 kg m^{-3} and field capacity and permanent wilting point were 0.20 and 0.08 m^3 m^{-3}, respectively (Jaria and Madramootoo, 2013).

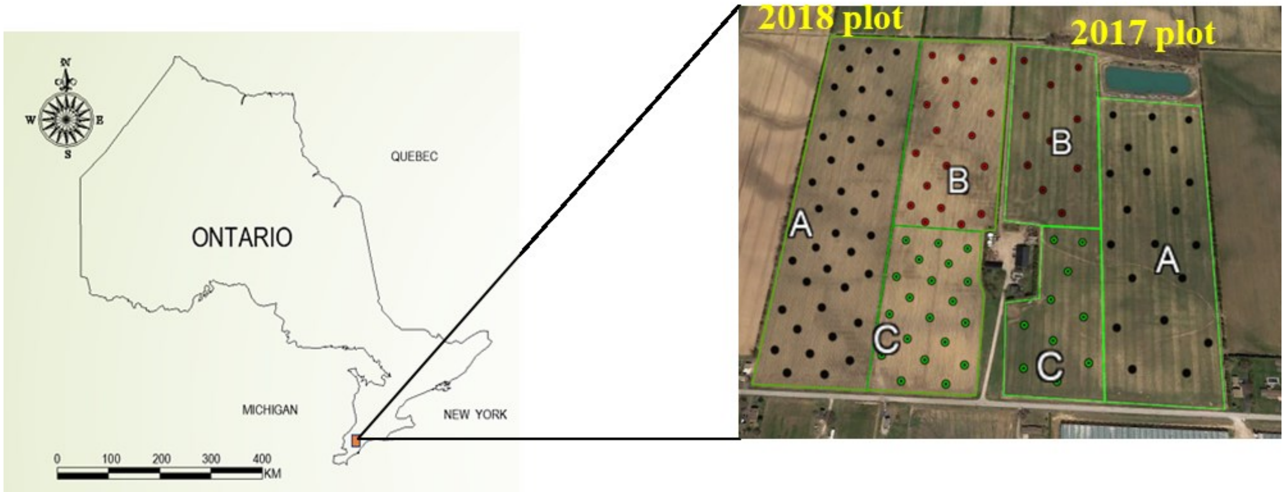

Fig. 6.1. Map of the experimental field showing various water treatments and georeferenced sampling points (A, B, and C represent 100%, 70, and 60% water treatments, respectively).

6.3.2. Experimental design and cropping details

The study was conducted during the 2017 and 2018 growing seasons (May-September) on a 10-hectare commercial farm cropped with processing tomatoes (*Lycopersicon esculentum* Mill. cultivar Heinz H9553). 42 days old seedlings were transplanted in soil with water content near field capacity in the top 30 cm on 25 May 2017 and 22 May 2018. The seedlings were planted at a spacing of 42 cm within rows that were spaced 50 cm apart. The plant density was 31,746 plants ha^{-1}. Pest and weeds were controlled in the farm according to conventional farm management practices.

The field was divided into three sections (A, B, and C) with areas of 10.5, 6, and 3.8 hectares in 2018 and 8.8, 5.3, and 3.2 hectares in 2017. Irrigation scheduling consisted of 100, 80, and 60% of replenishment of water in the plant root zone to field capacity for sections A, B, and C, respectively, in both seasons. Irrigation was applied through a drip system, with drip lines (irrigation tape, Streamline 636 006 F, Netafim Irrigation Inc., Fresno, CA) aligned along the surface of the bed. The inline emitters were spaced 30 cm apart, with a flow rate of 0.46 L h^{-1} @ 55 kPa, providing a uniform soil wetting pattern. The volume of water applied during each irrigation event to each treatment was determined as the product of the irrigation duration and the flow rate. Fertigation was applied through the micro drip irrigation system and all the treatments received the same amount of fertilizer during the growing season. The tomato plants were harvested after 112 days in 2017 (on 14 Sept.) and 121 days in 2018 (on 20 Sept.).

6.3.3. Data collection

In 2017, twenty (20) sampling points were selected from 100% treatment and ten (10) points were selected each from 80 and 60% treatments, while in 2018, forty (40) sampling points were selected from the 100% treatment, while twenty (20) points were selected each from the 80 and 60% treatments. The systematic grid sampling technique was used and the change in the number of sampling points between 2017 and 2018 seasons was to ensure better spatial coverage. All the sampling points were georeferenced for identification in the acquired images. The sampling points on the ground was a 3 × 3 m^2 plot. Measurements were taken from five (5) different plants within each plot and the average values were recorded. The coordinates of each plot were recorded with a Garmin GPSMAP 60CSx handheld GPS navigator, which has a spatial accuracy of 3 m.

Field measurements including leaf area index (LAI), leaf temperature, and soil moisture content were conducted in selected plants from georeferenced locations during the field campaigns at major phenological stages in the two growing seasons, as shown in Table 6.1. These measurements were taken to coincide with satellite image acquisitions and UAV flight campaigns. Average NDVI, defined as the weighted average of all the pixel-level NDVI values, was obtained from the

Table 6.1. Date of crop parameter measurements in the experimental site.

Year	DOY	DAT	Date	LAI	Tc	SMC	L8	S2	PS
2017	178	33	27-Jun	x	x	x	x		
	194	49	13-Jul	x	x	x	x		
	237	92	25-Aug	x	x	x	x		
2018	170	28	19-Jun	x	x	x		x	x
	180	38	29-Jun	x	x	x		x	x
	206	64	25-Jul	x	x	x		x	x
	228	86	13-Aug	x	x	x		x	x
	238	96	23-Aug	x	x	x		x	x

Where; DOY: Day of the year, DAT: Days after transplanting, LAI: Leaf area index, Tc: Leaf temperature, SMC: Volumetric soil moisture content, L8: Landsat 8, S2: Sentinel-2, and PS: PlanetScope images.

remotely sensed platforms within each plot. The pixel-level NDVI was computed for the UAV, Sentinel-2, and PlanteScope imagery using the conventional formula NDVI = (near-infrared - red)/(near-infrared + red) (Rouse, 1972). These NDVI values were compared with each other and statistical regression models were established using the field measurements and the average NDVI values.

6.3.3.1. In-situ crop measurements

Leaf temperature was measured with a portable infrared thermometer, with an emissivity of 0.95 W m^{-2} (Evett et al., 2000) (Fluke 572 model, Fluke Corporation, Everett, WA). The thermal sensor was placed 30 cm above the plant leaf with its laser point set at an angle of 90° to the horizontal. Measurements were conducted following standard procedures as adopted in Ihuoma and Madramootoo (2019a).

A portable canopy digital analyzer (LAI-2000 Plant Canopy Analyzer, LI-COR), was used to take non-destructive measurements of the LAI of the geo-referenced crops. An average of three (3) repetitions of eight (8) below canopy readings were taken within a 5 m radius of the georeferenced location to obtain the LAI value at each location. A view cap on the optical sensor, which has an open wedge of 180°, was used to avoid obstruction, like the operator of the sensor obstacles, as highlighted in Li-Cor (1992).

Portable Time Domain Reflectometers (TDR) (FieldScout TDR meters, Spectrum Technologies, Inc., IL, USA) was used to measure soil water content from the georeferenced points on days of data collection in 2017 and 2018. The TDR probes were inserted vertically into the soil at a depth of 30 cm such that it integrates the soil water content within the plant rooting depth. The TDR readings were calibrated with gravimetric soil moisture measurements.

6.3.3.2. Data acquisition from UAV

Two (2) different UAV flight campaigns were conducted on the farm in 2018 (25th July and 22nd August), and one UAV flight was conducted on 25th August 2017. The Parrot® Sequoia™ multispectral imaging sensor (Parrot Drones S.A.S, Paris, France), which captures the reflected light at four spectral bands with a field of view of 73.5° in the green (550 nm; 40 nm bandwidth), red (660 nm; 40 nm bandwidth), red-edge (735 nm; 10 nm bandwidth), and near-infrared (790 nm; 40 nm bandwidth), was mounted on a fixed-wing drone (GL, Hong Kong, China). The UAV was equipped with an irradiance sensor for measuring incident light in order to adjust for variation in ambient light during the flight. Ground images were acquired from calibration targets (AIRINOV Aircalib; AIRINOV, Paris, France), prior to each flight, in order to obtain reliable reflectance values. All images were taken under a clear sky condition. The Pixel size was 12 cm for images taken at flight altitude of about 70 m at a flight speed of 4 m/s.

The flight was conducted over the field through an automated flight pattern designed in the Atlas Flight application (MicaSense, Inc., Seattle, USA), ensuring 80% image overlap for both front and side laps. The Pix4Dmapper Pro (Pix4D S.A., Lausanne, Switzerland) was used to combine the single images to create an orthophoto mosaic in absolute reflectance values. The Pix4D takes both the calibration target images and the readings from the irradiance sensor into consideration in an automated workflow (Aasen et al., 2018 and Stavrakoudis et al., 2019). The UAV spectral data were resampled with Sentinel-2 spectral response to eliminate the mismatch in spectral resolution, as adopted in Kalacska et al. (2018).

6.3.3.3. Image acquisition from satellite platforms

Earth observation data were acquired from Copernicus Sentinel-2A and 2B satellite on five (5) different days (29th June, 9th July, 25th July, 13th August, and 23r^{d} August, 2018). Two (2) of these data sets were obtained on days closest to the UAVs flight campaigns in 2018. The Sentinel-2 mission consists of a constellation of two satellites (Sentinel-2A and Sentinel-2B; launched in 2015 and 2017, respectively) developed by European Space Agency for optimum coverage. The multispectral sensor on-board the Sentinnel-2 satellite platform have a combined 10 m spatial resolution (at the RGB and NIR wavebands) and a 5-day temporal resolution. The data are free and easily accessible and are utilized for understanding land cover, agriculture, and environment. The Sentinel-2 product was downloaded from the Copernicus Open Access Hub, which delivers orthorectified, georeferenced, and radiometrically calibrated into top-of-atmosphere (ToA) reflectance data (Vanino et al., 2018). In 2017, Landsat series (7 & 8) were acquired on three (3) different days (27th June, 13th July, and 25th August, 2017) from the field. But the data were enormously affected by cloud covers making them seemly unsuitable for agricultural studies.

Multispectral data were also acquired from PlanetScope satellite missions on days closest to Sentinel-2 data sets during the 2018 growing season. The PlanetScope has a daily revisit frequency with spatial resolution of 3 m at the RGB and NIR wavebands (Baloloy et al., 2018). The PlanetScope product was acquired as an Ortho Scene image, which is orthorectified, surface reflectance product, and delivered as analytic 4-band product. Multispectral image processing and analysis for obtaining NDVI were conducted with ESRI ArcGIS software (v10.5.1), as adopted in Saifuzzaman et al. (2019). NDVI was calculated according to the standard equation from the reflectance measurements in the near infrared and red bands.

6.3.4. Determination of actual evapotranspiration and crop coefficient

The crop evapotranspiration was estimated from Sentinel-2 images based on the empirical relationship between NDVI and Kc. The Kc was determined as the ratio of actual evapotranspiration (ETa) to the reference evapotranspiration (ETo). Daily ETa was estimated from the soil moisture balance approach (Eq. 6.1) based on daily soil moisture data collected in the field. Also, daily meteorological data collected from the same field using a portable weather station were used to estimate ETo, based on FAO-56 Penman-Monteith equation (Allen et al., 1998). NDVI values from georeferenced points were extracted from all the sentinel-2 images processed in the 2018 growing season. An empirical relationship between NDVI values and Kc values (which correspond with days of satellite image acquisition) was derived. Based on the equation of the linear relationship between NDVI and Kc, crop evapotranspiration for any day was estimated using the NDVI map of the field and daily ETo.

$$ET_a = \mathrm{P} + I + CR - D - R + \Delta S \ldots\ldots\ldots\ldots\ldots\ldots\ldots\ldots\ldots\ldots\ldots\ldots (6.1)$$

where, P: precipitation (mm), I: Irrigation depth since yesterday (mm), CR: Capillary rise from the groundwater table (mm), D: Deep percolation (mm), ETa: Actual crop evapotranspiration (mm), R: surface runoff (mm), ΔS: Soil water storage variation in the root zone (the top 45 cm soil layer) (mm). Deep percolation was ignored because there were low rainfall amounts. Efficient irrigation scheduling scheme ensured that the water applied did not exceed the field capacity. Surface runoff was ignored because the study site is relatively flat, and no runoff was observed during the growing season. The capillary rise from the groundwater table was ignored since the soil was sandy and the depth to ground water table is greater than 1 m (Jaria and Madramootoo, 2013).

To validate the ETc values gotten from the NDVI maps, the AquaCrop simulation model was also used to calculate ETc based on data collected from the field. The model uses the FAO 56-Penman Monteith module to estimate ETo (Steduto et al., 2009; Toumi et al., 2016). The ETc values are obtained based on the determination of the appropriate values of Kc using maximum soil evaporation and crop transpiration coefficients. Input parameters used by AquaCrop for calculation of ETc include climatic data, crop type, and cultivar, crop canopy cover, and soil water conditions (Araya et al., 2010). These parameters were measured in the field or estimated from experimental data, and input into the model for calculation of ETc. AquaCrop ETc was then compared with ETc estimated from NDVI maps.

6.3.4.1 Irrigation prescription maps

Irrigation prescription maps were generated from the combination of spatially-variable soil moisture data with an ETc map obtained from the Sentinel-2 platform. Soil moisture data collected from the georeferenced sampling points were used to produce the soil moisture map of the experimental field using ordinary kriging interpolation tool in ESRI ArcGIS software (v10.5.1). The ETc map from Sentinel-2 data was combined with soil moisture maps according to the soil moisture balance approach (Eq. 6.1) to produce the irrigation depth prescription maps.

6.3.5. Determination of crop irrigation water requirements (IWR)

The seasonal IWR was then calculated according to Eq. 6.2.

$$\mathrm{IWR} = ET_c - P_e \ldots\ldots\ldots\ldots\ldots\ldots. (6.2)$$

where ETc: Total monthly ETc data from AquaCrop model; P_e: is effective rainfall. Losses as a result of runoff and deep percolation were considered negligible because of low rainfall amount during the growing season. The effective precipitation was estimated using the USDA soil conservation service method according to Smith (1992) as follows:

$$\begin{cases} P_e = P_{tot} \times (125 - 0.2P_{tot})/125 & P_{tot} < 250\,mm \\ P_e = 125 + 0.1 \times P_{tot} & P_{tot} > 250\,mm \end{cases} \quad \cdots\cdots\cdots\cdots\cdots\cdots\cdots \ (6.3)$$

where P_{tot}: measured gross monthly precipitation.

6.3.6. Statistical analysis

The effects of water treatments on canopy - air temperature difference, LAI, and soil moisture content were described using the Pearson correlation ratio, as adopted by Ihuoma and Madramootoo (2020). Statistical analyses were carried out on NDVI from UAVs, Sentinel-2 images, canopy-air temperature difference, and LAI using the PROC/GLM (General Linear Model) procedure of SAS software (version 9.3, SAS Institute, Inc., Cary, NC, USA). Analysis of variance (ANOVA) was conducted on the data, and the significance of differences among treatments was separated using Fisher's Least Significant Difference (LSD) at a 5% probability level.

6.4. Results and discussion

This section focused on the analysis of the reflectance data from Sentinel-2A and 2B, UAVs, and PlanetScope and quality of the various sensors for the retrieval of NDVI and estimation of Kc and ETc for mapping irrigation water requirements.

6.4.1. Comparison of PlanetScope, UAV, and Sentinel-2 data

Fig. 6.2 shows the NDVI maps obtained from the UAV and satellite platforms on similar dates. The maps show that NDVI values ranged from 0.36 - 0.82 in Sentinel-2 images, 0.01 – 0.96 in UAV, and 0.34 – 0.82 in PlanetScope sensing platforms. These results show wide spatial variability in NDVI values within the field. Fig. 6.3 shows the average NDVI values acquired on 25th July 2018 for various platforms. The result indicates significant differences in NDVI from different remote sensing platforms, with the UAV recording the highest average NDVI values (0.89 ± 0.012) compared to PlanetScope (0.80 ± 0.01) and Sentinel-2 imagery (0.67 ± 0.008). The variation may be attributed to the radiometric differences as well as differences in spatial resolutions of the various imaging platforms. The UAV has a better resolution (12 cm) compared to the PlanetScope (3 m) and Sentinel-2 (10 m) imagery at the red and near infrared spectral regions. A further comparison of UAV and Sentinel-2 data is shown in Fig. 6.4. The histograms revealed that average NDVI values were centered around 0.9 for the UAV compared to Sentinel-2 values centered around 0.67.

(a)

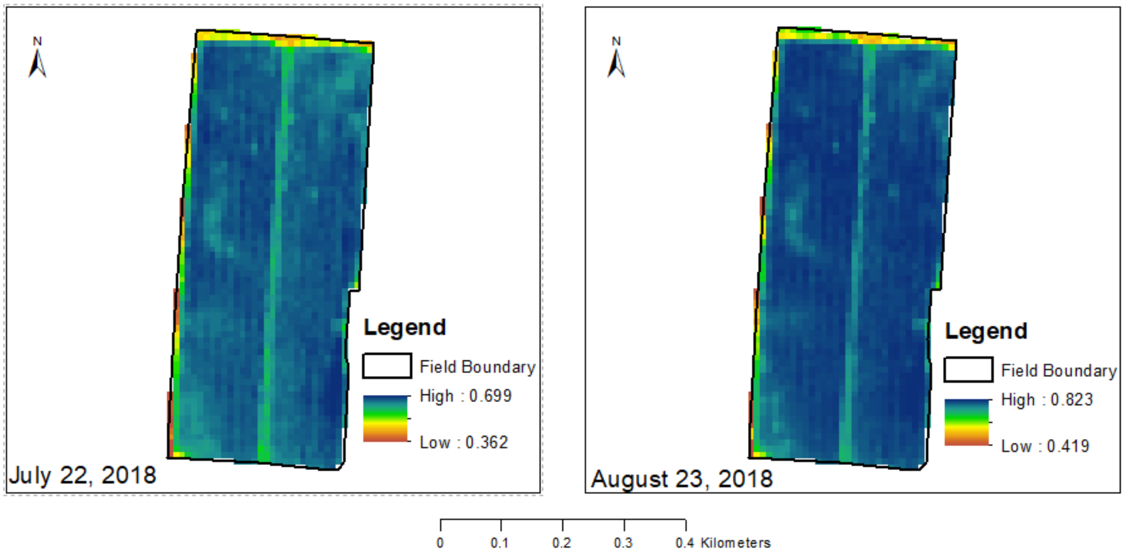
N
Legend
Field Boundary
High : 0.699
Low : 0.362
July 22, 2018
N
Legend
Field Boundary
High : 0.823
Low : 0.419
August 23, 2018
0
0.1
0.2
0.3
0.4 Kilometers

(b)

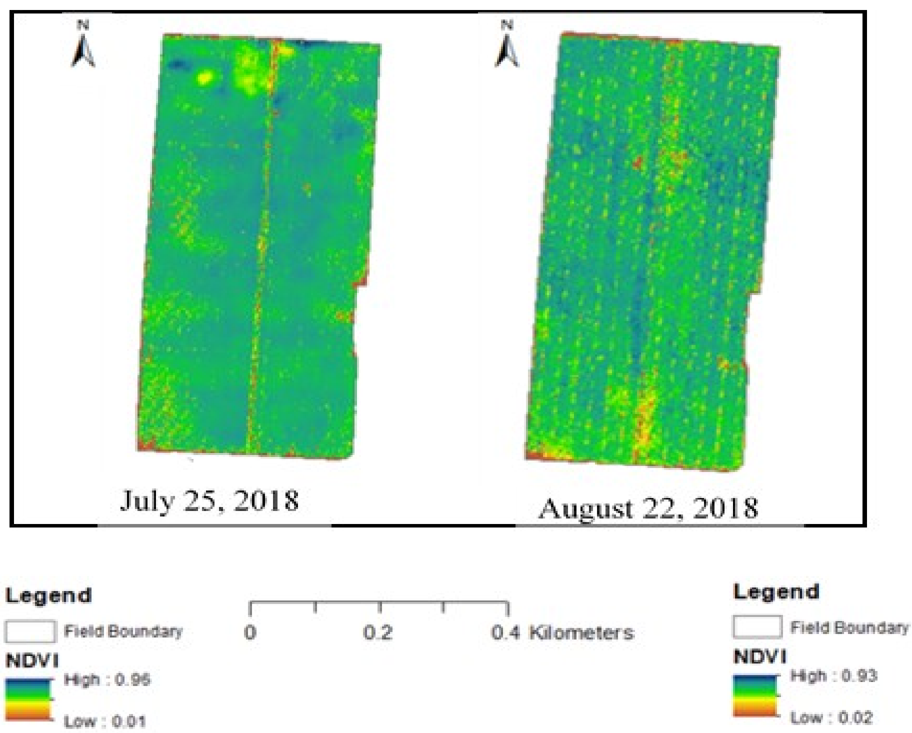
N
N
July 25, 2018
August 22, 2018
Legend
Field Boundary
NDVI
High : 0.96
Low : 0.01
0
0.2
0.4 Kilometers
Legend
Field Boundary
NDVI
High : 0.93
Low : 0.02

(c)

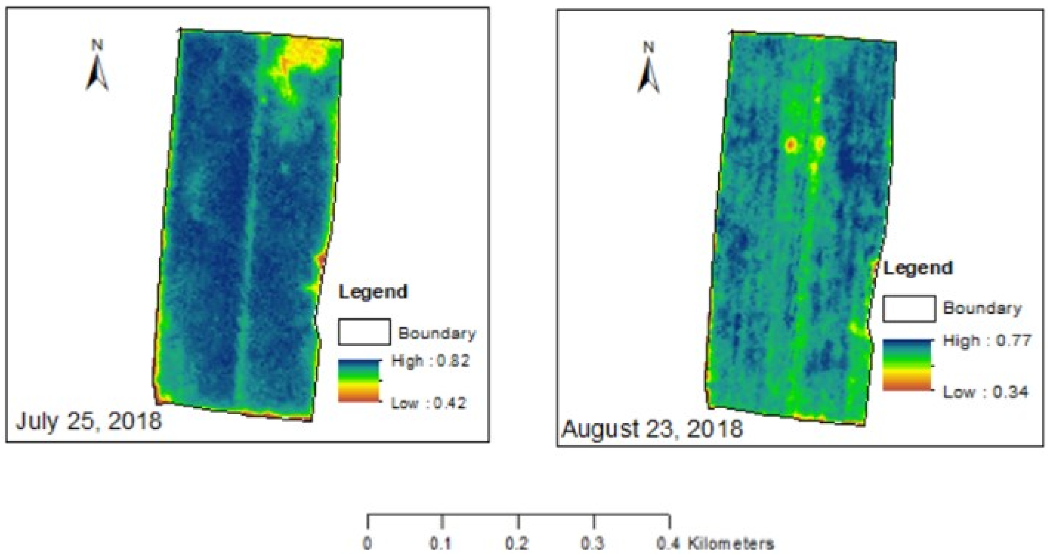

Fig. 6.2. Examples of NDVI maps estimated from (a) Sentinel-2; (b) UAV; (c) PlanetScope platforms in 2018.

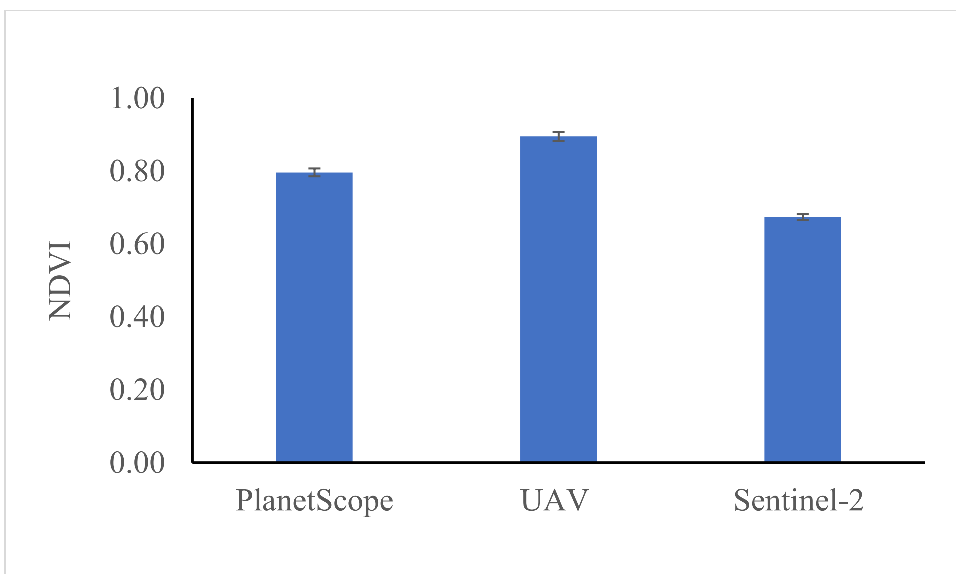

Fig. 6.3. Comparison of NDVI from UAV, Sentinel-2, and PlanetScope imagery acquired on 25th July 2018.

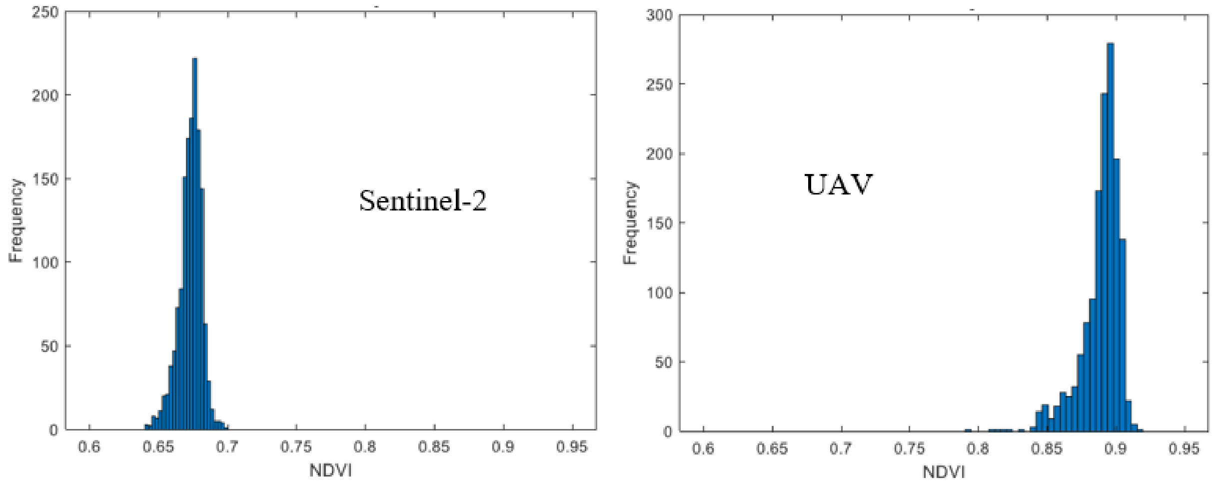

Fig. 6.4. Average NDVI from UAV acquired on July 25th, 2018 compared to Sentinel-2 imagery.

This average NDVI value from the UAV is relatively high because it was obtained in the field with about 85% vegetative cover (from site observation). Thus, the significant difference in average NDVI values between the UAV and satellite platforms suggests that the UAV overestimated the field NDVI. Although several authors have highlighted the suitability of UAV multispectral imagery for routine agricultural field assessment (Turner et al., 2012; Zarco-Tejada et al., 2013), UAV imagery also have some limitations. These limitations include the need to fly under very clear sky conditions, as well as the typically high cost of UAV and sensors, especially when several flights are needed during the growing season (Gago et al., 2015). The high value of NDVI from UAV in this study may be attributed to the potential calibration errors as well as the prevailing wind conditions during the flight campaigns. The limitations present a major drawback on the use of UAV to support precision agriculture.

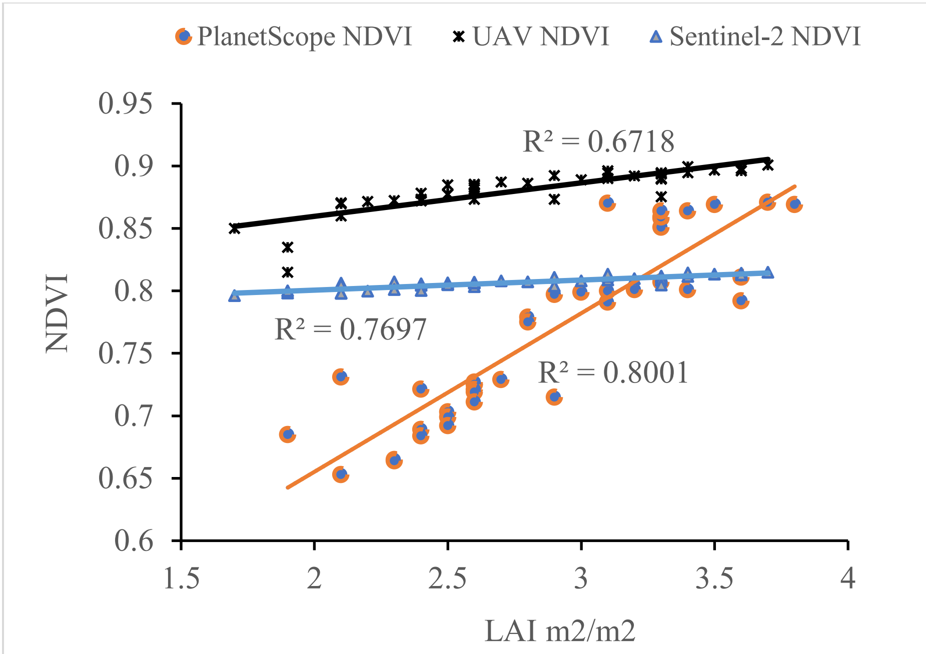

Fig. 6.5. Relationship between NDVI from PlanetScope, UAV, and Sentinel-2 data versus LAI

The relationships between LAI and NDVI computed from various imaging platforms are shown in Fig. 6.5. The result indicates a good correlation between LAI and NDVI data with $R^2 = 0.67$, $p < 0.001$; $R^2 = 0.77$, $p < 0.001$; and $R^2 = 0.80$, $p < 0.001$, for UAVs, Sentinel-2, and PlanetScope respectively. The strong correlation between NDVI and LAI observed in this experiment is consistent with previous studies (Rinaldi et al., 2014; Magney et al., 2016; Ihuoma and Madramootoo, 2017), indicating that water stress caused structural changes in tomato plants. The relationship between NDVI and LAI is essential for assessing the effects of water stress on yield. Providing suitable information on plant water requirements and spatiotemporal variability in field water status is essential for precise irrigation.

The result also shows that the PlanetScope data performed better than the UAV and Sentinel-2 data. This good correlation is due to the high spatial resolution of the PlanetScope satellite imagery, making it suitable for monitoring agricultural fields (Baloloy et al., 2018). Unlike Sentinel-2, PlanetScope data is not freely available to the public, and the relatively high cost of this data discourages its use by growers. The good correlation between Sentinel-2 date and LAI highlights the importance of Sentinel-2 imagery as a suitable alternative to UAV and other seemly costly satellite data. The Sentinel-2 data are easily accessible to the public and provide data to map large agricultural fields.

6.4.2. Water stress indicators

Water stress indicators were measured in the field during the plant growing seasons as indicated in Table 6.1. The descriptive statistics of tomato canopy grouped by irrigation treatments in 2017 and 2018 are presented in Table 6.2. The mean of LAI generally decreased with decreasing irrigation treatment levels, with 100 and 60% FC recording the highest and lowest LAI, respectively, the mean of Tc-Ta increased with decreasing water treatments. This decrease implies that water stressed plants have high canopy temperatures compared to non-stressed plants. The Tc-Ta showed good correlation, with $\eta^2 = 0.88$ and 0.62, in 2017 and 2018 respectively, while the LAI had correlation ratio, $\eta^2 = 0.86$ and 0.82, in 2017 and 2018, respectively. This result indicates that the irrigation treatments explained most of the variance in Tc-Ta and LAI during the two tomato growing seasons. Soil moisture content (SMC) showed significant variations for the various treatments. The SMC has $\eta^2 = 0.60$ and 0.73, for 2017 and 2018, respectively, indicating that the water treatments explained most of the variance in SMC. Average NDVI were not different for various irrigation treatments as shown in the NDVI maps (Fig. 6.2). The effects of irrigation treatments were probably not well pronounced in the canopy cover to be detected by NDVI. Ihuoma and Madramootoo (2020) observed that NDVI usually detects structural and morphological changes in plant canopies when there is a prolonged effect of stress in crops.

This concept explains why NDVI is useful for assessing plant yield and biomass, where the continued effects of stress would be noticeable (Rinaldi et al., 2014).

Table 6.2. Descriptive statistics (mean, standard deviation, and correlation ratio (η^2) of tomato plant canopy grouped by the irrigation treatments (100, 80, and 60% FC). Where Tc-Ta: air-canopy temperature difference (°C), LAI: Leaf Area Index ($m^2\ m^{-2}$), SMC: soil moisture content (%).

Stress indicators	2017 100%	2017 80%	2017 60%	2017 η^2	2018 100%	2018 80%	2018 60%	2018 η^2
Tc-Ta	-3.2± 0.5^a	-1.8± 0.5^b	0.9± 0.6^c	0.88	-5.3±1.5^a	-3.1±0.5^b	-1.1±1.6^c	0.62
LAI	3.3± 0.3^a	2.5± 0.2^b	1.8± 0.2^c	0.86	3.3±0.3^a	2.6±0.2^b	1.9±0.3^c	0.82
SMC	16.5± 1.1^a	13.3±1.2^b	11.4± 0.7^c	0.60	17.2±1.2^a	14.5±0.8^b	11.8±1.3^c	0.73

Treatments with the same letters are not statistically significant.

Table 6.3. Monthly (May-August) rainfall (mm) and mean temperature (°C) during the 2017 and 2018 growing seasons in comparison with 10-year (2008-2017) average.

	May	June	July	August	Mean
Temperature 2018 (°C)	17.1	20.5	22.6	22.9	20.8
Temperature 2017 (°C)	13.9	20.7	21.8	20.0	19.1
Temperature long-term average (°C)	14.7	20.3	22.3	21.6	19.7
Precipitation 2018 (mm)	122.1	98.1	30.2	37.6	72.0
Precipitation 2017 (mm)	108.6	100	50	42.7	75.3
Precipitation long-term average (mm)	84.9	95.5	56.1	41.1	69.4

6.4.3. Reference evapotranspiration and crop coefficient

Table 6.3 shows the weather conditions in 2017 and 2018 growing seasons compared to a 10-year average (2008 – 2017). The mean temperature was similar during the period of the experiment, recording a value of 19.1 °C in 2017 and 20.8 °C in 2018, and was similar to the 10-year average of 19.7 °C. Similarly, mean precipitation was not different for the two years, with 75.3 and 72.0 mm in 2017 and 2018, respectively. These values were higher than the long-term average of 69.4 mm.

Daily meteorological data were used to compute reference evapotranspiration (ETo) based on FAO-56 PM for 2017 and 2018. The seasonal variation of ETo for the 2-year period is shown in Fig. 6.6. Cumulative seasonal ETo was 486.8 mm (from 25th May – 14th September 2017) and 511.6 mm (from 22nd May – 20th September 2018). The average daily ETo was 4.31- and 4.19-mm d^{-1} in 2017 and 2018 growing seasons, respectively.

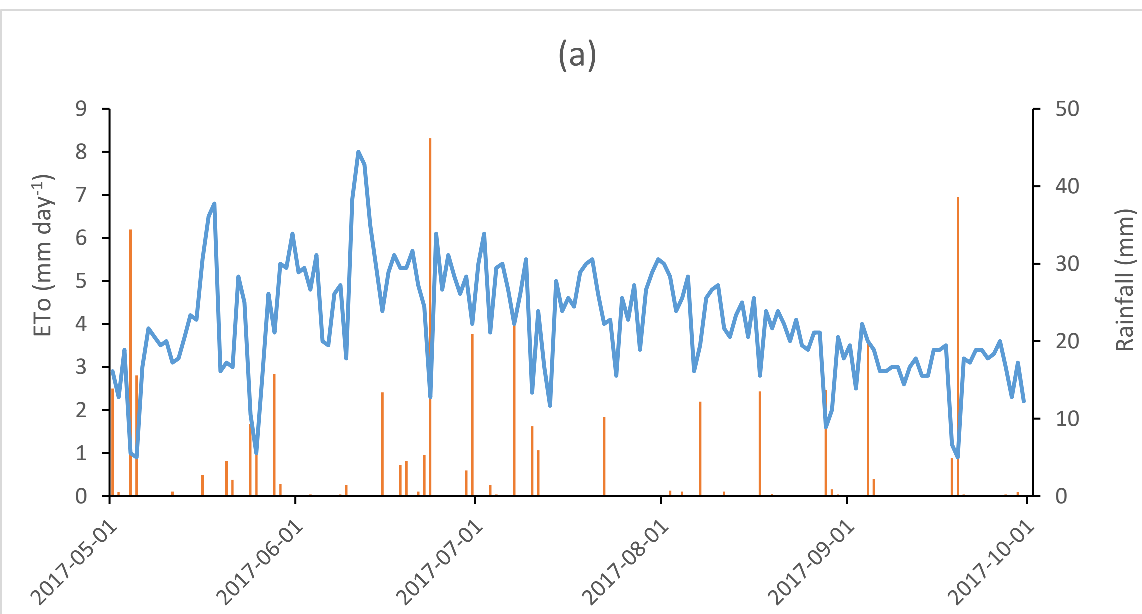

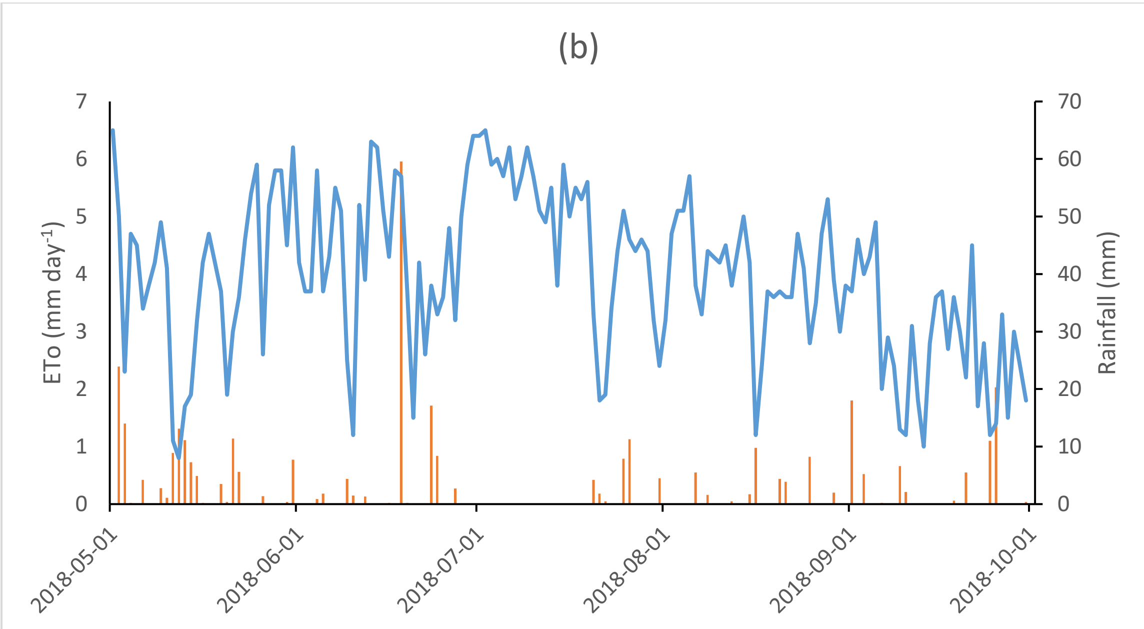

Fig. 6.6. Reference evapotranspiration (FAO-56 PM ETo, mm d^{-1}) and rainfall (mm) for the growing season 2017 (a) and 2018 (b) for the experimental site.

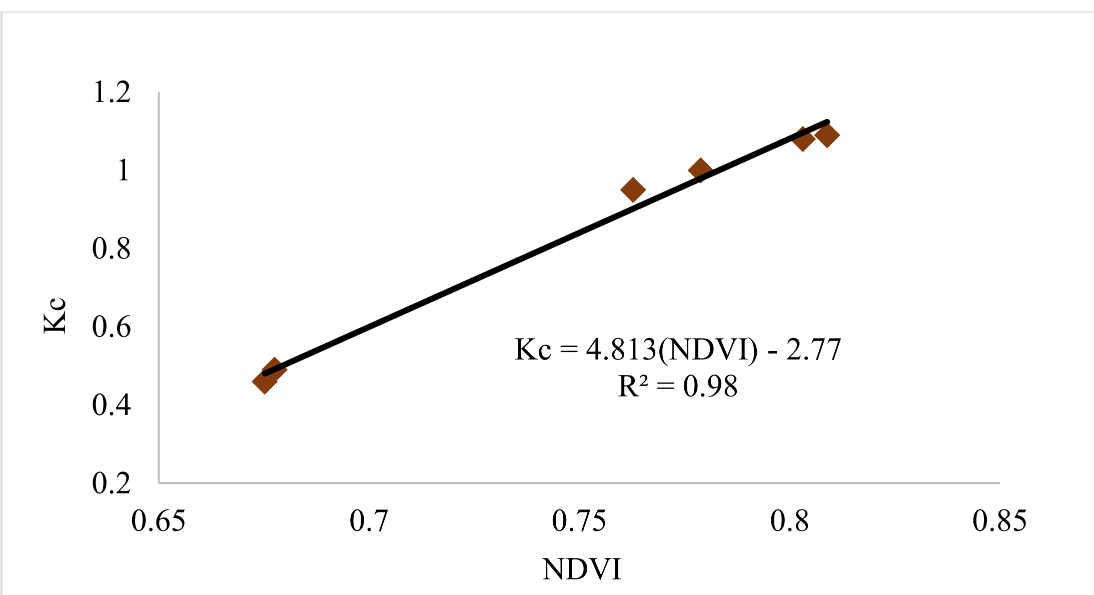

Fig. 6.7. Relationship between Kc and NDVI derived from sentinel-2 imagery.

6.4.4. Remote sensing-based estimates of crop evapotranspiration

Sentinel-2 imagery was selected for estimation of Kc, ETc, and IWR because of the perceived advantages of Sentinel-2 sensors over other sensing platforms considered in this study. NDVI values were extracted from georeferenced points in sentinel-2 images and were correlated with Kc values ($R^2 = 0.98$, $p < 0.001$) to establish a relationship between NDVI and Kc values (Fig. 6.7) on days of data collection. Kc depends mainly on the dynamics of plant canopy cover (Allen et al., 1998; Kullberg et al., 2017) and researchers have utilized its relationship with NDVI to map plant crop cover.

ETc maps were estimated from sentinel-2 imagery using the linear relationship between NDVI and Kc, as presented in Fig. 6.8. ETc derived from Sentinel-2 imagery ranged from 0.1 to 3.9 on 22nd July 2018 and 0.1 to 6.3 on 23rd August 2018. The spatial variability in ETc recorded in the field on both dates indicates the need for more efficient use of water in the field. Typically, the grower applies water uniformly in the field during the growing season, which implies that the grower either over/or under-irrigates the field. The result has implications on the allocation and use of limited water allocation resources in this intensely cultivated agricultural district. ETc prescription maps could be easily produced from remotely sensed platforms taking advantage of their quick turnaround time and high spatial resolution to optimize water use in these irrigated farmlands.

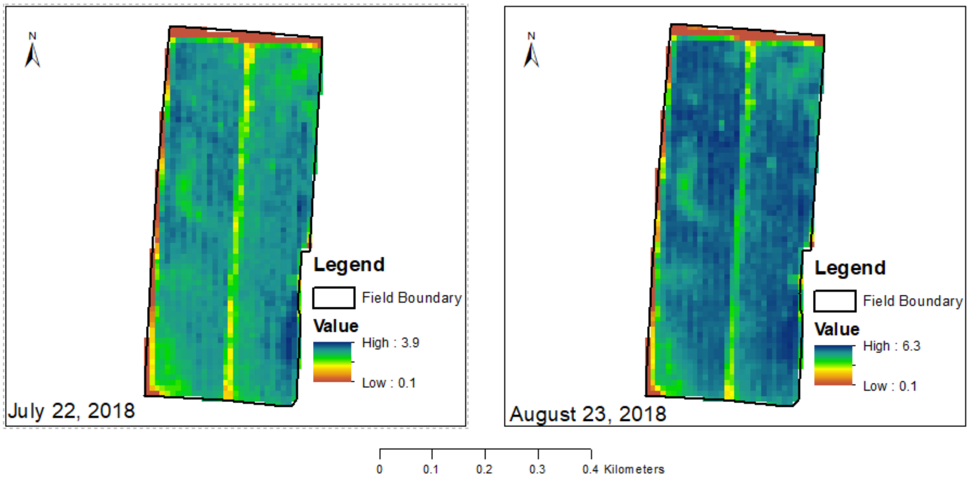

Fig. 6.8. Crop evapotranspiration maps estimated from Sentinel-2 imagery in 2018.

6.4.4.1. Verification of crop evapotranspiration using AquaCrop Simulation model

ETc was estimated from AquaCrop, as shown in Fig. 6.9, to verify the accuracy of remotely sensed estimates of ETc. Daily ETc from AquaCrop ranged from 0.6 to 6.2 mm d^{-1} and 0.7 to 6.2 mm d^{-1} in 2017 and 2018 growing seasons, respectively. ETo was generally higher during the flowering and maturity growth stages, corresponding to periods when the tomatoes needed more water for vegetal development.

Average ETc values estimated from Sentinel-2 imagery correlated with ETc estimated from AquaCrop model in 2018, with $R^2 = 0.92$ ($p < 0.01$), as shown in Fig. 6.10. The good correlation between ETc derived from AquaCrop and Sentinel-2 data shows the usefulness of Sentinel-2 imagery for mapping field ETc for improving precision irrigation. Although satellite platforms such as MODIS and Landsat are useful for mapping crop ET using METRIC and SEBAL algorithms (Senay et al., 2013), the utility of these satellite platforms and surface energy balance methods for assessing crop water stress is limited for field scale applications due to their coarse spatial resolution. The Sentinel-2 mission provides an alternative data with its 10 m spatial resolution and 5 days revisit time, an advantage that can be utilized to advance precision water management in the field.

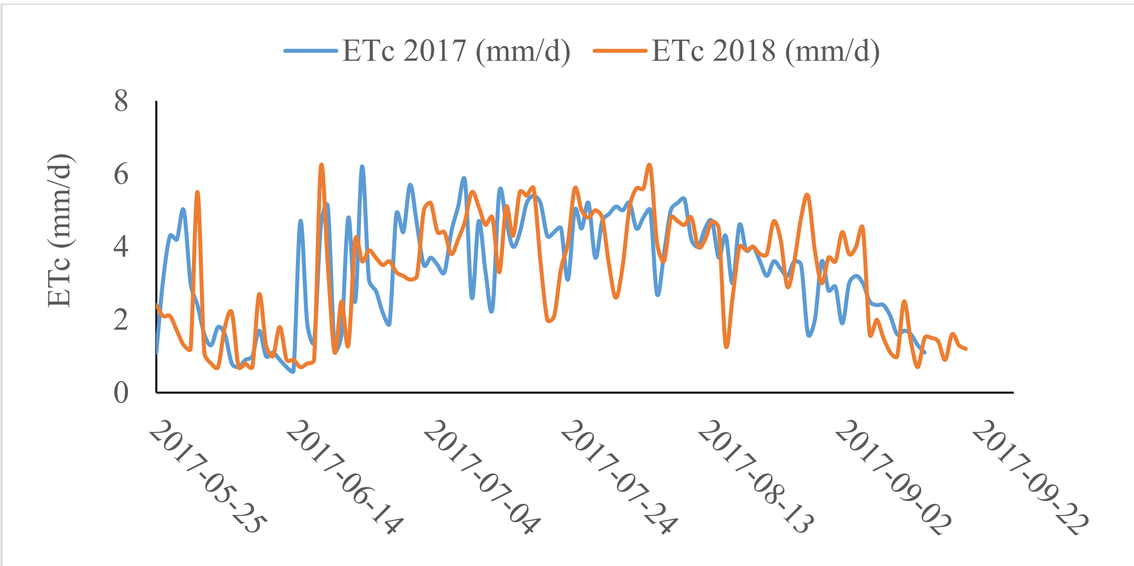

Fig. 6.9. Daily crop evapotranspiration estimated from Aqua Crop simulation model in 2017 and 2018 growing seasons.

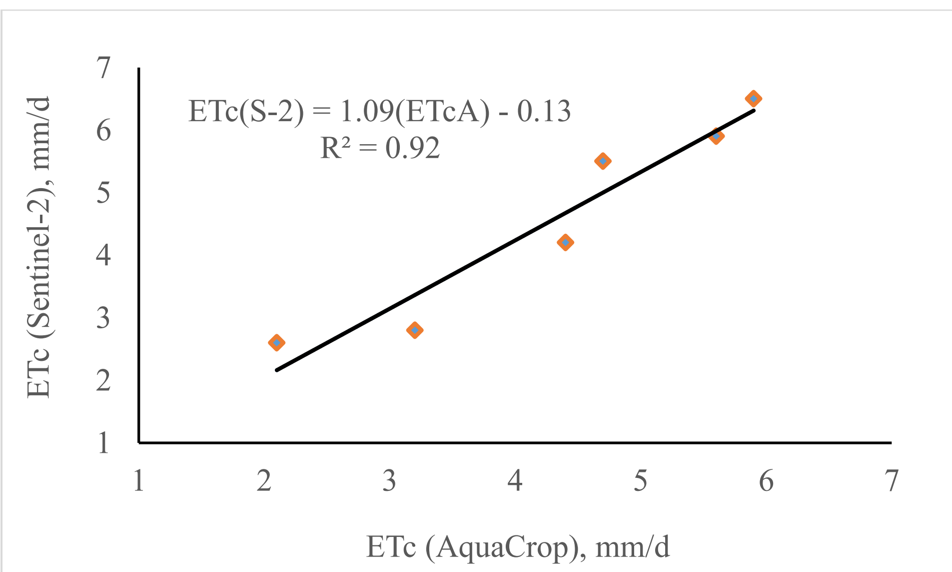

Fig. 6.10. Average ETc results estimated from sentinel-2 imagery (ETc S-2) compared with ETc estimated from Aqua Crop model (ETc A) in 2018.

6.4.5. Irrigation water requirements

Fig. 6.11 shows the maps of soil moisture content in the field during the sampling dates in 2018 while Fig. 6.12 shows the prescription maps of irrigation depths in the field. Irrigation depths varied from 4 – 33 mm within the field, during the sampling dates. The 100% treatment level requires less irrigation compared to 80 and 60% treatment levels, as seen in the maps. However, the results indicate substantial spatial variability in terms of crop water requirements during the growing season, which supports the use of a satellite-based approach for monitoring the growth conditions of plants. The result further proves the suitability of Sentinel-2 imagery for assessing crop canopy cover and IWR at the field scale. The findings of this study also show the prospect of integrating ETc data satellite imagery with spatially-variable soil moisture data for routine assessment of crop water status and optimization of water management in agricultural fields. Combining crop growth parameters and weather data with satellite imagery would aid growers, water resource managers, and policymakers to evaluate irrigation water volume needed at field and district scales.

Table 6.4 shows the seasonal IWR estimated from the effective rainfall and ETc in 2017 and 2018 growing seasons. IWR was highest in the months of July and August, which corresponds to the months when the plants require more water for growth. The estimated IWR was about 165 and 199 mm in 2017 and 2018 growing seasons, respectively. These estimates were lower than the actual amount of water applied by the farmer, which amounted to 198 and 247 mm in 2017 and 2018 growing seasons, respectively. These results indicate that the grower over-irrigated the tomato crops by 17% and 20% in 2017 and 2018 growing seasons, respectively. Assessing crop water needs from satellite imagery and incorporating this information into irrigation systems would essentially optimize crop water use.

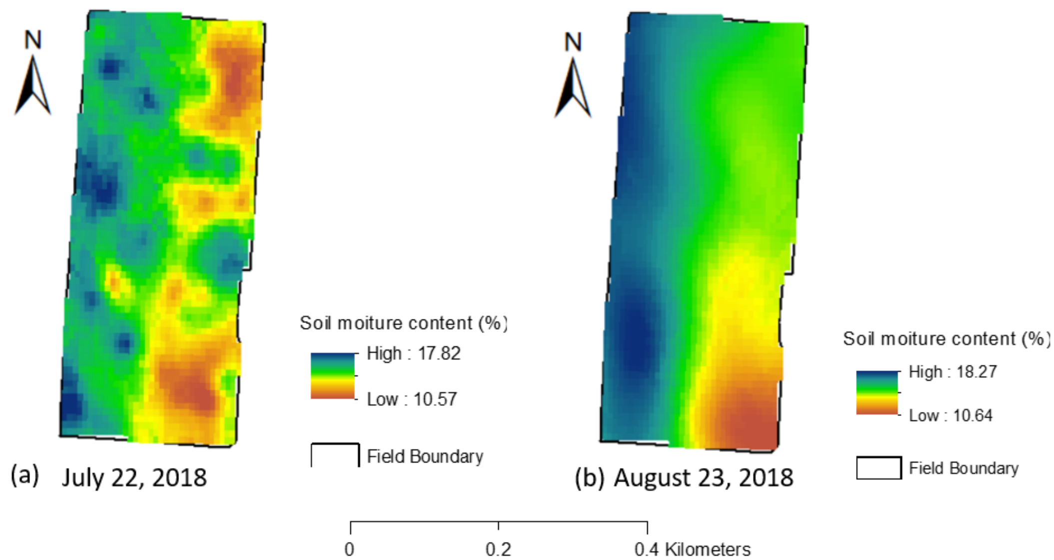

Fig. 6.11. Maps showing spatial variability of soil moisture content (%) in the field during the sampling dates in 2018 (a) July 22 and (b) August 23.

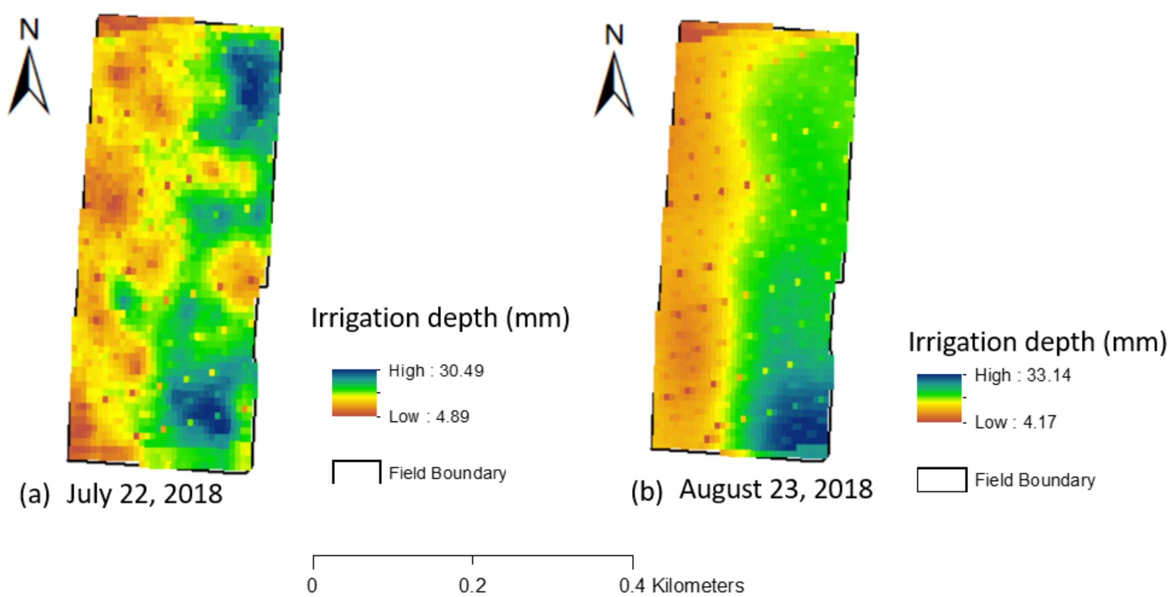

Fig. 6.12. Prescription maps showing irrigation depths (mm) in the field during the sampling dates in 2018 (a) July 22 and (b) August 23.

Table 6.4. Effective rainfall (Reff), crop evapotranspiration (ETc), and irrigation water requirement (IWR) during the growing seasons in 2017 and 2018.

Year	Month	Reff (mm)	ETc (mm)	IWR (mm)	Water applied (mm)
2017	May	24	27	3	7
	June	84	88	4	9
	July	46	121	75	88
	August	40	114	74	81
	September	22	31	9	13
	Total	215	381	165	198
2018	May	15	28	13	21
	June	83	87	4	11
	July	29	124	95	108
	August	35	116	81	94
	September	36	42	6	13
	Total	197	396	199	247

6.5. Summary and conclusion

This study described a methodology for integrating satellite based crop evapotranspiration (ETc) with soil moisture data for mapping irrigation application depth of processing tomato crops. We also evaluated UAV, Sentinel-2, and PlanetScope imagery for estimating crop coefficient (Kc) and ETc. Although PlanetScope data performed better than UAV and Sentinel-2 data, the relatively high cost of PlanetScope data limits its use for regular assessment of agricultural fields. However, Sentinel-2 satellite platform, with its enhanced spectral, spatial, and temporal resolutions, provides a reliable and non-invasive alternative for estimating Kc. Kc influences evapotranspiration fluxes and irrigation water requirements, and high correlation between Kc and NDVI reflects the good relationship between crop phenological development and canopy spectral reflectance. This study utilized this linear relationship to provide a better estimate of ETc, which was combined with soil moisture maps to predict irrigation water requirements. Results indicate a good agreement between ETc estimated from remotely sensed images and ETc measured by means of the AquaCrop model.

The findings reveal that the farmer tends to apply water uniformly in the field without recourse to the spatial variability of field ETc, thereby over/under-irrigating the crops. Typically, the grower over-irrigated the crops by 17-20% during the two growing seasons studied in this experiment. Providing timely information about the actual crop development and IWR from freely available satellite data allows the implementation of more efficient water applications based on the actual crop water requirements. Information and Communication Technologies facilitates timely delivery of satellite images using the internet, to provides near-real-time data to support irrigation management. This approach will equip farmers and policymakers with robust and qualitative information about the spatiotemporal variability of crop water requirements to enhance crop productivity.

CHAPTER VII

Summary and Conclusions

7.1. General summary

Traditional methods of water and nitrogen management rely on soil tests and sensors for measuring plant water and nitrogen requirements. These measurements are invasive and often do not account for spatial variability of soil and crop parameters, leading to uniform application of water and nitrogen. This in turn leads to over- and/or under-application of agricultural inputs in large fields, with its economic and environmental consequences. Spectral reflectance data provide a timely and non-destructive alternative to conventional approach of monitoring plant abiotic stress. This thesis evaluated reflectance indices for assessing crop stress, and coupled the indices with soil moisture data to provide more precise estimate of plant water and nitrogen requirements.

In order to better understand the use of spectral reflectance indices for plant stress assessment, intensive greenhouse and field experiments were undertaken using two widely cultivated high-value vegetable crops (bell pepper and tomato crops). The study evaluated nine reflectance indices for assessing plant stress, induced by varying irrigation water applications. The results indicated that the photochemical reflectance indices (PRI) centered at 553 nm (PRI_{553}) was the most useful index for detecting water stress in greenhouse grown bell pepper plants. The PRI centered at 550 nm (PRI_{550}) was suitable for assessing water stress in both greenhouse and field grown tomato crops. These results are in contrast with previous studies, which suggested the PRI centered at 570 nm (PRI_{570}) for monitoring water stress in most field crops, indicating that the reflectance indices threshold for water stress detection is crop and climate specific. Also, the Transformed Chlorophyll Absorption in Reflectance Index and the Renormalized Difference Vegetation Index (RDVI) were best suited for monitoring nitrogen status in tomato crops. The study further showed that the PRI, normalized by incorporating the RDVI and the red edge of the reflectance spectrum (wavelengths centered 600 and 70nm) was suitable to simultaneously estimate water and nitrogen status. The findings of these studies revealed the feasibility of monitoring crops using hyperspectral sensors to provide reliable, rapid, and non-invasive estimates of plant abiotic stress. Near-real-time analyses of leaf spectral features provides useful information to the growers for optimizing agricultural input and enhancing productivity.

The results of the greenhouse and field experiments were then scaled up to assess irrigation water requirements of tomato crops on large commercial vegetable fields. With the use of UAV technology, a drone outfitted with multispectral cameras, normalized difference vegetation indices were acquired and compared with PlanetScope and Sentinel 2A & 2B satellite imagery for estimating crop coefficient and evapotranspiration over a 10-hectare processing tomato field. The PlanetScope imagery were comparatively better than the UAV and Sentinel-2 data, but the high cost of acquiring PlanetScope data limits its use for routine agricultural field assessment. Sentinel-2 satellite data, with its enhanced resolutions, provide a reliable and non-invasive alternative for estimating Kc. AquaCrop simulation model was used to estimate daily crop evapotranspiration in the field and the results were compared with results obtained from Sentinel-2 satellite imagery. Crop evapotranspiration maps obtained from remotely sensed platforms were combined with soil moisture data to estimate and map irrigation depth, thereby accounting for spatial variability of soil and crop parameters.

The study revealed that uniform water application in the field caused about 17-20% over-application of irrigation water by the grower during the two growing seasons. The findings of this thesis confirm that providing timely information about the actual crop development and irrigation water requirements from freely available satellite data would allow the implementation of more efficient water applications based on actual crop water needs. Efficient use and management of irrigation water saves water and energy costs, minimizes leaching of agrochemicals, and reduces contamination of underlying aquifer. This study documented a protocol for utilizing satellite technology, especially the freely available Sentinel-2 imagery, to precisely map crop water requirements of large agricultural fields. This technique provides a valuable tool to farmers and policymakers for supporting precision agriculture.

7.2. Contributions to knowledge

As a result of these research results, the following are some of the commendable contributions to research.

1. This thesis demonstrated that leaf spectral data provide a non-destructive, reliable, and near real-time alternative to conventional methods of crop stress assessment. Suitable vegetation indices for monitoring crop abiotic stress in greenhouse and field grown high-value vegetable crops were identified. Measuring these indices with hyperspectral sensors provides timely spatial distribution information on crop conditions for optimizing agricultural water and nitrogen use.

2. This research project highlighted the suitability of Sentinel-2 satellite mission for mapping evapotranspiration and irrigation water requirements. The use of remotely sensed

reflectance data for agricultural applications is often limited by cloud cover and poor spectral resolution of satellite images. However, this study has shown that Sentinel-2 data have suitable spectral, spatial, and temporal resolutions for routine agricultural field assessments. With the high cost of unmanned aerial vehicle technology and other commercial satellite data such as PlanetScope imagery, Sentinel-2 imagery, which is freely available in the public domain, provides alternative data to regularly monitor agricultural fields.

3. This study created irrigation management zones based on crop characteristics, thereby advancing the concept of precision agriculture and variable rate irrigation. Previous management zones were created based on soil properties but, this research has confirmed that plant-based parameters, from remotely sensed images, provide a more reliable estimate of crop water needs for optimizing crop yield. This approach facilitates timely detection of water stress in crops to minimize yield loss, with the potential to increase water savings and enhance agricultural sustainability.

4. This thesis proposes a holistic methodology to precisely map crop irrigation water requirement based on the integration of spatially-variable soil moisture and crop evapotranspiration data, obtained from remotely sensed images. The integration of crop evapotranspiration and soil moisture content leads to a better estimate of irrigation water requirements. This approach provides high resolution maps for optimizing agricultural water use efficiency, aimed at improving crop yield.

7.3. Recommendations for future research

1. Leaf spectral properties are not solely dependent on plant water status. Factors such as soil background, canopy structure, leaf thickness, leaf age, and variations in leaf angle could influence the spectral response of leaves. Therefore, future research should focus on the integration of thermal and narrow-band hyperspectral imagery to provide more precise information about plant water status.

2. Future studies should test the vegetation indices for monitoring water and nitrogen stresses in actual fertigation management practices, to fully establish the practicality of this approach for improving precision agricultural management.

3. Operationalizing this concept for practical use in crop stress management requires more data points to generate response surface curves of the suitable indices versus water and nitrogen application rates. With the indices, more precise estimates of water and nitrogen rates can be obtained from the response surface curve to support decision making in fertigation management.

4. Further research in crop water stress studies should fuse satellite observations of crop evapotranspiration and soil moisture with daily climate data to generate near real-time prescription maps for site-specific irrigation applicable to thousands of hectares within irrigation/water management districts.

References

Aasen, H.; Honkavaara, E.; Lucieer, A.; Zarco-Tejada, P.; Aasen, H.; Honkavaara, E.; Lucieer, A.; Zarco-Tejada, P.J., 2018. Quantitative Remote Sensing at Ultra-High Resolution with UAV Spectroscopy: A Review of Sensor Technology, Measurement Procedures, and Data Correction Workflows. Remote Sens. 10, 1091.

Afzal, A., Duiker, S. W., Watson, J. E., Luthe D., 2017. Leaf thickness and electrical capacitance as measures of plant water status. Transactions of the ASABE, 60(4), 1063-1074.

Agam, N., Cohen, Y., Berni, J., Alchanatis, V., Kool, D., Dag, A., Yermiyahu, U., Ben-Gal, A., 2013. An insight to the performance of crop water stress index for olive trees. Agric. Water Manage. 118, 79–86.

Aguilar, C., Zinnert, J. C., Polo, M. J., & Young, D. R., 2012. NDVI as an indicator for changes in water availability to woody vegetation. Ecological Indicators, 23, 290-300.

Al Zayed, I. S., Elagib, N. A., Ribbe, L., Heinrich, J., 2016. Satellite-based evapotranspiration over Gezira Irrigation Scheme, Sudan: A comparative study. Agri Water Mgt., 177, 66 – 76.

Aladenola, O., Madramootoo, C., 2014. Response of greenhouse-grown bell pepper (Capsicum annuum L.) to variable irrigation. Canadian J. Plant Sci. 94, 303–310.

Alchanatis, V., Cohen, Y., Cohen, S., Moller, M., Sprinstin, M., Meron, M., Tsipris, J., Saranga, Y., Sela, E., 2010. Evaluation of different approaches for estimating and mapping crop water status in cotton with thermal imaging. Precision Agric. 11, 27–41.

Ali, M. H., 2011. Practices of irrigation and on-farm water management: *Vol. 2.* New York, NY: Springer.

Allen, R. G., Pereira, L. S., Raes, D., Smith, M., 1998. Crop evapotranspiration-Guidelines for computing crop water requirements-FAO Irrigation and drainage paper 56. FAO, Rome, 300, D05109.

Allen, R.G., Pereira, L.S., Smith, M., Raes, D., Wright, J.L., 2005. The FAO-56 dual crop coefficient method for predicting evaporation from soil and application extensions. J. Irrig. Drain. Eng. 131, 2–13.

Allen, R.G., Tasumi, M., Trezza, R., 2007. Satellite-based energy balance for mapping evapotranspiration with internalized calibration (METRIC) – model. J. Irrig. Drain. 133, 380–394.

Alves, I., Pereira, L.S., 2000. Non-water-stressed baselines for irrigation scheduling with infrared thermometers: a new approach. Irrig. Sci. 19 (2), 101–106.

Amatya, S., Karkee, M., Alva, A. K., Larbi, P., & Adhikari, B. 2012. Hyperspectral imaging for detecting water stress in potatoes. Paper Number: 12-1345197. In American society of agricultural and biological engineers, meeting Presentation.

Ameglio, T., Archer, P., Cohen, M., Valancogne, C., Daudet, F., Dayau, S., Cruiziat, P., 1999. Significance and limits in the use of predawn leaf water potential for tree irrigation. Plant and Soil 207, 155–167.

Araya, A., Solomon, H., Kiros, M. H., Afewerk, K., Taddese, D., 2010. Test of AquaCrop model in simulating biomass and yield of water deficient and irrigated barley (Hordeumvulgare). Agric. Water Manage., 97, pp. 1838-1846.

Ballester, C., Jimenez-Bello, M., Castel, J., Intrigliolo, D., 2013. Usefulness of thermography for plant water stress detection in citrus and persimmon trees. Agricultural and Forest Meteorology 168, 120–129.

Baloloy, A. B., Blanco, A. C., Candido, C. G., Argamosa, R. J. L., Dumalag, J. B. L. C., Dimapilis, L. L. C., Paringit, E. C., 2018. Estimation of mangrove forest aboveground biomass using multispectral bands, vegetation indices and biophysical variables derived from optical satellite imageries: rapideye, planetscope and sentinel-2. ISPRS Annals of the Photogrammetry, Remote Sensing and Spatial Information Sciences, Volume IV-3, ISPRS TC III Mid-term Symposium "Developments, Technologies and Applications in Remote Sensing", 7–10 May, Beijing, China.

Baluja, J., Diago, M.P., Balda, P., Zorer, R., Meggio, F., Morales, F., Tardaguila, J., 2012. Assessment of vineyard water status variability by thermal and multispectral imagery using an unmanned aerial vehicle (UAV). Irrig. Sci. 30 (6), 511–522.

Bandyopadhyay, K. K., Pradhan, S., Sahoo, R. N., Singh, R., Gupta, V. K. 2014. Characterization of water stress and prediction of yield of wheat using spectral indices under varied water and nitrogen management. Agricultural Water Management, 146, 115-123

Bastiaanssen, W. G., Menenti, M., Feddes, R., & Holtslag, A., 1998. A remote sensing surface energy balance algorithm for land (SEBAL). Formulation. Journal of hydrology, 198-212.

Bausch, W., Trout, T., Buchleiter, G., 2011. Evapotranspiration adjustments for deficit-irrigated corn using canopy temperature: a concept. Irrig. and Drain. 60, 682–693.

Behmann, J., Steinrücken, J., Plümer, L., 2014. Detection of early plant stress responses in hyperspectral images. ISPRS J. Photogramm. Remote Sens. 93, 98–111.

Bellvert, J., Marsal, J., Girona, J., Gonzalez-Dugo, V., Fereres, E., Ustin, S.L., Zarco-Tejada, P.J., 2016. Airborne thermal imagery to detect the seasonal evolution of crop water status in peach, nectarine and saturn peach orchards. Remote Sens. 8, 39.

Berni, J. A., Zarco-Tejada, P. J., Suárez, L., Fereres, E., 2009a. Thermal and narrowband multispectral remote sensing for vegetation monitoring from an unmanned aerial vehicle. Geoscience and Remote Sensing, IEEE Transactions on, 47, 722-738.

Berni, J. A., Zarco-Tejada, P. J., Suárez, L., Fereres, E., 2009b. Thermal and narrowband multispectral remote sensing for vegetation monitoring from an unmanned aerial vehicle. *Geoscience and Remote Sensing, IEEE Transactions on,* 47**,** 722-738.

Bhattarai, N.; Quackenbush, L.J.; Dougherty, M.; Marzen, L.J., 2015. A simple Landsat-MODIS fusion approach for monitoring seasonal evapotranspiration at 30 m spatial resolution. *Int. J. Remote Sens. 36*, 115–143.

Bisquert, M., Sánchez, J.M., López-Urrea, R., Caselles, V., 2016. Estimating high resolution evapotranspiration from disaggregated thermal images. Remote Sens. Environ. 187, 423–433.

Bouraima, A.-K., Zhang, W.H., Wei, C.F., 2015. Irrigation water requirements of rice using Cropwat model in Northern Benin. Int. J. Agric. Biol. Eng. 8 (2), 58–64.

Calera, A., Campos, I., Osann, A., D'Urso, G., Menenti, M., 2017. Remote sensing for crop water management: from ET modelling to services for the end users. Sensors 17, 1104.

Campos, I., González-Piqueras, J., Carrara, A., Villodre, J., Calera, A., 2016. Estimation of total available water in the soil layer by integrating actual evapotranspiration data in a remote sensing-driven soil water balance. J. Hydrol. 534, 427–439.

Carter, G.A., 1991. Primary and secondary effects of water concentration on the spectral reflectance of leaves. Am. J. Bot. 78, 916–924.

Cheng, X.-J., Wang, D., 2014. Estimating canopy water content in wheat based on new vegetation water index. Spectrosc. Spectral Anal. 34, 3391–3396.

Choudhury, B.J., Ahmed, N.U., Idso, S.B., Reginato, R.J., Daughtry, C.S.T., 1994. Relations between evaporation coefficients and vegetation indices studies by model simulations. Remote Sens. Environ. 50, 1–17.

Chung, S., Breshears, L. E., Yoon, J. 2018. Smartphone near infrared monitroring of plant stress. *Computers and Electronics in Agriculture,* 154, 93 – 98.

Clarke, T.R., 1997. An empirical approach for detecting crop water stress using multispectral airborne sensors. Hort Technol. 7, 9–16.

Cohen, Y., Alchanatis, V., Meron, M., Saranga, Y., Tsipris, J., 2005. Estimation of leaf water potential by thermal imagery and spatial analysis. J. Exp. Botany 56, 1843–1852.

Collaizzi, P., Kustas, William P., Anderson, Martha C., Agam, Nurit; Tolk, Judy A., Evett, Steven R., Howell, Terry A., Gowda, Prasanna H., O'Shaughnessy, Susan A., 2012. Two-source energy balance model estimates of evapotranspiration using component and composite surface temperatures. Publications from USDA-ARS /UNL Faculty. Paper 1147. http://digitalcommons.unl.edu/usdaarsfacpub/1147.

Colombo, R., Meroni, M., Busetto, L., Rossini, M., Panigada, C., 2011. Optical remote sensing of vegetation water content. In: Thenkabail, P.S., Lyon, J.G., Huete, A. (Eds.), Hyperspectral Remote Sensing of Vegetation. CRC Press, Taylor and Francis Group (USA), 227–244.

Colombo, R., Meroni, M., Marchesi, A., Busetto, L., Rossini, M., Giardino, C., Panigada, C., 2008. Estimation of leaf and canopy water content in poplar plantations by means of hyperspectral indices and inverse modeling. *Remote Sensing of Environment,* 112, 1820–1834.

Corti, M., Gallina, M. P., Cavalli, D., & Cabassi, G. (2017). Hyperspectral imaging of spinach canopy under combined water and nitrogen stress to estimate biomass, water, and nitrogen content. Biosystems Engineering, 158, 38 – 50.

Dangwal, N., Patel, N., Kumari, M., Saha, S., 2015. Monitoring of water stress in wheat using multispectral indices derived from Landsat-TM. Geocarto International**,** 1-12.

Danson, F., Steven, M., Malthus, T., Clark, J., 1992. High-spectral resolution data for determining leaf water content. Int. J. Remote Sens. 13, 461–470.

Dawson, T., Curran, P., North, P., Plummer, S., 1999. The propagation of foliar biochemical absorption features in forest canopy reflectance: a theoretical analysis. Remote Sens. Environ. 67, 147–159.

Dejonge, K.C., Taghvaeian, S., Trout, T.J., Comas, L.H., 2015. Comparison of canopy temperature-based water stress indices for maize. Agric. Water Manage. 156, 51–62.

Dubey, S.K., Sharma, D., 2018. Assessment of climate change impact on yield of major crops in the Banas River Basin, India. Science of the Total Environment 635, 10–19.

Eastham, J., Gray, S.A., 1998. A preliminary evaluation of the suitability of sap flow sensors for use in scheduling vineyard irrigation. American J. Enol. Viticulture 49, 171–176.

Ehret, D.L., Lau, A., Bittman, S., Lin, W., Shelford, T., 2001. Automated monitoring of greenhouse crops. Agronomie 21, 403–414.

Ehsani, R., Wulfsohn, D., Das, J., Lagos, I.Z., 2016. Yield estimation: a low–hanging fruit for application os small UAS. ASABE Resource magazine. Available from http://bt.e-ditionsbyfry.com/publication/?i=316822.

Elston, J., 2016. Why unmanned aircraft for agriculture? ASABE Resource magazine. Available from http://bt.e-ditionsbyfry.com/publication/?i=316822.

Evain, S., Flexas, J., Moya, I., 2004. A new instrument for passive remote sensing: 2.Measurement of leaf and canopy reflectance changes at 531 nm and their relationship with photosynthesis and chlorophyll fluorescence. *Remote Sens. Environ.,* 91(2), 175-185.

Evanidi, A., Katsoulas, N., Augoustaki, D., Loulou, I., & Kittas, C., 2018. Crop reflectance measurements for nitrogen deficiency detection in a soilless tomato crop. Biosystems Engineering. 176, 1-11.

Evanidi, A., Katsoulas, N., Bartzanas, T., Ferentinos, K. P., Kittas, C., 2017. Crop water assessment in controlled environment using crop reflectance and temperature measurements. Precis. Agric. 18, 332-349.

Evett, S. R., Howell, T. A., Schneider, A. D., Upchurch, D. R. and Wanjura, D. F. 2000. Automatic drip irrigation system of corn and soybean. Pages 401-408 in R. G. Evans et al., eds. Proc. Decennial Natl. Irrig. Symp., Phoenix, AZ.

Fereres, E., Goldhamer, D.A., 2003. Suitability of stem diameter variations and water potential as indicators for irrigation scheduling of almond trees. J. Horticultural Sci. Biotechnol. 78, 139–144.

Filion, R., Bernier, M., Paniconi, C., Chokmani, K., Melis, M., Soddu, A., Talazac, M., Lafortune, F., 2016. Remote sensing for mapping soil moisture and drainage potential in semi-arid regions: applications to the Campidano plain of Sardinia, Italy. Sci. Total Environ. 543, Part B, 862–876.

Flexas, J., Escalona, J.M., Evain, S., Gulías, J., Moya, I., Osmond, C.B., Medrano, H., 2002. Steady-state chlorophyll fluorescence (Fs) measurements as a tool to follow variations of net CO2 assimilation and stomatal conductance during water-stress in C3 plants. Physiologia plantarum 114, 231–240.

Foster, T., Brozovic, N., Butler, A. P., Neale, C. M. U., Raes, D., Steduto, P., Fereres, E., Hsiao, T. C., 2017. AqaCrop-OS: An open source version of FAO's crop water productivity model. Agricultural Water Management, 181, 18–22.20.

Frias-Moreno, N.. Nuñez-Barrios, A.. Perez-Leal, R.. Gonzalez-Franco, A. C.. Hernandez-Rodriguez, A.. RoblesHernandez, L.. 2014: Effect of Nitrogen Deficiency and Toxicity in Two Varieties of Tomatoes (Lycopersicum esculentum L.). Agric. Sci., 5:1361-1368.

Gago, J., Douthe, C., Coopman, R .E., Gallego, P. P., Ribas-Carbo , M., Flexas, J., Escalona, J., Medrano, H., 2015. UAVs challenge to assess water stress for sustainable agriculture. Agricultural Water Management, 153, 9-19.

Gago, J., Martorell, S., Tomás, M., Pou, A., Millán, B., Ramón, J., Ruiz, M., Sánchez, R., Galmés, J., Conesa, M.A., Cuxart, J., Tardáguila, J., Ribas-Carbó, M., Flexas, J., Medrano, H., Escalona, J.M., 2013. High-resolution aerial thermal imagery for plant water status assessment in vineyards using a multicopter-RPAS. First Conference of the International Society for Atmospheric Research using Remotely-piloted Aircraft, (ISARRA), Palma de Mallorca (Spain).

Gallardo, M., Thompson, R., Valdez, L., Fernández, M., 2006. Response of stem diameter variations to water stress in greenhouse-grown vegetable crops. J. Horticultural Sci. Biotechnol. 81, 483–495.

Gamon, J., 2015. Reviews and Syntheses: optical sampling of the flux tower footprint. Biogeosciences*,* 12, 4509-4523.

Gamon, J., Penuelas, J., Field, C., 1992. A narrow-waveband spectral index that tracks diurnal changes in photosynthetic efficiency. Remote Sensing of environment*,* 41**,** 35-44.

Gamon, J., Serrano, L., Surfus, J., 1997. The photochemical reflectance index: an optical indicator of photosynthetic radiation use efficiency across species, functional types, and nutrient levels. *Oecologia,* 112**,** 492-501.

Gao, B., 1996. NDWI – a normalized difference water index for remote sensing of vegetation liquid water from space. Remote Sens. Environ. 58, 257–266.

Garbulsky, M.F., Peñuelas, J., Gamon, J.A, Inoue, Y., Filella, I., 2011. The Photochemical Reflectance Index (PRI) and the remote sensing of leaf, canopy and ecosystem radiation use efficiencies; a review and meta-analysis. *Remote Sens. Environ.,* 115, 281-297.

Garces-Restrepo, C., Vermillion, D., Mu~noz, G., 2007. Irrigation management transfer. Worldwide efforts and results. FAO, Rome. pp. 62.

Genc, L., Demirel, K., Camoglu, G., Asik, S., & Smith, S. 2011. Determination of plant water stress using spectral reflectance measurements in watermelon (Citrullus vulgaris), American-Eurasian. Journal of Agriculture and Environmental Science. 11, 296 - 304.

Gianquinto, G., Orsini, F., Mezzetti, M., Sambo, P., Bona, S., 2011. A methodological approach for defining spectral indices for assessing tomato nitrogen status and yield. European Journal of Agronomy, 35, 135-143.

Giorio, P., Giorio, G., 2003. Sap flow of several olive trees estimated with the heatpulse technique by continuous monitoring of a single gauge. Environ. Exp.Botany 49, 9–20.

González-Dugo, M., Moran, M., Mateos, L., Bryant, R., 2006. Canopy temperature variability as an indicator of crop water stress severity. Irrigation Science. 24**,** 233-240.

Gonzalez-Dugo, V., Zarco-Tejada, P.J., Fereres, E., 2014. Applicability and limitations of using the crop water stress index as an indicator of water deficits in citrus orchards. Agric. For. Meteorol. 198–199.

Granier, A., 1987. Evaluation of transpiration in a Douglas-fir stand by means of sap flow measurements. Tree Physiol. 3, 309–320.

Haboudane, D., Miller, J.R., Tremblay, N., Zarco-Tejada, P.J., Dextraze, L., 2002. Integrated narrow-band vegetation indices for prediction of crop chlorophyll content for application to precision agriculture. Remote Sens. Environ. 81, 416–426.

Hargreaves, G.H., Samani, Z.A., 1985. Reference crop evapotranspiration from temperature. Appl. Eng. Agric. 1 (2), 96–99.

Hartz, T.K., Johnstone, P.R., Francis, D.M., Miyao, E.M. 2005. Processing tomato yield and fruit quality improved with potassium fertigation. HortScience. 40, 1862-1867.

Hernández-Clemente, R., Navarro-Cerrillo, R.M., Suárez, L., Morales, F., Zarco-Tejada, P.J., 2011. Assessing structural effects on PRI for stress detection in conifer forests. Remote Sens. Environ. 115, 2360–2375.

Hirich, A., Fatnassi, H., Ragab, R., Choukr-Allah, R., 2016. Prediction of climate change impact on corn grown in the south of morocco using the saltmed model. Irrig. and Drain. 65, 9–18.

Horticulture for People (IHC2010): International Symposium on 922. 23–34. Jones, H., 2012. Remote sensing of plant stresses and its use in irrigation management. VII Int. Symp. Irrig. Horticultural Crops 1038, 239–247.

Hsiao, T.C., Heng, L., Steduto, P., Rojas-Lara, B., Raes, D.,Fereres, E., 2009. AquaCrop—the FAO crop model to simulate yield response to water: III. Parameterization and testing for maize. Agron. J., 101 (3), 448-459.

Huang, J., Wang, H., Dai, Q., Han, D., 2014. Analysis of NDVI data for crop identification and yield estimation. *IEEE J. Sel. Top. Appl. Earth Observ. Remote Sens.*, 7(4), 4374–4384.

Huguet, J.-G., Li, S., Lorendeau, J.-Y., Pelloux, G., 1992. Specific micromorphometric reactions of fruit trees to water stress and irrigation scheduling automation. J. Horticultural Sci. 67, 631–640.

Idso, S., Jackson, R., Pinter, P., Reginato, R., Hatfield, J., 1981. Normalizing the stress-degree-day parameter for environmental variability. Agricultural Meteorology. 24**,** 45-55.

Idso, S.B., Jackson, R.D. and Reginato, R.J. 1978. Remote sensing for agricultural water management and crop yield prediction. Agric. Water Manage. 1, 299-310.

Ihuoma, S. O., & Madramootoo, C. A., 2017. Recent advances in crop water stress detection: A review. Computer and Electronics in Agriculture*.,* 141, 267-275.

Ihuoma, S. O., & Madramootoo, C. A. (2019a). Crop reflectance indices for mapping water stress in greenhouse grown bell peppers. Agri. Water Mgt., 219, 49-58.

Ihuoma, S. O., & Madramootoo, C. A. (2019b). Sensitivity of spectral vegetation indices for monitoring water stress in tomato plants. Computers and Electronics in Agriculture, 163, 104860.

Ihuoma, S. O., & Madramootoo, C. A. (2020). Narrow-band reflectance indices for mapping the combined effects of water and nitrogen stress in field grown tomato crops. Biosystems Engineering, 192, 133-143.

Irmak, A., Ratcliffe, I., Ranade, P., Hubbard, K., Singh, R. K., Kamble, B., Kjaersgaard, J., 2011. Estimation of land surface evapotranspiration with a satellite remote sensing procedure. *Great Plains Res.,* 21, 73–88.

Irmak, S., Haman, D.Z., Bastug, R., 2000. Determination of crop water stress index for irrigation timing and yield estimation of corn. Agron. J. 92 (6), 1221–1227.

Jaria, F., Madramootoo, C.A., 2013. Thresholds for Irrigation Management of Processing Tomatoes Using Soil Moisture Sensors in Southwestern Ontario. T. ASABE. 56, 155- 166.

Jayanthi, H., Neale, C. M. U., Wright, J. L., 2000. Seasonal evapotranspiration estimation using canopy reflectance: a case study involving pink beans. In: proceedings of remote sensing and hydrology, Santa Fe, NM, USA, 2–7 April 2000. pp. 302–305.

Jiang, C., Johkan, M., Hohjo, M., Tsukagoshi, S., Maruo, T., 2017. A correlation analysis on chlorophyll content and SPAD value in tomato leaves. Hort. Research, 71, 37－42.

Jones, H. G., 2004. Irrigation scheduling: advantages and pitfalls of plant-based methods. *Journal of experimental botany,* 55, 2427-2436.

Jones, H. G., 2007. Monitoring plant and soil water status: established and novel methods revisited and their relevance to studies of drought tolerance. *Journal of experimental botany,* 58, 119-130.

Jones, H., 2010. Remote detection of crop water stress and distinguishing it from other stresses. XXVIII International Horticultural Congress on Science and

Jones, H., 2012. Remote sensing of plant stresses and its use in irrigation management. VII International Symposium on Irrigation of Horticultural Crops 1038, 239-247.

Jones, H.G., Vaughan, R.A., 2010. Remote sensing of vegetation: principles, techniques, and applications. Oxford University Press.

Kalacska, M., Arroyo-Mora, J. P., Soffer, R. J., Roulet, N. T., Moore, T. R., Humphreys, E., Leblanc, G., Lucanus, O., Inamdar, D., 2018. Estimating Peatland Water Table Depth and Net Ecosystem Exchange: A Comparison between Satellite and Airborne Imagery. *Remote Sens.*, *10*(5), 687.

Kamble, B., Irmak, A., Hubbard, K., 2013. Estimating Crop Coefficients Using Remote Sensing-Based Vegetation Index. *Remote Sens.,* 5, 1588-1602.

Katsoulas, N., Elvanidi, A., Ferentinos, K. P., Bartzanas, T., Kittas, C., 2016. Crop reflectance monitoring as a tool for water stress detection in greenhouses: A review. Biosystems Engineering.

Kim, Y., Glenn, D. M., Park, J., Ngugi, H. K., & Lehman, B. L., 2010. Hyperspectral image analysis for plant stress detection. In American society of agricultural and biological engineers, Annual international meeting, Pittsburgh, Pennsylvania.

Kirnak, H., Kaya, C., Higgs, D., Tas, I., 2003. Response of drip irrigated bell pepper to water stress and different nitrogen levels with or without mulch cover. J. Plant Nutr., 26, 263 – 277.

Kittas, C., Elvanidi, A., Katsoulas, N., Ferentinos, K. P., Bartzanas, T., 2016. Reflectance indices for the detection of water stress in greenhouse tomato (Solanum lycopersicum). Acta Horticulturae. 1112, 63-70.

Koksal, E. S., 2011. Hyperspectral reflectance data processing through cluster and principal component analysis for estimating irrigation and yield related indicators. Agricultural Water Management. 98, 1317-1328.

Kullberg, E.G., DeJonge, K.C., Chávez, J.L., 2017. Evaluation of thermal remote sensing indices to estimate crop evapotranspiration coefficients. Agric. Water Manage. 179, 64–73.

Kumar, V., Udeigwe, T.K., Clawson, E.L., Rohli, R.V., Miller, D.K., 2015. Crop water use and stage-specific crop coefficients for irrigated cotton in the mid-south, United States. Agric. Water Manage. 156, 63–69.

Laurent, V.C.E., Schaepman, M.E., Verhoef, W., Weyermann, J., Chávez, R.O., 2014. Bayesian object-based estimation of LAI and chlorophyll from a simulated sentinel-2 top-of-atmosphere radiance image. Remote Sens. Environ. 140, 318–329.

Lei, Y., Zhang, H., Chen, F., Zhang, L., 2016. How rural land use management facilitates drought risk adaptation in a changing climate—A case study in arid northern China. Sci. Total Environ. 550, 192–199.

Leroux, L., Baron, C., Zoungrana, B., Traoré, S. B., Seen, D. L., Bégué, A., 2016. Crop Monitoring Using Vegetation and Thermal Indices for Yield Estimates: Case Study of a Rainfed Cereal in Semi-Arid West Africa. *IEEE Journal of Selected Topics in Applied Earth Observations and Remote Sensing,* 9, 347-362.

Liang, L., Zhang, L., Lin, H., Li, C., & Yang, M. (2013). Estimating canopy leaf water content in wheat based on derivative spectra. Scientia Agricultura Sinica, 46, 18–29.

Li-Cor, 1992. LAI-2000 Plant Canopy Analyser: Instruction Manual. Nebraska Li-Cor, Inc., Lincoln (179 pp.).

Limpus, S., 2009. Isotropic and anisotropic characterisation of vegetable crops. In: Fisheries, D.O.P.I.A. (Ed.).

Lohr, D., Ti;;mann, P., Zerche, S., Druege, U., Rath, T., & Meinken, E. (2016). Non-destructive measurement of nitrogen status of leafy ornamental cuttings by near infrared reflectance spectroscopy (NIRS) for assessment of rooting capacity. Biosystems Engineering, 148, 157 – 167.

Lorenzo-Minguez, P., Ceulemans, R., Gabriels, R., Impens, I., Verdonck, O., 1985. Effect of short-term water stress on leaf gas exchange processes and plant water potential in Schefflera. Hort Sci. 20, 932–934.

Maes, W., Achten, W., Reubens, B., Muys, B., 2011. Monitoring stomatal conductance of Jatropha curcas seedlings under different levels of water shortage with infrared thermography. Agric. Forest Meteorol. 151, 554–564.

Magney, T. S., Vierling, L. A., Eitel, J. U., Huggins, D. R., Garrity, S. R., 2016. Response of high frequency Photochemical Reflectance Index (PRI) measurements to environmental conditions in wheat. *Remote Sensing of Environment,* 173, 84-97.

Meroni, M., Rossini, M., Guanter, L., Alonso, L., Rascher, U., Colombo, R., Moreno, J., 2009. Remote sensing of solar-induced chlorophyll fluorescence: review of methods and applications. Remote Sens. Environ. 113, 2037–2051.

Meroni, M., Rossini, M., Picchi, V., Panigada, C., Cogliati, S., Nali, C., Colombo, R., 2008. Assessing steady-state fluorescence and PRI from hyperspectral proximal sensing as early indicators of plant stress: the case of ozone exposure. Sensors 8, 1740–1754. method. Nat. Sci. Rep. 1–9.

model for apple canopy water content prediction using the equidistant sampling

Moya, I., Camenen, L., Evain, S., Goulas, Y., Cerovic, Z., Latouche, G., Flexas, J., Ounis, A., 2004. A new instrument for passive remote sensing: 1. Measurements of sunlight-induced chlorophyll fluorescence. Remote Sens. Environ. 91, 186–197.

Nielsen, D.C., Gardner, B.R., 1988. Scheduling irrigation for corn with the crop water stress index (CWSI). Appl. Agric. Res. 2 (5), 295–300.

Norman, J. M., Kustas, W. P., Humes, K.S. 1995. Source approach for estimating soil and vegetation energy fluxes in observation of directional radiometric surface temperature. Agric. For. Meteorol., 77, 263-293.

Numata, I., Khand, K., Kjaersgaard, J., Cochrane, M. A., and Silva, S.S., 2017. Evaluation of Landsat-Based METRIC Modeling to Provide High-Spatial Resolution Evapotranspiration Estimates for Amazonian Forests. Remote sensing. Vol. 9, 46. doi:10.3390/rs9010046.

Nyathi, M.K., van Halsema, G.E., Annandale, J.G. Struik, P.C., 2018. Calibration and validation of the AquaCrop model for repeatedly harvested leafy vegetables grown under different irrigation regimes. Agricultural Water Management, 208, 107–119.

OMAFRA, 2016. Irrigation update. Ontario Ministry of Agriculture, Food and Rural Affairs.

O'Shaughnessy, S.A., Evett, S.R., Colaizzi, P.D., Howell, T.A., 2012. A crop water stress index and time threshold for automatic irrigation scheduling of grain sorghum. Agr. Water Manage. 107, 122–132.

Orta, A. H., Erdem, T. and Erdem, Y. 2002. Determination of water stress index in sunflower. Helia 37, 27-38.

Osakabe, Y.1., Osakabe, K., Shinozaki, K.1., Lam-Son, P., 2014. Response of plants to water stress. Front Plant Sci. 5, 86.

Osroosh, Y., Peters, R.T., Campbell, C.S., Zhang, Q., 2015. Automatic irrigation scheduling of apple trees using theoretical crop water stress index with an innovative dynamic threshold. Comp. Electron. Agric. 118, 193–203.

Osroosh, Y., Peters, R.T., Campbell, C.S., Zhang, Q., 2016. Comparison of irrigation automation algorithms for drip-irrigated apple trees. Comp. Electron. Agric. 128, 87–99.

Padilla, F. M., Pena-Fleitas, M. T., Gallardo, M., Thompson, R. B. (2015). Threshold values of canopy reflectance indices and chlorophyll meter readings for optimal nitrogen nutrition of tomato. Annals of Applied Biology166 (2), 271-285.

Paltineanu, C., Septar, L., Moale, C., 2013. Crop Water Stress in Peach Orchards and Relationships with Soil Moisture Content in a Chernozem of Dobrogea. J. Irrig. Drain Eng., 139 (1), 20–25.

Panigada, C., Rossini, M., Meroni, M., Cilia, C., Busetto, L., Amaducci, S., Boschetti, M., Cogliati, S., Picchi, V., Pinto, F., Marchesi, A., Colombo, R., 2014. Fluorescence, PRI and canopy temperature for water stress detection in cereal crops. *International Journal of Applied Earth Observation and Geoinformation,* 30**,** 167-178.

Patel, A., Sharda, R., Patel, S., Meena, P., 2017. Reference evapotranspiration estimation using cropwat model at ludhiana district (Punjab). Int. J. Sci., Environ. Technol. 6 (1), 620–629.

Payero, J. O. and Irmak, S., 2006. Variable Upper and Lower Crop Water Stress Index Baselines for Corn and Soybean. Biological Systems Engineering.

Pelgrum, H., Miltenburg, I., Cheema, M., Klaasse, A., Bastiaanssen, W., 2010. ETLook a novel continental evapotranspiration algorithm. Remote Sensing and Hydrology Symposium, 10875-10877.

Peñuelas, J., Filella, I., 1998. Visible and near-infrared reflectance techniques for diagnosing plant physiological status. Trends in Plant Sci. 3, 151–156.

Peñuelas, J., Garbulsky, M. F., Filella, I., 2011. Photochemical reflectance index (PRI) and remote sensing of plant CO_2 uptake. *New Phytologist,* 191, 596-599.

Peñuelas, J., Pinol, J., Ogaya, R., Filella, I., 1997. Estimation of plant water concentration by the reflectance water index WI (R900/R970). Int. J. Remote Sens. 18, 2869–2875.

Petropoulos, S. A., Fernandes, A., Katsoulas, N., Barros, L., Ferreira, I., 2019. The effect of covering material on the yield, quality and chemical composition of greenhouse-grown tomato fruit. J Sci Food Agric. 99: 3057–3068.

Prasad, P.V.V., Staggenborg, S.A., Ristic, Z., 2008. Impacts of drought and/or heat stress on physiological, developmental, growth, and yield processes of crop plants. In: Ahuja, L.H., Saseendran, S.A. (Eds.), Response of Crops to Limited Water: Understanding and Modeling Water Stress Effects on Plant Growth Processes. Advances in Agricultural Systems Modeling Series 1. ASA-CSSA, Madison, Wisconsin.

Rahimzadeh-Bajgiran, P., Munehiro, M., Omasa, K., 2012. Relationships between the photochemical reflectance index (PRI) and chlorophyll fluorescence parameters and plant pigment indices at different leaf growth stages. Photosynthesis Res. 113, 261–271.

Rinaldi, M., Castrignanò, A., De Benedetto, D., Sollitto, D., Ruggieri, S., Garofalo, P., Santoro, F., Figorito, B., Gualano, S., Tamborrino, R., 2014. Discrimination of tomato plants under different irrigation regimes: analysis of hyperspectral sensor data. Environmetrics. 26, 77-88.

Rinaldi, M., Garofalo, P., Vonella, A.V., 2015. Productivity and Water Use Efficiency in Processing Tomato under Deficit Irrigation in Southern Italy. Acta Horticulturae. 1081, 97-104.

Roerink, G. J., Su, Z., Menenti, M., 2000. S-SEBI: a simple remote sensing algorithm to estimate the surface energy balance. Phys. Chem. Earth, 25,147-157.

Ronga, D., Rizza, F., Badeck, F., Milc, J., Laviano, L., Montevecchi, G., Pecchioni, N., Francia, E. (2018). Physiological responses to chilling in cultivars of processing tomato released and cultivated over the past decades in Southern Europe. Scientia Horticulturae, 231, 118-125.

Rossini, M., Fava, F., Cogliati, S., Meroni, M., Marchesi, A., Panigada, C., Giardino, C., Busetto, L., Migliavacca, M., Amaducci, S., Colombo, R., 2013. Assessing canopy PRI from airborne imagery to map water stress in maize. ISPRS Journal of Photogrammetry and Remote Sensing. 86, 168-177.

Roujean, J.L., Breon, F.M., 1995. Estimating PAR absorbed by vegetation from bidirectional reflectance measurements. Remote Sens. Environ. 51, 375–384.

Rouse, J. W., Haas, R. H., Schell, J. A., Deering, D. W., 1974. Monitoring vegetation systems in the Great Plains with ERTS. In: Fraden, S.C., Marcanti, E.P., Becker, M. A. (Eds.), Third ERTS-1 Symposium, 10–14 Dec. 1973, NASA SP-351, Washington D.C.. NASA, 309–317.

Rozenstein, O., Haymann, N., Kaplan, G., Tanny, J., 2018. Estimating cotton water consumption using a time series of Sentinel-2 imagery. Agricultural Water Management, 207, 44 – 52.

Samuel, A., Girma, A., Zenebe, A., Ghebreyohannes, T., 2018. Spatio-temporal variability of evapotranspiration and crop water requirement from space. Journal of Hydrology, 567, 732-742.

Scholander, P.F., Hammel, H., Bradstreet, E.D., Hemmingsen, E., 1965. Sap pressure in vascular plants. Science 148, 339–346.

Senay, G.B.; Bohms, S.; Singh, R.K.; Gowda, P.H.; Velpuri, N.M.; Alemu, H.; Verdin, J.P., 2013. Operational evapotranspiration mapping using remote sensing and weather datasets: A new parameterization for the SSEB approach. J. Am. Water Resour. Assoc. 49, 577–591.

Sentek Sensor Technologies. 2003. Access Tube Installation Guide Version 1.0 for EnvironSCAN, EnviroSMART and Diviner 2000. Sentek Pty Ltd. Stepney, South Australia.

Sezen, S. M., Yazar, A., Dasgan, Y., Yucel, S., Akyildiz, A., Tekin, S., Akhoundnejad, Y., 2014. Evaluation of crop water stress index (CWSI) for red pepper with drip and furrow irrigation under varying irrigation regmes. *Agricultural water management,* 143, 59 – 70.

Shamshiri, R. R., Kalantari, K., Ting, K. C., Thorp, K. R., Hameed, I. A., Weltzien, C., Ahmad, 608 D., Shad, M. Z., 2018. Advances in greenhouse automation and controlled environment 609 agriculture: A transition to plant factories and urban agriculture. Internatonal Journal of 610 Agricultural and Biological Engineering. 11, 1 – 22.

Siad, S. M., Iacobellis, V., Zduli, P., Gioia, A., Stavi, I., Hoogenboom, G., 2019. A review of coupled hydrologic and crop growth models. Agricultural Water Management, 224, 105746.

Silva, E. C., Nogueira, R. J. M. C., Silva, M. A., Albuquerue, M. B., 2011. Drought stress and plant nutrition. Plant Stress 5 (Special Issue 1), 32-41.

Singh, A.K., Madramootoo, C.A., Smith, D.L., 2010. Water balance and corn yield under different water table management scenarios in Southern Quebec. In: 9th international drainage symposium held jointly with CIGR and CSBE/SCGAB proceedings, 13–16 June 2010, Québec City convention centre, Quebec City, Canada. American Soc. Agric. Biol. Engineers, 1.

Smith, M., 1992. CROPWAT: a Computer program for irrigation planning and management. Food and Agricultural Organization of the United Nations.

Stagakis, S., González-Dugo, V., Cid, P., Guillén-Climent, M.L., & Zarco-Tejada, P.J. (2012). Monitoring water stress and fruit quality in an orange orchard under regulated deficit irrigation using narrow-band structural and physiological remote sensing indices. Journal of Photogrammetry and Remote Sensing, 71, 47–61.

Stavrakoudis, D., Katsantonis, D., Kadoglidou, K., Kalaitzidis, A., Gitas, I. Z., 2019. Estimating rice agronomic traits using drone-collected multispectral imagery. Remote Sens., 11, 545.

Steduto, P., Hsiao, T.C., Raes, D., Fereres, E., 2009. AquaCrop-the FAO crop model to simulate yield response to water: I. Concepts and underlying principles. Agron. J., 101, 426-437.

Steele, D.D., Stegman, E.C., Gregor, B.L., 1994. Field comparison of irrigation scheduling methods for corn. Trans. ASAE 37 (4), 1197–1203.

Steidle Neto, A. J., Lopes, D. C., Pinto, F, A. C., & Zolnier, S. (2017). Vis/NIR spectroscopy and chemometrics for non-destructive estimation of water and chlorophyll status in sunflower leaves. Biosystems Engineering, 155, 124 - 133.

Stockle, C.O., Dugas, W.A., 1992. Evaluating canopy temperature based indices for irrigation scheduling. Irrig. Sci. 13, 31–37.

Su, Z., 2002. The surface energy balance system (SEBS) for estimation of turbulent heat fluxes. Hydrol. Earth Syst. Sci. Discuss., 6 (1), 85-100.

Suárez, L., Zarco-Tejada, P. J., Berni, J. A., González-Dugo, V., Fereres, E., 2009. Modelling PRI for water stress detection using radiative transfer models. Remote Sensing of Environment. 113, 730-744.

Suárez, L., Zarco-Tejada, P., Berni, J., González-Dugo, V., Fereres, E., 2010. Orchard Water Stress detection using high-resolution imagery. XXVIII international horticultural congress on science and horticulture for people (IHC2010): international symposium on 922. 35–39.

Surendran, U., Sushanth, C.M., Mammen, G., Joseph, E.J., 2017. FAO-CROPWAT model-based estimation of crop water need and appraisal of water resources for sustainable water resource management: Pilot study for Kollam district –humid tropical region of Kerala, India. Current Sci. 112 (1), 76–86.

Taghvaeiana, S., Comas, L., DeJonge, K.C., Trout, T.J., 2014. Conventional and simplified canopy temperature indices predict water stress in sunflower. Agric. Water Manage. 144, 69–80.

Toumi, J., Er-Raki, S., Ezzahar, J., Khabba, S., Jarlan, L., Chehbouni, A., 2015. Performance assessment of AquaCrop model for estimating evapotranspiration, soil water content and grain yield of winter wheat in Tensift Al Haouz (Morocco): Application to irrigation management. Agricultural Water Management, Vol. 163, pp 219-235.

Tremblay, N., Wang, Z., & Cerovic, Z. G. (2012). Sensing crop nitrogen status with fluorescence indicators: A review. Agron. Sustain. Dev. 32, 451 – 464.

Tsakmakis, I.D. Kokkos, N.P. Gikas, G.D. Pisinaras, Hatzigiannakis, V. E., Arampatzis, G., Sylaios, G.K., 2019. Evaluation of AquaCrop model simulations of cotton growth under deficit irrigation with an emphasis on root growth and water extraction patterns. Agricultural Water Management 213, 419–432.

Turner, D., Lucieer, A., Watson, C., 2012. An automated technique for generating georectified mosaics from ultra-high resolution unmanned aerial vehicle (UAV) imagery, based on structure from motion (SfM) point clouds. Remote Sens.. 4(5), 1392. 1410.

USDA-NRCS (U.S. Department of Agriculture, National Resources and Conservation Service). (2000). Soil Texture Calculator.

Vanino, S., Nino, P., De Michele, C., Bolognesi, S. F., D'Urso, G., Di Bene, C., Pennelli, B., Vuolo, F., Farina, R., Pulighe, G., Napoli, R., 2018. Capability of Sentinel-2 data for estimating maximum evapotranspiration and irrigation requirements for tomato crop in Central Italy. Remote Sensing of Environment, 215, 452 – 470.

Vanuytrecht, E., Raes, D., Steduto, P., Hsiao, T.C., Fereres, E., Heng, L.K., Vila, M. G., Moreno, P. M., 2014. AquaCrop: FAO's crop water productivity and yield response model. Environ. Model. Softw, 62, 351-360.

Verrelst, J., Rivera, J.P., Veroustraete, F.,Muñoz-Marí, J., Clevers, J.G.P.W.,Camps-Valls, G., Moreno, J., 2015. Experimental Sentinel-2 LAI estimation using parametric, nonparametric and physical retrieval methods - a comparison. ISPRS J. Photogramm. Remote Sens. 108, 260–272.

Wang, X., Zhao, C., Guo, N., Li, Y., Jian, S., Yu, K., 2015. Determining the Canopy Water Stress for Spring Wheat Using Canopy Hyperspectral Reflectance Data in Loess Plateau Semiarid Regions. Spectroscopy Letters. 48**,** 492-498.

Yazar, A., Howell, T.A., Dusek, D.A., Copeland, K.S., 1999. Evaluation of crop water stress index for LEPA irrigated corn. Irrig. Sci. 18 (4), 171–180.

Yildirim, M., Demirel, K., Bahar, E., 2012. Effect of restricted water supply and stress development on growth of bell pepper (Capsicum Annuum L.) under drought conditions. J. Agro Crop Sci. 3, 1–9.

Zarco-Tejada, P. J., González-Dugo, V., Berni, J. A., 2012. Fluorescence, temperature and narrow-band indices acquired from a UAV platform for water stress detection using a micro-hyperspectral imager and a thermal camera. Remote Sensing of Environment. 117**,** 322-337.

Zarco-Tejada, P. J., González-Dugo, V., Williams, L., Suárez, L., Berni, J. A., Goldhamer, D., Fereres, E., 2013. A PRI-based water stress index combining structural and chlorophyll effects: Assessment using diurnal narrow-band airborne imagery and the CWSI thermal index. *Remote sensing of environment,* 138**,** 38-50.

Zarco-Tejada, P.J., Berni, J.A., Suárez, L., Sepulcre-Cantó, G., Morales, F., Miller, J., 2009. Imaging chlorophyll fluorescence with an airborne narrow-band multispectral camera for vegetation stress detection. Remote Sens. Environ. 113, 1262–1275.

Zarco-Tejada, P.J., Rueda, C.A., Ustin, S.L., 2003. Water content estimation in vegetation with MODIS reflectance data and model inversion methods. Remote Sens. Environ. 2003 (85), 109–124.

Zhang, H., Han, M., Chavez, J.L., Lan, Y., 2017a. Improvement in estimation of soil water deficit by integrating airborne imagery data into a soil water balance model. Int. J. Agric. Biol. Eng. 10 (3), 37–46.

Zhang, H., Xiong, Y., Huang, G., Xu, X., Huang, Q., 2017b. Effects of water stress on processing tomatoes yield, quality and water use efficiency with plastic mulched drip irrigation in sandy soil of the Hetao irrigation district. Agric. Water Manage. 179, 205–214.

Zhao, H., Zhu, X., Li, C., Zhao, G., Jiang, Y., 2017. Improving the Accuracy of the Hyperspectral Model for Apple Canopy Water Content Prediction using the Equidistant Sampling Method. *Nature - Scientific Reports,* 1 – 9.

Zhao, T., Stark, B., Chen, Y., Ray, A. L., Doll, D., 2015. A detailed field study of direct correlations between ground truth crop water stress and normalized difference vegetation index (NDVI) from small unmanned aerial system (sUAS). Unmanned Aircraft Systems (ICUAS), 2015 International Conference on IEEE. 520–525.

Zhao, Z., Li, X., Yin, Y. B., Tang, J., & Zhou, S. B. (2010). Analysis of spectral features based on water content of desert vegetation. *Spectroscopy and Spectral Analysis* **30**, 2500–2503.